THE UNIVERSITY OF CHICAGO

THE PBAF CHROMATIN REMODELER CONTROLS MOTOR NEURON REGIONAL IDENTITY IN *CAENORHABDITIS ELEGANS*

A DISSERTATION SUBMITTED TO

THE FACULTY OF THE DIVISION OF THE BIOLOGICAL SCIENCES

AND THE PRITZKER SCHOOL OF MEDICINE

IN CANDIDACY FOR THE DEGREE OF

DOCTOR OF PHILOSOPHY

COMMITTEE ON NEUROBIOLOGY

BY

ANTHONY OSUMA

CHICAGO, ILLINOIS

JUNE 2024

TABLE OF CONTENTS

CHAPTER 2: RESULTS

LIST OF FIGURES

LIST OF TABLES

ACKNOWLEDGMENTS

My time in graduate school has been one of the most challenging yet rewarding experiences of my life. Over the years there have been many people who I've learned from, worked with, and received much needed support from.

First and foremost, I would like to thank my mentor Paschalis Kratsios. I could not have asked for a better mentor throughout my graduate training. I so appreciate the hands-on academic training and guidance you have provided me over the last 8 years. Your personality and passion for *C. elegans* and neuroscience is infectious, and clearly bleeds into the wonderful lab environment you have created. I will forever be grateful to you for taking the chance on bringing me into your lab as a volunteer and then technician, affording me the opportunity to prove I could succeed as a graduate student. I have no doubt that the Kratsios Lab will continue to grow and succeed with you at its helm.

I would also like to thank all the members of my committee, Elizabeth Grove, Edwin Ferguson, and Ellie Heckscher, for providing their time, mentorship, and guidance during my time in graduate school. I appreciate that your comments and advice have always challenged and pushed me to think critically and become a better scientist, whether it be through our committee meetings, TAships, or rotations spent together.

Thank you as well to all current and former members of the Kratsios Lab! It is a special thing to thoroughly enjoy going into work because of the people there. All of you have made the experience worthwhile. I especially want to thank Yinan Li, Manasa Prahlad, and Jihad Aburas who directly contributed to the work in this thesis, as well as Weidong Feng, Edgar Correa, Catarina Catela, and Kailong Wen. You made the earliest, quietest days of the lab so enjoyable!

Thank you to the entire Neuroscience community at the University of Chicago, especially Elena Rizzo, Dan McGehee, and Ruth Anne Eatock for believing in me and granting me the opportunity to work here as a graduate student.

Lastly, I would like to thank my family and friends for their love and support throughout graduate school. I would first like to thank my parents, Denise and Tobi Osuma, who have been there every step of the way. Words cannot describe how thankful I am to call you my parents. You have always gone above and beyond to support me and provide lifetime opportunities, while also pushing me to be better as both a student and person. Thank you! I would like to thank my friends whose companionship and support have made getting through graduate school that much easier, especially fellow scientists Shannon Miller and Nicholas Kowalski (commiserating about graduate school always made me feel better!) as well as Elliott Chen, Joe Cariz, and Srinivas Panchamukhi. I always look forward to our weekly chats while playing Halo as a brief reprieve from the daily grind of graduate school. Finally, I want to thank my wife and life partner, Madeline Osuma. You have been by my side supporting me through the process of graduate school for nearly a decade now. From reading over applications, to listening to countless practice presentations, or even just listening to me vent about failed experiments, thank you so much for your unwavering love and support. I would not have been able to reach this point without you.

ABSTRACT

A fundamental feature of the nervous system is its topographic organization. The motor system, for example, is topographically organized, as the position of motor neuron cell bodies in the central nervous system (CNS) correlates with which muscle targets will be innervated at the periphery. For their proper topographic organization, motor neurons must acquire their regional identity features, such as neurotransmitter receptors, signaling proteins, ion channels, etc. Many studies across model systems have focused on elucidating the transcriptional mechanisms that govern motor neuron regional identity. While much has been discovered in terms of transcription factor involvement in these mechanisms, whether and how epigenetic modifications (e.g., DNA modifications, histone modifications, chromatin modifications) control motor neuron regional identity remains poorly understood. In this thesis, we leveraged the *Caenorhabditis elegans* motor system to uncover a new role of a highly conserved chromatin remodeling complex (polybromo-associated BRG1-associated factor (PBAF), part of the switch/sucrose non-fermentable (SWI/SNF) family of chromatin remodelers) in motor neuron regional identity. We first show that mutant *C. elegans* animals lacking critical PBAF subunits display ectopic expression of the glutamate receptor *glr-4/GRIK4* in ventral nerve cord motor neurons, while also displaying loss of expression of other terminal identity features (*itr-1/ITPR1, avr-15/GLRA1-3, glr-5/GRIK1/3, ser-2/HTR1A*) in tail motor neurons. Second, we observe that PBAF repression of *glr-4/GRIK4* is cell-autonomous and occurs only in specific motor neuron subtypes. Finally, we describe another conserved transcription factor, *mab-9/Tbx20*, that also represses *glr-4/GRIK4* in ventral nerve cord motor neurons, suggesting a model for the observed specificity of PBAF activity. That is, a sequence-specific transcription factor (MAB-9/Tbx20) may recruit PBAF to the *glr-4/GRIK4* cis-regulatory region to accomplish repression.

Altogether, the data in this thesis presents a novel role for the PBAF chromatin remodeler as an activator in specific motor neuron subtypes of the ventral nerve cord and a repressor in tail motor neurons, and thus as a critical regulator of motor neuron regional identity.

CHAPTER I: INTRODUCTION

1.1 Background on Central Nervous System Development

Development of the human nervous system begins during the earliest stages of life. A single fertilized egg (zygote) undergoes a series of rapid cell divisions resulting in the formation of the blastocyst, a single-layered ball of cells containing an inner cell mass of embryonic stem cells, roughly 5-6 days following fertilization. At about 2 weeks the blastocyst undergoes a process called gastrulation, a critical step during development in which the single-layered cluster of cells is formed into a three-layered embryo. The differentiation of embryonic stem cells into these three germ layers gives rise to all the various structures and organs found in the body. The endoderm forms the gut, lungs, and liver. The mesoderm is responsible for forming muscle, bone, cartilage, and blood. Finally, the ectoderm gives rise to the skin as well as the nervous system.

At 3-4 weeks, formation of the central nervous system (CNS) begins during a process called neurulation. At this time, the notochord, a cord of mesodermal cells which later form the vertebral column, releases signaling proteins which induce the overlying ectoderm to differentiate into the neural plate. The neural plate then folds in on itself and closes, forming the neural tube which will eventually become the brain and spinal cord. The neural tube subsequently undergoes morphogenesis, during which it begins to form a regionalized CNS. The neural tube is subdivided into 4 distinct regions: the forebrain, midbrain, hindbrain, and spinal cord. Along the length of the neural tube, the dorsal-ventral (D-V) axis is patterned due to the secretion of several signaling molecules (e.g., sonic hedgehog [SHH], Wnt family members, bone morphogenic proteins [BMPs], and retinoic acid [RA]). This results in the differential expression of transcription factors along the D-V axis, leading compartments of neural

progenitors to differentiate into various post-mitotic neuron and glial cell types. Among these cell types are motor neurons (MNs), which originate from neural progenitors on the ventral side of the neural tube (the pMN domain) and require SHH and RA signaling for the expression of critical transcription factors (such as Olig2) necessary for MN differentiation (Cave and Sockanathan, 2018[1]). However, the precise mechanisms through which post-mitotic MNs achieve their terminal fates to carry out their diverse functions remains elusive and will be the focus of the work presented in this thesis.

1.2 The Problem of Neuronal Identity

In order to diversify and perform their specific functions along the anterior-posterior (A-P) axis, MNs must differentiate to achieve their unique terminal identities. How this is accomplished is a problem that dates back to the earliest days of neuroscience. The work of Santiago Ramón y Cajal established what we know today as the "neuron doctrine"; that is, that the nervous system is comprised of a network of discrete, independent processing units called neurons, which form the functional basis for the entire nervous system. These neurons were first classified based on their distinct anatomical features (cell body shape, size, axon length, etc.) (Bota and Swanson, 2007[2]) (**Fig. 1.1a**). Electrophysiological properties were then later used as a means of neuron classification with the development of new electrophysiology techniques (e.g., patch clamp) (Neher and Sakmann, 1976[3], Hamill et. al., 1981[4], Sakmann and Neher, 1984[5]). More recently, sequencing techniques have been used to further classify neurons based on their unique molecular profiles (the types of proteins they express in combination, such as neurotransmitter receptors, ion channels, etc.) (**Fig. 1.1b**). As a result, neurons are typically

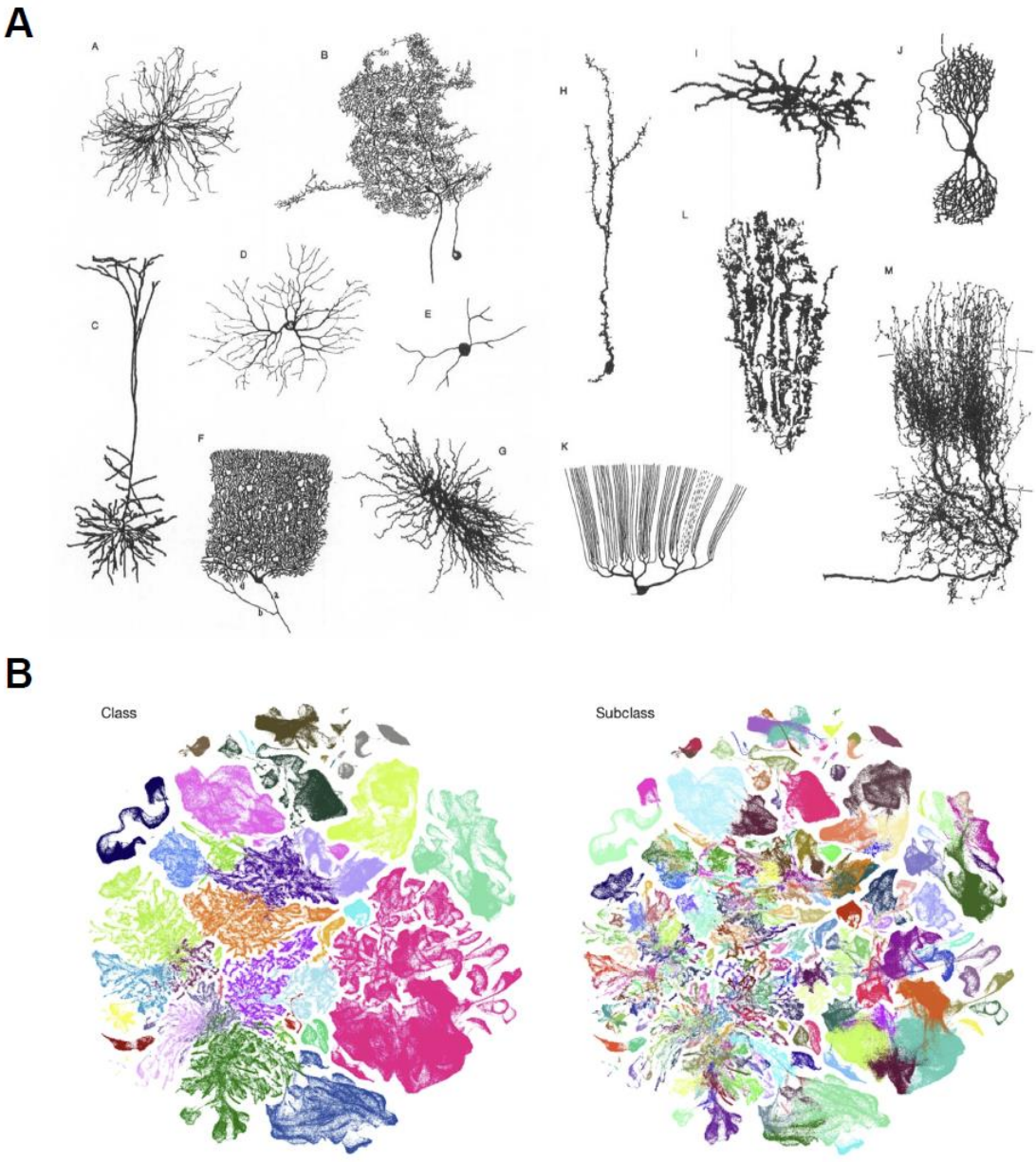

Figure 1.1 Morphology and molecular identity reveal neuron subtype diversity in the cortex

(**A**) Various neuron types display a high degree of morphological diversity, as seen in their dendrites, axonal projections, and soma locations. Adapted from Mel, B.W. Neural Computation 1994.

(**B**) scRNA-seq data for whole adult mouse brain. UMAP representation of neuron types (left), of which there are over 30, and neuron subtypes (right), of which there are over 330. Adapted from Yao et. al., 2023. Differences in morphology, molecular identity, and function together shape neuron subtypes.

divided into neuron subtypes; i.e., a categorical grouping of neurons based on a combination of their distinct morphological, molecular, and functional properties that define subtype identity. This principle holds true in the human motor system, which can be subdivided into over 600 MN subtypes (Zuccaro et. al., 2021[6]). The diversity represented across groups of neurons is the result of complex gene regulatory networks of proteins (usually sequence-specific transcription factors) that are expressed in unique combinations to promote or repress distinct molecular features in a cell. These molecular features (called terminal identity genes) are comprised of neurotransmitter receptors, signaling proteins, ion channels, etc., which ultimately determine a neuron's terminal identity. While there has been much progress in the elucidation of these gene regulatory networks, open questions remain preventing our full understanding of how neuronal subtypes are both established during development and maintained throughout life. What are the epigenetic mechanisms (e.g., DNA or histone modifications, chromatin remodeling) that control neuronal subtype diversification? How do such mechanisms influence the activity of sequence-specific transcription factors?

1.3 Topographic Organization of the Motor System

Topographic maps are used throughout the human nervous system as a fundamental organizational feature. That is, there is an ordered relationship between the position of neurons (cell body position) in the CNS and sensory fields (e.g., retina, skin) or muscle targets. Evidence for topographic maps emerged from experiments – initially conducted in primates – including electrical stimulation of cortex (Leyton and Sherrington, 1917[7]) and studying acute cortical lesions (Holmes, 1918[8]), and were later cemented with microelectrode stimulation and recording practices (Adrian, 1941[9], Marshall and Talbot, 1942[10]). The lateral geniculate nucleus (LGN) and

primary visual cortex (V1), for example, are organized via a retinotopic map, in that a specific area of the retina is mapped to a specific area in the LGN and visual cortex (Allman and Kass, 1975[11]). Meanwhile, auditory cortex has been documented to be tonotopically organized in relation to the range of frequencies detected be specific areas of the cochlea (Humphries et. al., 2010[12]).

Like sensory systems, motor systems also display striking topographical organization in motor neuron cell body position and the muscle targets they innervate. We can see this in both the developing hindbrain and spinal cord along the dorsal-ventral (D-V), medial-lateral (M-L), and anterior-posterior (A-P) axes. For example, the hindbrain, divided into segments during development called rhombomeres, contains nuclei of MNs which project to specific muscle groups based on their location along the A-P axis. MNs in rhombomere segments r1-r3 innervate muscles of the jaw, whereas MNs in r4 and r5 innervate muscles of the face and eyes (Sannes et. al., 2012[13]). Likewise, lower MNs in the spinal cord are organized topographically along the A-P axis. MN cell bodies located in the lower cervical and brachial regions of the spinal cord extend their axons to innervate muscles of the arms, while MN cell bodies located in the lumbar region of the spinal cord innervate muscles of the legs (Khan and Lui, 2023[14]). Thus, in both the hindbrain and spinal cord, control of specific muscles in the periphery is directly related to the position of MNs along the A-P axis (Jessell et. al., 2011[15]).

In order for these MNs to achieve their differences in functional output, they must display a high degree of diversity between one another. Specifically, there must be molecular mechanisms in place (intrinsic or extrinsic) that enable MNs to occupy specific positions in the developing nervous system. Their unique molecular identities then guide the formation of connections with different cells, thus enabling MNs to exhibit different functions (i.e., control different muscles).

This leads to the fundamental question: How is diversity between MNs achieved during development?

As discussed above, we know that MNs located in similar regions may also share similar functions (such as in the hindbrain and spinal cord). Thus, as a further means of classification, MNs also carry a distinct regional identity (i.e., the unique combination of molecular features expressed in MNs across the same region), a concept which originates from studies of Hox genes in the *Drosophila* embryo (discussed further in chapter 1.4). This MN regional identity is necessary for the establishment of topography in the motor system. As with MN subtype identity, MN regional identity is also established through conserved gene regulatory networks. Specifically, members of the highly conserved Hox family of homeodomain proteins act to confer regional identity to MNs in the developing nervous system.

1.4 The Role of Hox Genes in Establishing MN Regional Identity

One of the most well-studied protein families during development is a homeodomain sub-family of transcription factors known as Hox proteins. Hox genes are highly conserved genes which contain a 180bp homeobox sequence encoding for the homeodomain (DNA binding domain) in Hox proteins. Hox genes were first discovered through the work of Edward Lewis in the fruit fly model *Drosophila melanogaster*. Two striking mutations resulted in homeotic transformations (the transformation of one body structure to the likeness of another). A dominant mutation in the *Antennapedia* complex resulted in the transformation of antennae into legs, while a recessive mutation in the *bithorax* complex resulted in the transformation of halteres into wings (Lewis, 1978[16], Lappin et. al., 2006[17]). These studies also highlighted that the order of Hox genes

on the chromosome is related to the order in which those genes are expressed along the A-P axis (i.e. spatial collinearity). Thus, these gene complexes were found to be responsible for establishing the regional identity of body segments in *Drosophila* along the anterior-posterior (A-P) axis.

While *Drosophila* have 8 Hox genes, mammals have a total of 39 Hox genes (13 genes across 4 clusters, a-d, on separate chromosomes). As in *Drosophila*, Hox genes have been shown to play a similar role in determining body plan formation along the A-P axis in several species. In mammals, Hox proteins are combinatorically expressed across specific regions along the A-P axis, where they bind to the regulatory regions of a myriad of downstream transcription factors to promote or restrict their expression in that particular region. The result is a vast gene regulatory network of transcription factors which work in consort with one another to specify a cell's terminal fate.

This principle, again, holds true for the developing motor system and is the primary factor in why we observe its topographic organization (Averof and Akam, 1995[18], Noden, 1991[19], Tumpel et. al., 2009[20]). For example, the mouse spinal cord is organized into distinct motor columns, where each column houses a specific set of MNs that innervate distinct muscle groups along the A-P axis (Catela and Kratsios, 2021[21], Catela et. al., 2022[22]) – e.g., lateral motor column (LMC) MNs are generated in brachial and lumbar spinal cord regions and innervate limb muscles, while medial motor column (MMC) MNs exist throughout cervical, brachial, thoracic, and lumbar spinal cord regions and innervate axial muscles (Stifani, 2014[23]). These motor columns are generated through the unique expression of transcription factors in a particular region, such as *Foxp1* that is expressed only in the preganglionic motor column (PGC) and in the LMC and is necessary for the proper specification of these MNs (Dasen et. al., 2008[24], Rousso et. al., 2008[25]).

The expression of these transcription factors is, in turn, determined by the combination of Hox genes expressed in that region. In this way, Hox genes control the regional identity of MNs, a role that has been well documented in the worm, fly, and mammalian nervous systems. Therefore, the motor system is an ideal model system to elucidate the underlying mechanisms which establish regional neuron identity.

1.5 *C. elegans* as a Model to Investigate MN Regional Identity and Diversification

To probe the question of MN regional identity, this research focuses on the use of *Caenorhabditis elegans* motor system as a model. Use of the nematode *C. elegans* as a model to study the nervous system was established by Sydney Brenner (Brenner, 1973[26], Brenner, 1974[27]), who sought a simpler model system than zebrafish or fruit flies to study nervous system development. There are several compelling reasons why *C. elegans* presents a powerful model to study MN development.

First, the entire animal contains only 302 neurons, a number far lower than that of many other model organisms. The invariance of cellular development across individual animals allowed the determination of the complete embryonic cell lineage in *C. elegans* from zygote to newly hatched larva (Sulston et. al., 1983[28]), as well as the complete mapping of the *C. elegans* connectome (White et. al., 1986[29], Albertson and Thompson, 1976[30]). The small size of its genome also resulted in *C. elegans* being the first multicellular organism to have its complete genome sequenced (*C. elegans* Sequencing Consortium, 1998[31]).

Second, *C. elegans* are easily grown and maintained in a laboratory setting. Adult animals are only 1-1.5 mm long and have a fast reproductive cycle of just 3 days. While males exist and

offer a means of sexual reproduction, hermaphrodites (instead of females) offer another means of reproduction through self-fertilization. Thus, it is easy to isolate isogenic clones of *C. elegans* and hundreds of offspring can be obtained from a single hermaphrodite. Animals can be maintained on an agar pad with an easily culturable bacterial lawn (*E. coli*) as a food source. They also appear as semi-transparent making them an ideal model for the use of transgenic techniques using fluorescent proteins, allowing individual neurons in the worm to be seen and imaged under a fluorescent microscope.

Third, the *C. elegans* model is very conducive to genetic manipulations and sequencing techniques. Not only are transgenic lines easily produced via microinjection of a DNA fragment or plasmid, but they can also be manipulated through CRISPR/Cas9 gene editing as well as RNAi, which was first discovered in *C. elegans* (Fire et. al., 1998[32]). *C. elegans* is a powerful tool for gene discovery as it is conducive to using genetic screens (both forward and reverse), while also supporting the use of various sequencing techniques (RNA-seq, ChIP-seq, ATAC-seq).

Finally, *C. elegans* MNs are divided into several subpopulations while also carrying a regional identity. *C. elegans* MNs are split into 9 distinct types based on gross morphological criteria: SAB, DA, DB, VA, VB, AS, VC, DD, and VD. Seven of the types use the neurotransmitter acetylcholine (SAB, DA, DB, VA, VB, AS, VC), while the other two are GABAergic MN types (DD, VD). The MNs in each of these types are interspersed throughout the ventral side of the animal along the A-P axis and innervate 95 body wall muscles along the ventral and dorsal sides of the animal, allowing for locomotion (Altun and Hall, 2011[33]). However, these MNs can be further classified into subtypes with a distinct regional identity. *C. elegans* MNs can be divided into 3 distinct regions: retrovesicular ganglion (RVG), ventral nerve

cord (VNC), and preanal ganglion (PAG) (**Fig. 1.2**). Recent single-cell RNA-seq data has shown that these MNs differ in their molecular profiles along the A-P axis (Smith et. al., 2024[34]), with the largest differences being found when comparing MNs between RVG, VNC, and PAG. As a result, while each region contains neurons of all types, MNs in the same region also share molecular properties. Thus, *C. elegans* presents a useful model to study MN regional identity and development.

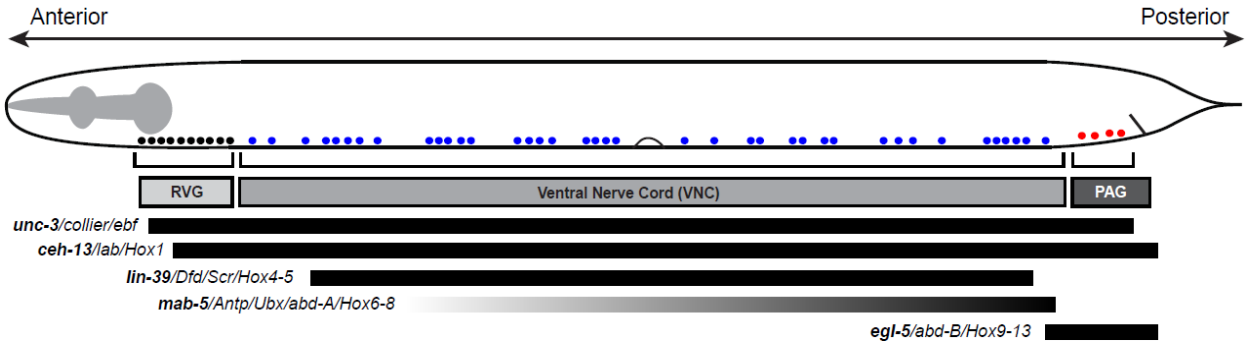

Figure 1.2 *C. elegans* cholinergic MNs differ in cell body position

(Top) Schematic of *C. elegans* cholinergic MNs, segregated by region: retrovesicular ganglion (black), ventral nerve cord (blue), and preanal ganglion (red). (Bottom) Regions of expression for *unc-3* and C. elegans Hox genes *ceh-13*, *lin-39*, *mab-5*, and *egl-5*.

1.6 Terminal Selectors: Determinants of Post-Mitotic MN Cell Fate

Terminal selector genes are a specialized class of transcription factors that broadly control gene expression and thus differentiation in a specific cell type. In other words, they are primarily responsible for helping a given group of cells achieve their terminal identity. Terminal selectors have been discovered in several species thus far, including mice (Cobaleda et. al., 2007[35]), flies (Chanut-Delalande et. al., 2006[36]), and worms (Hobert, 2008[37], Hobert, 2016[38], Kratsios et. al., 2011[39]), and have been especially well studied in the developing nervous system. They generally have in common two key defining features. First, they are required to initiate the expression of

several functionally unrelated terminal identity features (Deneris and Hobert, 2014[40]). In the case of MNs, this includes features such as ion channels, neurotransmitter receptors, signaling proteins, etc. Second, they are continuously expressed throughout the life of the animal and their removal results in the loss of these terminal identity features. As such, they are considered to be "master regulators" of terminal identity.

In the *C. elegans* motor system, it has been previously found that the conserved transcription factor UNC-3, the sole ortholog of the Collier/Olf/Ebf (COE) family of transcription factors, acts as a terminal selector in cholinergic MNs (Kratsios et. al., 2011[39]). UNC-3 directly binds to its conserved COE motif and activates genes critical for cholinergic MN function and terminal differentiation (such as genes important for the acetylcholine pathway, as well as terminal identity features). UNC-3 is also continuously required, and its absence results in the loss of all cholinergic MN terminal identity features. However, while some of these features are shared by all cholinergic MNs (i.e., acetylcholine pathway genes), many others are expressed only in specific MN subtypes, or even within subsets of MN subtypes. Thus, other factors must coordinate to work with or against UNC-3 in order to generate this subtype-specific expression pattern of terminal identity genes. While a number of transcription factors have been observed to coordinate with or antagonize UNC-3 function, very little is known regarding the involvement of epigenetic mechanisms in MN specification. In the next few sections, I will provide a brief background on histone modifications and chromatin remodeling, as well as introduce one remodeler, PBAF, that is the central topic of this thesis.

1.7 Histone Post-Translational Modifications Regulate Chromatin Structure and Accessibility

Every cell in the body contains a complete copy of the entire genome. This enormous amount of DNA must be efficiently packaged in the nucleus, and thus exists as a complex of DNA and proteins called chromatin. Strings of nucleosomes form the structural basis of chromatin, each composed of an octamer core of histone proteins wrapped in approximately 1.65 turns (or 146 base pairs) of DNA(Annunziato, 2008[41]). While this method of packaging is extremely effective for condensing DNA in the nucleus, it also renders it largely inaccessible to DNA binding proteins. Chromatin thus exists in two different states: heterochromatin and euchromatin. Heterochromatin is a highly consolidated form of chromatin in which DNA is compacted into nucleosomes, largely inaccessible to DNA binding proteins, and thus is typically not associated with gene transcription. Euchromatin on the other hand is a much more lightly packed form of chromatin where, instead of being tightly wound around histones, specific regions of DNA are much more accessible to DNA binding proteins and is therefore typically associated with gene transcription (Huisinga et. al., 2006[42]) (**Fig. 1.3a**). However, each cell differs in terms of which genes are expressed and when those genes are expressed. Chromatin must therefore be highly dynamic and able to switch between its condensed and accessible states when necessary. This would not be possible without the activity of histone modifying enzymes and chromatin remodelers, complexes of proteins that function to restructure chromatin.

One of the primary mechanisms through which the remodeling of chromatin is regulated is histone post-translational modifications. Such modifications are wide ranging, including acetylation, methylation, phosphorylation, and ubiquitination among others (Alhamwe et. al., 2018[43]). These modifications are targeted towards specific amino acids, usually within N-

terminal histone tails. While several types of post-translational modifications have been observed in the literature, two of these, acetylation and methylation, have been studied quite extensively and seen to be highly involved in chromatin remodeling, affecting the initiation or suppression of gene transcription (Lee et. al., 2020[44]). These specific modifications are executed by the histone modifying enzymes histone acetyltransferase and histone methyltransferase. Acetyltransferases acetylate specific, conserved lysine residues on histone tails (H3K14, H3K27, etc.) by transfer of an acetyl group to these amino acids from acetyl-CoA. Likewise, methyltransferases methylate specific lysine and arginine residues on histone tails (H3R2, H3K4, H3K9, etc.) via the donation of a methyl group to these amino acids from S-adenosylmethionine (Bannister and Kouzarides, 2011[45]). The variations in these modifications are dependent on their intended functional output (i.e., if the target gene is to be activated or inactivated). This functions to effectively mark nucleosomes for remodeling, and these marks are subsequently recognized by specific protein domains residing in chromatin remodeling complexes. Thus, histone modifying enzymes are often referred to as "writers" of histone post-translational modifications, while chromatin remodelers are often referred to as "readers" of histone post-translational modifications. These modifications, however, are usually not permanent and therefore need to be removed in order to reverse the changes to chromatin state. Other histone modifying enzymes (e.g., deacetylases and demethylases) serve to remove changes made to histone tails by writers and are thus often referred to as "erasers" (Gillette and Hill, 2015[46], Biswas and Rao, 2018[47]). This precise dynamic between histone post-translational modifications and chromatin remodelers (discussed further in chapter 1.8) is essential for regulating several nuclear processes including gene transcription.

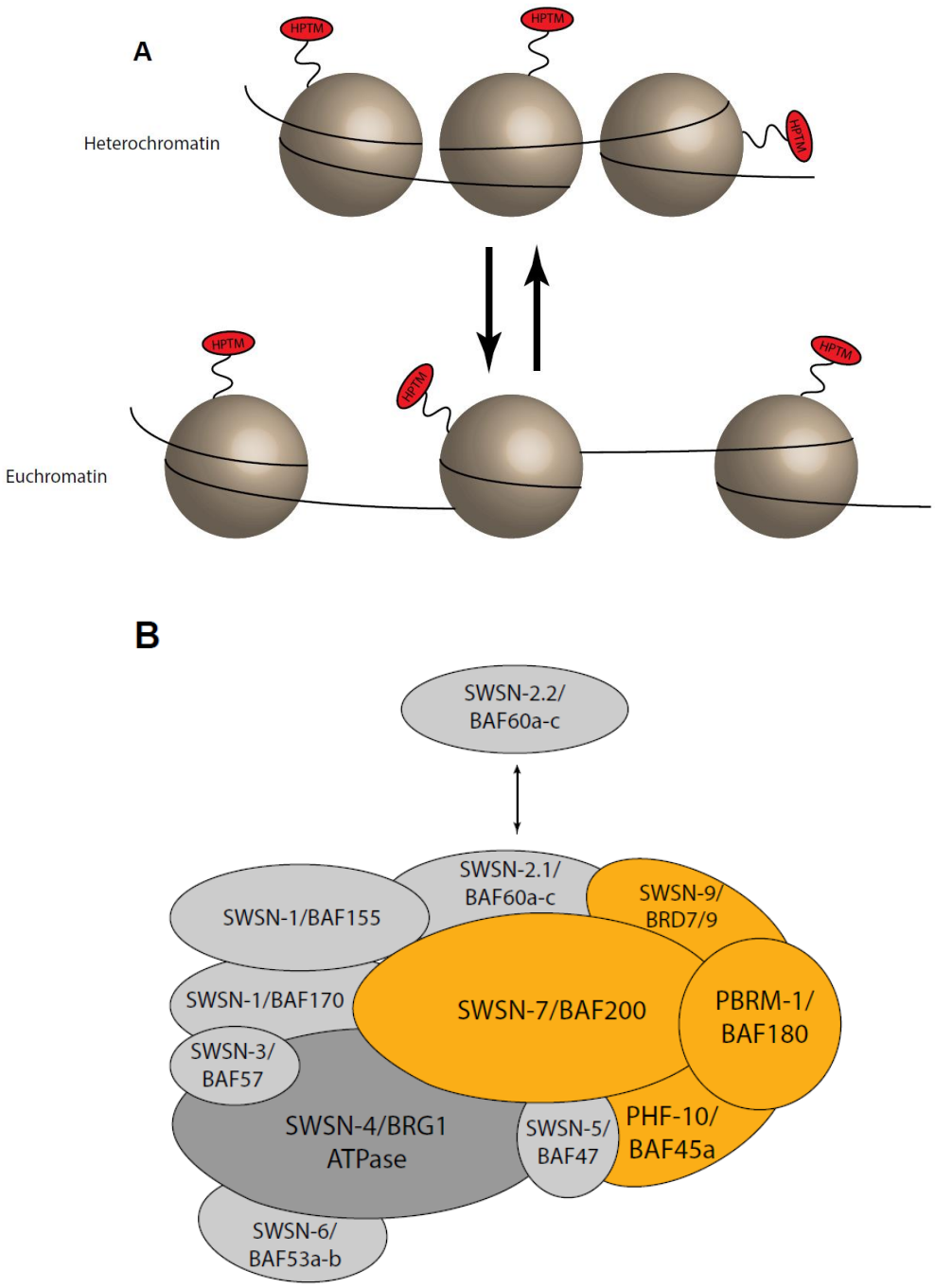

Figure 1.3 Chromatin structure is dynamic and is altered by ATP dependent chromatin remodelers

(A) Cartoon of chromatin states with histone post-translational modifications. Heterochromatin (top) is a compact state of chromatin with largely inaccessible DNA. Euchromatin (bottom) is an open form of chromatin with accessible DNA, associated with gene transcription.

Figure 1.3 cont.
(B) Schematic of the PBAF chromatin remodeling complex, with the names of each component in *C. elegans* and their mammalian orthologs. Contains the ATPase swsn-4/BRG1 (dark gray), a core of accessory subunits shared by the BAF remodeler (light gray), and PBAF specific subunits (orange).

1.8 Chromatin Remodelers: Readers of Histone Post-Translational Modifications

Chromatin remodelers are ATP dependent protein complexes that use the energy generated from ATP hydrolysis to weaken the contacts between DNA and histones, resulting in the restructuring, sliding, or ejection of nucleosomes. There exist four families of chromatin remodelers which have been identified in the literature, those being the switch/sucrose non-fermentable (SWI/SNF), imitation switch (ISWI), chromodomain helicase DNA-binding (CHD), and inositol auxotrophy 80 (INO80) families of remodelers (Tyagi et. al., 2016[48], Reyes et. al., 2021[49]). Each of these families contains at least two unique remodeling complexes, all of which have a catalytic subunit with a Snf2 (a family of helicase-like proteins) ATPase domain. This domain is characterized by two distinct parts – the DExx (N-terminal domain of helicase superfamilies 1 and 2) and HELICc (C-terminal domain of helicase superfamilies 1 and 2) domains, which function to utilize the power of ATP hydrolysis to translocate the enzyme onto double stranded DNA, acting as a motor to physically break the contact between DNA and histones, and thereby facilitating change in the conformation of chromatin (Clapier and Cairns, 2009[50]).

While all four families of chromatin remodelers have in common a Snf2 catalytic subunit, they differ in their domains that flank the ATPase domain. In particular, the SWI/SNF family of remodelers contains a helicase-SANT (HSA) domain, essential for complex assembly by binding actin related proteins, and a bromodomain flanking the ATPase domain. Specifically,

bromodomains serve to give the SWI/SNF remodeler its reader functionality by recognizing and binding acetylated lysine residues on histone tails. This specific mechanism of reading histone post-translational modifications distinguishes the SWI/SNF family from others, such as the CHD family which contains chromodomains (instead of a bromodomain) flanking its ATPase domain and function to recognize methylated lysine residues on histone tails (Tyagi et. al., 2016[48], Clapier and Cairns, 2009[50]).

1.9 Known Roles for the PBAF Chromatin Remodeler in Disease and Neurodevelopment

The SWI/SNF family of chromatin remodelers was originally discovered in yeast through independent genetic screens resulting in mutations which affected multiple SWI/SNF subunits (Cairns et. al., 1994[51], Stern et. al., 1984[52], Neigeborn and Carlson, 1984[53]). These mutations manifested as mating-type switching (SWI) and sucrose non-fermenting (SNF) phenotypes, hence giving SWI/SNF its name. Of particular interest in this thesis is the SWI/SNF chromatin remodeler polybromo-associated BRG1-associated factor (PBAF) (**Fig. 1.3b**). PBAF is a highly conserved chromatin remodeler found in mammals, flies (PBAP), and worms, and is characterized by two distinguishing features: Its ATPase *swsn-4/BRG1* (shared by the closely related chromatin remodeler BRG1-associated factor, BAF) as well as its many conserved bromodomains.

While PBAF/BAF mutations have been implicated in several disease states, these chromatin remodelers have been largely studied within the context of cancer. A myriad of human malignancies (up to 20%) have been reported to show mutations in BAF complexes (Hodges et. al., 2016[54]), and evidence in the literature suggests that these complexes can even act as both a

tumor suppressor (loss of *swsn-5*/*BAF47*) and oncogene (*SS18*) (Alfert et. al., 2019[55]). Importantly, mutations in PBAF/BAF chromatin remodelers have been linked to several neurodevelopmental and neurodegenerative disorders including Coffin-Siris syndrome, Nicolaides-Baraitser syndrome, Kleeftra's syndrome, autism spectrum disorders, amyotrophic lateral sclerosis, and schizophrenia (Chesi et. al., 2013[56], Koga et. al., 2009[57]). However, while these remodeling complexes have been observed to play a role in certain aspects of neural development such as neural progenitor proliferation, we are far from having a complete understanding of their function in the developing nervous system. As such, a distinct role for PBAF as a regulator of regional MN identity in the developing nervous system remains unclear.

1.10 Aim of this Thesis

The motor system is a critical unit of the nervous system responsible for generating all forms of movement. MNs extend their axons out from the CNS to the periphery, where they synapse with various muscle groups to coordinate locomotion. During development MNs adopt a distinct regional identity, as evidenced by their topographical organization, in that certain molecular features are shared between MNs of the same region. While many studies have focused on the early development of MN regional identity, such as the role of Hox genes during MN differentiation, how post-mitotic MNs achieve their terminal regional identities remains poorly understood.

To probe the question of MN regional identity, this thesis will use the *C. elegans* motor system as a model, primarily focusing on the expression of the terminal identity gene *glr-4/GRIK4* (a glutamate receptor). Known to be directly controlled and activated by the terminal

selector UNC-3, we find that *glr-4/GRIK4* is repressed in the VNC by a highly conserved chromatin remodeling complex called PBAF. While chromatin remodelers, typically broadly expressed, are known to be involved in the broad expression and repression of genes, very little is known regarding chromatin factor involvement in establishing MN regional identity. Furthermore, although previous studies have tied PBAF to aspects of neural development and disease, a role in generating MN regional identity has not been described.

Chapter 2 of this thesis aims to show a novel role for the PBAF chromatin remodeler as a key regulator of MN regional identity. We see that, despite its broad expression pattern, PBAF is required and acts cell-autonomously in post-mitotic MNs to repress *glr-4/GRIK4* in the VNC, while also being required to activate calcium channel and chloride channel subunits *itr-1/ITPR1* and *avr-15/GLRA1-3* (among others) in the posterior tail region (PAG). These MNs display differences in the expression of only select terminal identity features while other features remain unchanged, and thus adopt a "mixed" MN identity. The findings in this thesis may provide valuable insight into the role that chromatin factors play in establishing MN regional identity, as well as mechanistic information on how broadly expressed chromatin factors exert remarkably specific effects on gene expression.

1.11 References

1. Cave C, Sockanathan S. Transcription Factor Mechanisms Guiding Motor Neuron Differentiation and Diversification. *Curr Opin Neurobiol*. 2018;53:1-7. doi:10.1016/j.conb.2018.04.012

2. Bota M, Swanson LW. The neuron classification problem. *Brain Res Rev*. 2007;56(1):79. doi:10.1016/j.brainresrev.2007.05.005

3. Neher E, Sakmann B. Single-channel currents recorded from membrane of denervated frog muscle fibres. *Nature*. 1976;260(5554):799-802. doi:10.1038/260799a0

4. Hamill OP, Marty A, Neher E, Sakmann B, Sigworth FJ. Improved patch-clamp techniques for high-resolution current recording from cells and cell-free membrane patches. *Pflugers Arch*. 1981;391(2):85-100. doi:10.1007/BF00656997

5. Sakmann B, Neher E. Patch Clamp Techniques for Studying Ionic Channels in Excitable Membranes. *Annu Rev Physiol*. 1984;46(1):455-472. doi:10.1146/annurev.ph.46.030184.002323

6. Zuccaro E, Piol D, Basso M, Pennuto M. Motor Neuron Diseases and Neuroprotective Peptides: A Closer Look to Neurons. *Front Aging Neurosci*. 2021;13:723871. doi:10.3389/fnagi.2021.723871

7. Leyton ASF, Sherrington CS. Observations on the Excitable Cortex of the Chimpanzee, Orang-Utan, and Gorilla. *Q J Exp Physiol*. 1917;11(2):135-222. doi:10.1113/expphysiol.1917.sp000240

8. Holmes G. Disturbances of Vision by Cerebral Lesions. *Br J Ophthalmol*. 1918;2(7):353-384.

9. Adrian ED. Afferent discharges to the cerebral cortex from peripheral sense organs. *J Physiol*. 1941;100(2):159-191.

10. Marshall WH, Talbot SA. Recent evidence for neural mechanisms in vision leading to a general theory of sensory acuity. In: *Visual Mechanisms*. Jacques Cattell; 1942:117-164.

11. Allman JM, Kass JH. The dorsomedial cortical visual area: A third tier area in the occipital lobe of the owl monkey (aotus trivirgatus). *Brain Res*. 1975;100(3):473-487. doi:10.1016/0006-8993(75)90153-5

12. Humphries C, Liebenthal E, Binder JR. Tonotopic organization of human auditory cortex. *NeuroImage*. 2010;50(3):1202-1211. doi:10.1016/j.neuroimage.2010.01.046

13. Sanes DH, Reh TA, Harris WA. 4 - Determination and differentiation. In: Sanes DH, Reh TA, Harris WA, eds. *Development of the Nervous System (Third Edition)*. Academic Press; 2012:77-104. doi:10.1016/B978-0-12-374539-2.00008-2

14. Khan YS, Lui F. Neuroanatomy, Spinal Cord. In: *StatPearls*. StatPearls Publishing; 2024. Accessed February 5, 2024. http://www.ncbi.nlm.nih.gov/books/NBK559056/

15. Jessell TM, Sürmeli G, Kelly JS. Motor Neurons and the Sense of Place. *Neuron*. 2011;72(3):419-424. doi:10.1016/j.neuron.2011.10.021

16. Lewis EB. A gene complex controlling segmentation in Drosophila. *Nature*. 1978;276(5688):565-570. doi:10.1038/276565a0

17. Hox Genes: Seductive Science, Mysterious Mechanisms - PMC. Accessed February 5, 2024. https://www.ncbi.nlm.nih.gov/pmc/articles/PMC1891803/

18. Averof M, Akam M. Hox genes and the diversification of insect and crustacean body plans. *Nature*. 1995;376(6539):420-423. doi:10.1038/376420a0

19. Noden DM. Cell movements and control of patterned tissue assembly during craniofacial development. *J Craniofac Genet Dev Biol*. 1991;11(4):192-213.

20. Tümpel S, Wiedemann LM, Krumlauf R. Chapter 8 Hox Genes and Segmentation of the Vertebrate Hindbrain. In: *Current Topics in Developmental Biology*. Vol 88. Genes. Academic Press; 2009:103-137. doi:10.1016/S0070-2153(09)88004-6

21. Catela C, Kratsios P. Transcriptional mechanisms of motor neuron development in vertebrates and invertebrates. *Dev Biol*. 2021;475:193-204. doi:10.1016/j.ydbio.2019.08.022

22. Catela C, Chen Y, Weng Y, Wen K, Kratsios P. Control of spinal motor neuron terminal differentiation through sustained Hoxc8 gene activity | eLife. Accessed February 5, 2024. https://elifesciences.org/articles/70766

23. Stifani N. Motor neurons and the generation of spinal motor neurons diversity. *Front Cell Neurosci*. 2014;8. Accessed February 5, 2024. https://www.frontiersin.org/articles/10.3389/fncel.2014.00293

24. Dasen JS, De Camilli A, Wang B, Tucker PW, Jessell TM. Hox Repertoires for Motor Neuron Diversity and Connectivity Gated by a Single Accessory Factor, FoxP1. *Cell*. 2008;134(2):304-316. doi:10.1016/j.cell.2008.06.019

25. Rousso DL, Gaber ZB, Wellik D, Morrisey EE, Novitch BG. Coordinated Actions of the Forkhead Protein Foxp1 and Hox Proteins in the Columnar Organization of Spinal Motor Neurons. *Neuron*. 2008;59(2):226-240. doi:10.1016/j.neuron.2008.06.025

26. Brenner S. The Genetics of Behaviour. *Br Med Bull*. 1973;29(3):269-271. doi:10.1093/oxfordjournals.bmb.a071019

27. Brenner S. The Genetics of Caenorhabditis Elegans. *Genetics*. 1974;77(1):71-94. doi:10.1093/genetics/77.1.71

28. Sulston JE, Schierenberg E, White JG, Thomson JN. The embryonic cell lineage of the nematode Caenorhabditis elegans. *Dev Biol*. 1983;100(1):64-119. doi:10.1016/0012-1606(83)90201-4

29. White JG, Southgate E, Thomson JN, Brenner S. The structure of the nervous system of the nematode Caenorhabditis elegans. *Philos Trans R Soc Lond B Biol Sci*. 1997;314(1165):1-340. doi:10.1098/rstb.1986.0056

30. Albertson DG, Thompson JN, Brenner S. The pharynx of Caenorhabditis elegans. *Philos Trans R Soc Lond B Biol Sci*. 1997;275(938):299-325. doi:10.1098/rstb.1976.0085

31. The C. Elegans Sequencing Consortium. Genome Sequence of the Nematode C. elegans: A Platform for Investigating Biology. *Science*. 1998;282(5396):2012-2018. doi:10.1126/science.282.5396.2012

32. Fire A, Xu S, Montgomery MK, Kostas SA, Driver SE, Mello CC. Potent and specific genetic interference by double-stranded RNA in Caenorhabditis elegans. *Nature*. 1998;391(6669):806-811. doi:10.1038/35888

33. Altun ZF, Hall DH. Hermaphrodite - Nervous System - General Overview. Accessed February 5, 2024. https://www.wormatlas.org/hermaphrodite/nervous/Neuroframeset.html

34. Smith JJ, Taylor SR, Blum JA, Gitler AD, Miller DM, Kratsios P. A molecular atlas of adult C. elegans motor neurons reveals ancient diversity delineated by conserved transcription factor codes. Published online August 6, 2023:2023.08.04.552048. doi:10.1101/2023.08.04.552048

35. Cobaleda C, Schebesta A, Delogu A, Busslinger M. Pax5: the guardian of B cell identity and function. *Nat Immunol*. 2007;8(5):463-470. doi:10.1038/ni1454

36. Chanut-Delalande H, Fernandes I, Roch F, Payre F, Plaza S. Shavenbaby Couples Patterning to Epidermal Cell Shape Control. *PLOS Biol*. 2006;4(9):e290. doi:10.1371/journal.pbio.0040290

37. Hobert O. Regulatory logic of neuronal diversity: Terminal selector genes and selector motifs. *Proc Natl Acad Sci*. 2008;105(51):20067-20071. doi:10.1073/pnas.0806070105

38. Hobert O. Chapter Twenty-Five - Terminal Selectors of Neuronal Identity. In: Wassarman PM, ed. *Current Topics in Developmental Biology*. Vol 116. Essays on Developmental Biology, Part A. Academic Press; 2016:455-475. doi:10.1016/bs.ctdb.2015.12.007

39. Kratsios P, Stolfi A, Levine M, Hobert O. Coordinated regulation of cholinergic motor neuron traits through a conserved terminal selector gene. *Nat Neurosci*. 2012;15(2):205-214. doi:10.1038/nn.2989

40. Deneris ES, Hobert O. Maintenance of postmitotic neuronal cell identity. *Nat Neurosci*. 2014;17(7):899-907. doi:10.1038/nn.3731

41. Annunziato AT. DNA Packaging: Nucleosomes and Chromatin. Published 2008. Accessed February 5, 2024. http://www.nature.com/scitable/topicpage/dna-packaging-nucleosomes-and-chromatin-310

42. Huisinga KL, Brower-Toland B, Elgin SCR. The contradictory definitions of heterochromatin: transcription and silencing. *Chromosoma*. 2006;115(2):110-122. doi:10.1007/s00412-006-0052-x

43. Alaskhar Alhamwe B, Khalaila R, Wolf J, et al. Histone modifications and their role in epigenetics of atopy and allergic diseases. *Allergy Asthma Clin Immunol*. 2018;14(1):39. doi:10.1186/s13223-018-0259-4

44. Lee HT, Oh S, Ro DH, Yoo H, Kwon YW. The Key Role of DNA Methylation and Histone Acetylation in Epigenetics of Atherosclerosis. *J Lipid Atheroscler*. 2020;9(3):419-434. doi:10.12997/jla.2020.9.3.419

45. Bannister AJ, Kouzarides T. Regulation of chromatin by histone modifications. *Cell Res*. 2011;21(3):381-395. doi:10.1038/cr.2011.22

46. Gillette TG, Hill JA. Readers, writers and erasers: Chromatin as the Whiteboard of Heart Disease. *Circ Res*. 2015;116(7):1245-1253. doi:10.1161/CIRCRESAHA.116.303630

47. Biswas S, Rao CM. Epigenetic tools (The Writers, The Readers and The Erasers) and their implications in cancer therapy. *Eur J Pharmacol*. 2018;837:8-24. doi:10.1016/j.ejphar.2018.08.021

48. Tyagi M, Imam N, Verma K, Patel AK. Chromatin remodelers: We are the drivers!! *Nucleus*. 2016;7(4):388-404. doi:10.1080/19491034.2016.1211217

49. Reyes AA, Marcum RD, He Y. Structure and Function of Chromatin Remodelers. *J Mol Biol*. 2021;433(14):166929. doi:10.1016/j.jmb.2021.166929

50. Clapier CR, Cairns BR. The Biology of Chromatin Remodeling Complexes. *Annu Rev Biochem*. 2009;78(1):273-304. doi:10.1146/annurev.biochem.77.062706.153223

51. Cairns BR, Kim YJ, Sayre MH, Laurent BC, Kornberg RD. A multisubunit complex containing the SWI1/ADR6, SWI2/SNF2, SWI3, SNF5, and SNF6 gene products isolated from yeast. *Proc Natl Acad Sci U S A*. 1994;91(5):1950-1954.

52. Stern M, Jensen R, Herskowitz I. Five SWI genes are required for expression of the HO gene in yeast. *J Mol Biol*. 1984;178(4):853-868. doi:10.1016/0022-2836(84)90315-2

53. Neigeborn L, Carlson M. Genes Affecting the Regulation of SUC2 Gene Expression by Glucose Repression in Saccharomyces Cerevisiae. *Genetics*. 1984;108(4):845-858. doi:10.1093/genetics/108.4.845

54. Hodges C, Kirkland JG, Crabtree GR. The Many Roles of BAF (mSWI/SNF) and PBAF Complexes in Cancer. *Cold Spring Harb Perspect Med*. 2016;6(8):a026930. doi:10.1101/cshperspect.a026930

55. Alfert A, Moreno N, Kerl K. The BAF complex in development and disease. *Epigenetics Chromatin*. 2019;12:19. doi:10.1186/s13072-019-0264-y

56. Chesi A, Staahl BT, Jovičić A, et al. Exome sequencing to identify de novo mutations in sporadic ALS trios. *Nat Neurosci*. 2013;16(7):851-855. doi:10.1038/nn.3412

57. Koga M, Ishiguro H, Yazaki S, et al. Involvement of SMARCA2/BRM in the SWI/SNF chromatin-remodeling complex in schizophrenia. *Hum Mol Genet*. 2009;18(13):2483-2494. doi:10.1093/hmg/ddp166

CHAPTER II: RESULTS

*This chapter is a partial reprint of our manuscript in progress. As a note, the manuscript here has not been formally peer-reviewed and may undergo revisions.

*Author contributions to the work presented in this chapter: Anthony Osuma – The work presented in figures 2.2, 2.4, 2.7, and supplementary figures 2.2 and 2.4 was completed as a technician in the Kratsios lab. All other work was completed as a graduate student in the Kratsios lab. Yinan Li – Provided data for figure 2.6 B-C. Manasa Prahlad – Assisted in building and imaging strains for figure 2.3 E and G. Laura Mathies – Provided *C. elegans* strains and reagents that were used for this research. Paschalis Kratsios – Principal investigator of the project.

The PBAF chromatin remodeling complex controls regional identity in *C. elegans* motor neurons

Anthony Osuma, Yinan Li, Manasa Prahlad, Laura Matthies, Paschalis Kratsios

2.1 Abstract

In the motor system, motor neurons (MNs) are organized topographically in the developing hindbrain and spinal cord. There exists a complex gene regulatory network of transcription factors, including the highly conserved HOX family of homeodomain proteins, which work together to specify MN regional identity (i.e. the unique combination of molecular features expressed in MNs across the same region). However, we know very little about the role chromatin factors play in determining MN regional identity. Here we show that the broadly expressed chromatin remodeler PBAF plays a distinct role in controlling MN regional identity in *C. elegans* MNs. We observe that PBAF represses the conserved glutamate receptor subunit *glr-4/GRIK4* in the nerve cord, while activating several MN identity genes in the posterior ganglion (*itr-1/ITPR1, avr-15/GLRA1-3, glr-5/GRIK1/3, ser-2/HTR1A*). Furthermore, we show that PBAF

repression of *glr-4* is cell-autonomous and occurs in specific MN subtypes (DA, VA, and AS). Finally, we identify another conserved transcription factor which represses *glr-4* in AS MNs of the nerve cord, *mab-9/TBX20*, suggesting that PBAF may be recruited to target loci by subtype-specific transcription factors. Altogether, our results demonstrate a novel role for PBAF in regulating regionally expressed genes critical for MN identity in specific MN subtypes.

2.2 Introduction

Motor systems are a fundamental facet of the nervous system, containing both central and peripheral structures which work together to coordinate locomotion. To generate this complex system, each of its individual functional units (neurons) must differentiate from a progenitor to a mature cell, attaining their unique molecular profiles in the process.

One key organizational feature of motor systems is the presence of topographical maps – there is an ordered relationship between the position of motor neurons (MNs) in the CNS and the muscle targets they innervate. For example, in humans, hindbrain MNs in rhombomere segments r1-r3 innervate muscles of the jaw, while MNs in r4 and r5 innervate face and eye muscles (Sanes et. al., 2012[1]). Similarly, lower MNs with cell bodies located in the lower cervical and brachial region of the spinal cord extend their axons to innervate muscles of the arms, while lower MNs with cell bodies in the lumbar region innervate leg muscles (Khan and Lui, 2023[2]). Thus, control over specific muscles in the periphery is directly linked to MN cell body position in hindbrain and spinal cord (Jessell et. al., 2011[3]).

In the mouse hindbrain, motor neurons are organized in nuclei – each nucleus contains a specific set of MNs that innervates distinct muscles of the head (Guthrie, 2007[4]). In the mouse spinal cord, MNs are organized into columns – each column contains a specific set of MNs that

innervates distinct muscle groups along the rostro-caudal body axis (Catela and Kratsios, 2021[5], Catela et. al., 2022[6]). For example, MNs of the lateral motor column (LMC) are generated in brachial and lumbar regions of the spinal cord and innervate limb muscles. Meanwhile, MNs of the medial motor column (MMC) are generated throughout cervical, brachial, thoracic, and lumbar regions of the spinal cord and innervate axial muscles (Stifani, 2014[7]). Seminal studies have shown that the topographic organization of MNs in the hindbrain and spinal cord can, at least to some extent, be defined by distinct molecular signatures. A specific set of highly conserved transcription factors, the HOX family of homeodomain proteins, are known to define the regional identity of developing MNs in the hindbrain and spinal cord (Hughes and Kaufman, 2002[8], Mallo et. al., 2010[9]). These factors are expressed in unique combinations along the rostro-caudal axis to confer regional identity to MN progenitors (Averof and Akam, 1995[10], Noden, 1991[11], Tumpel et. al., 2009[12]). For example, *Hox1-Hox4* (across all Hox clusters) are expressed primarily in the hindbrain and most rostral brachial MNs, while *Hox9-Hox11* have their expression restricted to lumbar and the most caudal thoracic MNs. Hox factors also work together with several other transcription factors to generate MN diversity. *Foxp1* expression, for example, is promoted only in the preganglionic motor column (PGC) and highly in the LMC and is necessary for the proper specification of these MNs (Dasen et. al, 2008[13], Rousso et. al., 2008[14]). These gene regulatory networks that which define MN regional identity are highly conserved, as similar codes have been found in both worms and flies. While much progress has been made in elucidating how the combinatorial expression of transcription factors generates these networks, we know very little about chromatin factors that define MN regional identity.

Here, we use the *C. elegans* motor system as a model to explore this fundamental problem. *C. elegans* contain 95 body wall muscles which are found on both the ventral and

dorsal sides along the entire length of the animal (Gieseler et. al., 2017[15]). These muscles are innervated by MNs located in three different regions: the ventral nerve cord and its two flanking ganglia. As in flies and mice, the regional identity of these MNs is at least in part defined by distinct Hox gene expression codes. Previous work has shown that HOX factors are not only continuously required to maintain MN identity, but they also cooperate with other transcription factors, such as UNC-3, sole ortholog of Collier/Olf/Ebf (COE), and UNC-30, sole ortholog of the PITX family transcription factors (Dubois and Vincent, 2001[16], Feng et. al., 2022[17]). Beyond these TF-based programs, whether and how chromatin factors control MN regional identity remains unclear.

To identify such factors in an unbiased manner, we performed a forward genetic screen. Using this approach, we identified one gene (*pbrm-1*) for which a single base pair substitution (C -> T nucleotide substitution causing a premature stop) was sufficient to result in loss of regional MN identity, and instead caused MNs to adopt a "mixed" MN identity. In other words, MNs properly expressed some, but not all, of the molecular features required for them to achieve their unique regional identity.

Curiously, our primary gene of interest, *pbrm-1*, is a critical component of the highly conserved chromatin remodeling complex polybromo-associated BRG1-associated factor (PBAF). PBAF belongs to the SWI/SNF family of remodelers, one of the four known families of chromatin remodelers (Clapier and Cairns, 2009[18]). SWI/SNF was originally discovered in yeast through independent genetic screens, in which mutations that affected multiple SWI/SNF subunits resulted in mating-type switching (SWI) and sucrose non-fermenting (SNF) phenotypes (Cairns et. al., 1994[19], Stern et. al., 1984[20], Neigeborn and Carlson, 1984[21]). PBAF is characterized by two distinguishing features: First is by its ATPase *swsn-4/BRG1*, which is

shared by PBAF and the closely related remodeler BRG1-associated factor (BAF). PBAF/BAF use ATP hydrolysis to weaken the contacts between histones and DNA, thereby allowing for restructuring of the nucleosome (Zhou et. al., 2016[22]). This in turn allows remodelers to regulate the conformation of chromatin (in the "closed" heterochromatin state or "open" euchromatin state) as well as have some level of control over the access of transcriptional machinery to their target binding sites on DNA. Second is by its highly conserved bromodomains, which serve to recognize acetylated lysine residues on histone tails, critical for its function as a reader of histone post-translational modifications (Zeng and Zhou, 2002[23]).

PBAF/BAF mutations have also been implicated in several disease states, largely within the context of cancer. It has been previously reported that up to 20% of human cancers show mutations in the BAF remodeling complex (Alfert et. al., 2019[24]). Additionally, mutations in the PBAF/BAF remodelers have been linked to several neurodevelopmental disorders such as Coffin-Siris syndrome, Nicolaides-Baraitser syndrome, Kleeftra's syndrome, and autism spectrum disorders. However, the extent of PBAFs/BAFs role in the developing nervous system remains largely unclear.

Here, we describe a unique role for the PBAF chromatin remodeler as a key regulator of MN regional identity in two ways. We find that, despite its broad expression pattern, PBAF is required to repress glutamate receptor *glr-4/GRIK4* in the VNC, while it is also required to activate calcium channel and chloride channel subunits *itr-1/ITPR1* and *avr-15/GLRA1-3* (among others) in the posterior tail region. The findings of this research are significant for several reasons: First, we describe a novel role for PBAF chromatin remodeler as a regulator of regional MN identity in post-mitotic MNs. Second, despite its broad expression pattern and the fact that chromatin remodelers are not typically known to bind DNA in a sequence specific manner

(Sudarsanam and Winston, 2000[25], Yu et. al., 2013[26]), we observe PBAFs ability to regulate gene expression in specific subtypes of MNs across regions, indicating that PBAF may be recruited by subtype specific transcription factors to its target sites as well as highlighting the diversity of ways in which chromatin remodelers may regulate transcription. Finally, these findings have functional disease relevance as PBAF/BAF mutations have been directly linked to several neurodevelopmental disorders.

2.3 Results

2.3.1 An unbiased genetic screen for *C. elegans* mutants with defects in regional motor neuron identity

To study how post-mitotic MNs of different regions acquire their unique molecular identity, we leverage the topographic organization of the *C. elegans* motor system, which contains nine MN classes in hermaphrodites: (a) Neurons of the SAB class are specifically located at a ganglion close to the head (retrovesicular ganglion [RVG]) and innervate head muscles (**Fig. 2.1a**). (b) egg-laying MNs of the VC class are only found in the ventral nerve cord and innervate vulva muscles. (c) MNs of the remaining seven classes (AS, DA, DB, DD, VA, VB, and VD) innervate body wall muscles and are essential for locomotion. Individual MNs of all these classes (except SAB) intermingle along the nerve cord and its flanking ganglia (RVG, PAG) (**Fig. 2.1a**).

To identify factors critical for regional MN identity in an unbiased manner, we conducted a forward genetic screen on animals carrying a red fluorescent reporter (*tagRFP*) for *glr-4*, ortholog of human *GRIK4 (glutamate receptor, ionotropic, kainite 4)* (**Fig. 2.2a**) (Li et. al.,

2023[27]). Expression of *glr-4*^{prom}*::tagRFP* is region-specific: the SAB neurons in the anterior ganglia (RVG) and the DA9 neuron in the posterior ganglia (PAG) strongly express

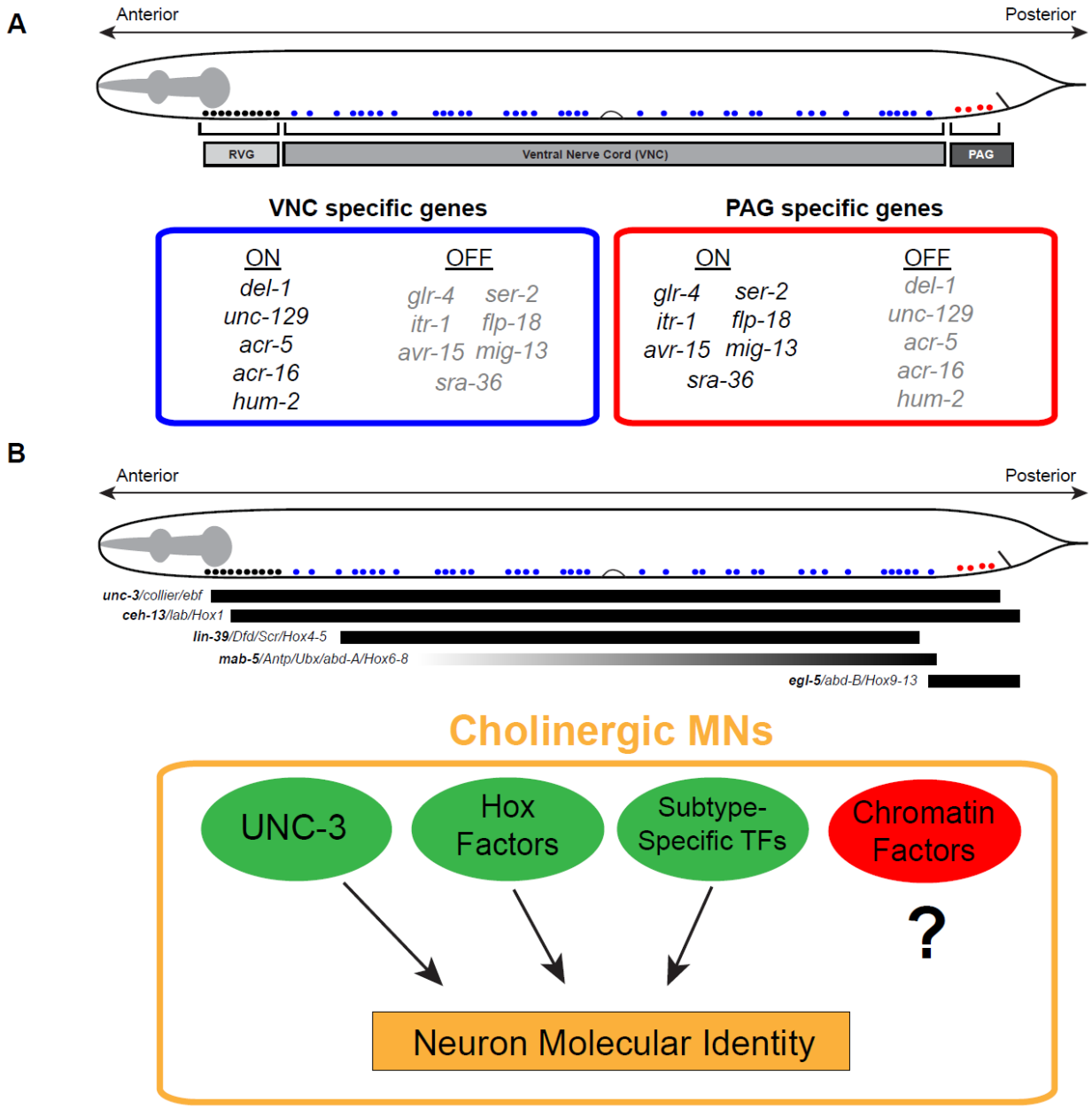

Figure 2.1. *C. elegans* cholinergic MNs belong to distinct regions and vary in their terminal identity gene expression

(A) Schematic of C. elegans MNs divided by region (top) - retrovesicular ganglion (RVG), ventral nerve cord (VNC), preanal ganglion (PAG). Known terminal identity genes expressed in VNC or PAG only (bottom).

Figure 2.1 cont.
(B) Schematic for regionally restricted expression of UNC-3 and hox genes (top). Little is known about chromatin factor involvement in MN regional identity (bottom).

glr-4^{prom}::tagRFP, but only 1-2 MNs along the nerve cord express this reporter. Following random ethyl methanesulfonate (EMS) mutagenesis of the P0 generation, we screened F2 progeny for mutants displaying altered *glr-4^{prom}::tagRFP* expression at larval stage 4 (L4) (**Fig. 2.2a**). We retrieved one mutant strain (carrying the mutation *ot792*) showing region-specific effects in MNs: *glr-4^{prom}::tagRFP* expression was unaffected in anterior SAB and posterior DA9 neurons, but strong expression was observed in MNs of the nerve cord (11.6 ± 2.2 cells in *ot792* mutant animals versus 0.6 ± 0.9 cells in control animals, $p < .0001$) (**Fig 2.2b-e**). We obtained similar results with an endogenous *glr-4::mScarlet* reporter (**Suppl. Fig. 2.1c, d**) (Li et. al., 2023[27]). Hence, *ot792* mutants display ectopic *glr-4* expression only in nerve cord MNs, suggesting regional MN identity is affected in these animals.

2.3.2 *pbrm-1/PBRM1* selectively represses *glr-4/GRIK4* expression in motor neurons of the ventral nerve cord

Upon single nucleotide polymorphism (SNP) mapping and whole genome sequencing, we identified the molecular lesion in *ot792* mutants: a C -> T nucleotide substitution (7,115 bp from ATG) generates a premature stop (TAG, amber) codon in the 12th exon of *pbrm-1*, ortholog of human polybromo 1 (PBRM1/BAF180), likely affecting all *pbrm-1* isoforms (**Fig 2.2e**). We also

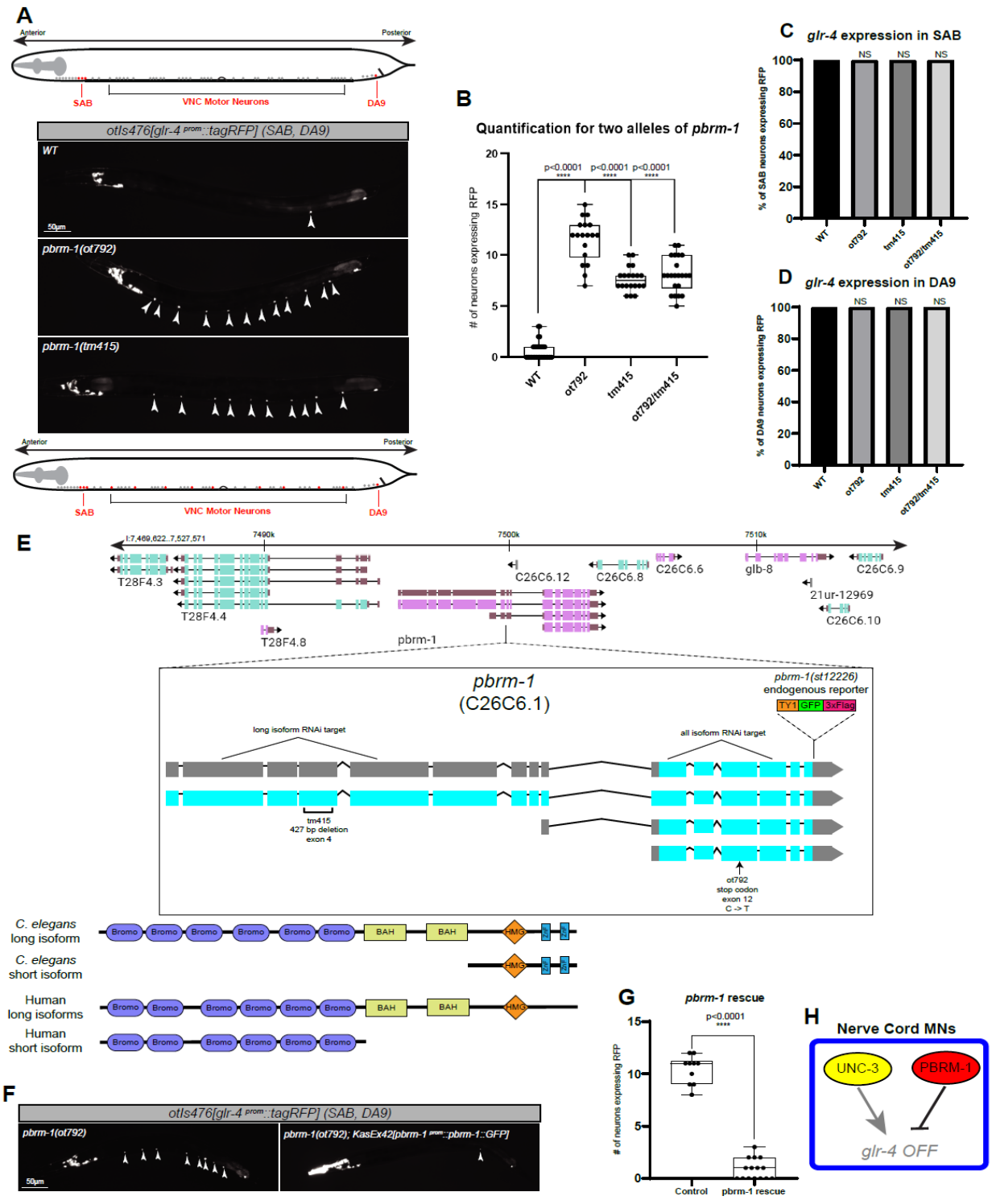

Figure 2.2. *pbrm-1/PBRM1* selectively represses *glr-4/GRIK4* expression VNC MNs

(A) Expression of *glr-4*^{prom}*::tagRFP* in VNC MNs (white arrowheads). *pbrm-1* mutants show ectopic expression of *glr-4* in the VNC. Worm schematics represent *glr-4*^{prom}*::tagRFP* expression in WT (top) and *pbrm-1* mutant (bottom) animals.

Figure 2.2 cont.
(B-D) Quantification of **A** showing number of MNs expressing *glr-4* in VNC (C), RVG (D), and PAG (E). Animals imaged at L4 stage. WT n=35; *ot792* n=18; *tm415* n=20; *ot792/tm415* n=22. Unpaired Welch's t-test, p<.05 = *; p<.01 = **; p<.001 = ***; p<.0001 = ****.

(E) Diagram of the *pbrm-1* gene locus in *C. elegans* with the location of two mutant alleles, two RNAi targets, and one endogenous reporter. used in our analysis (top). Protein domains of PBRM-1 long and short isoforms in *C. elegans* and humans (bottom), which include bromodomains, bromo-adjacent homology (BAH) domains, high mobility group (HMG) box domains, and zinc finger (Znf) domains.

(F) *pbrm-1(ot792)* animals injected with *pbrm-1^{prom}::pbrm-1::GFP* show near complete rescue of the WT phenotype.

(G) Quantification of **F** showing number of MNs expressing *glr-4* in VNC. Animals imaged at L4 stage. Control n=10; *pbrm-1* rescue n=15. Unpaired Welch's t-test, p<.05 = *; p<.01 = **; p<.001 = ***; p<.0001 = ****.

(H) Schematic of PBRM-1 and UNC-3 effects on *glr-4* in the VNC.

used an independent *pbrm-1* allele *(tm415)*, and again observed similar, albeit weaker, region-specific effects on *glr-4^{prom}::tagRFP* compared to *pbrm-1(ot792)* animals (**Fig 2.2b-e**). The *tm415* allele contains a 427 nucleotide-long deletion in the 4th *pbrm-1* exon, selectively affecting the long, but not the short, *pbrm-1* isoforms (**Fig 2.2e**). Thus, the stronger *glr-4^{prom}::tagRFP* phenotype of *pbrm-1(ot792)* mutants compared to *pbrm-1(tm415)* is likely due to *ot792* affecting all *pbrm-1* isoforms.

Further, complementation testing showed that transheterozygote animals carrying both alleles (*ot792* and *tm415*) also displayed ectopic expression of *glr-4* in nerve cord MNs (7.7 ± 1.2 cells, p < .0001), indicating *pbrm-1* gene activity is necessary to repress *glr-4* (**Fig. 2.2b**). Finally, transgenic supply of *pbrm-1* cDNA with its endogenous promoter (*pbrm-1^{prom}::pbrm-1 cDNA*) completely rescued the *glr-4* phenotype in *pbrm-1(ot792)* mutants (**Fig. 2.2f, g**).

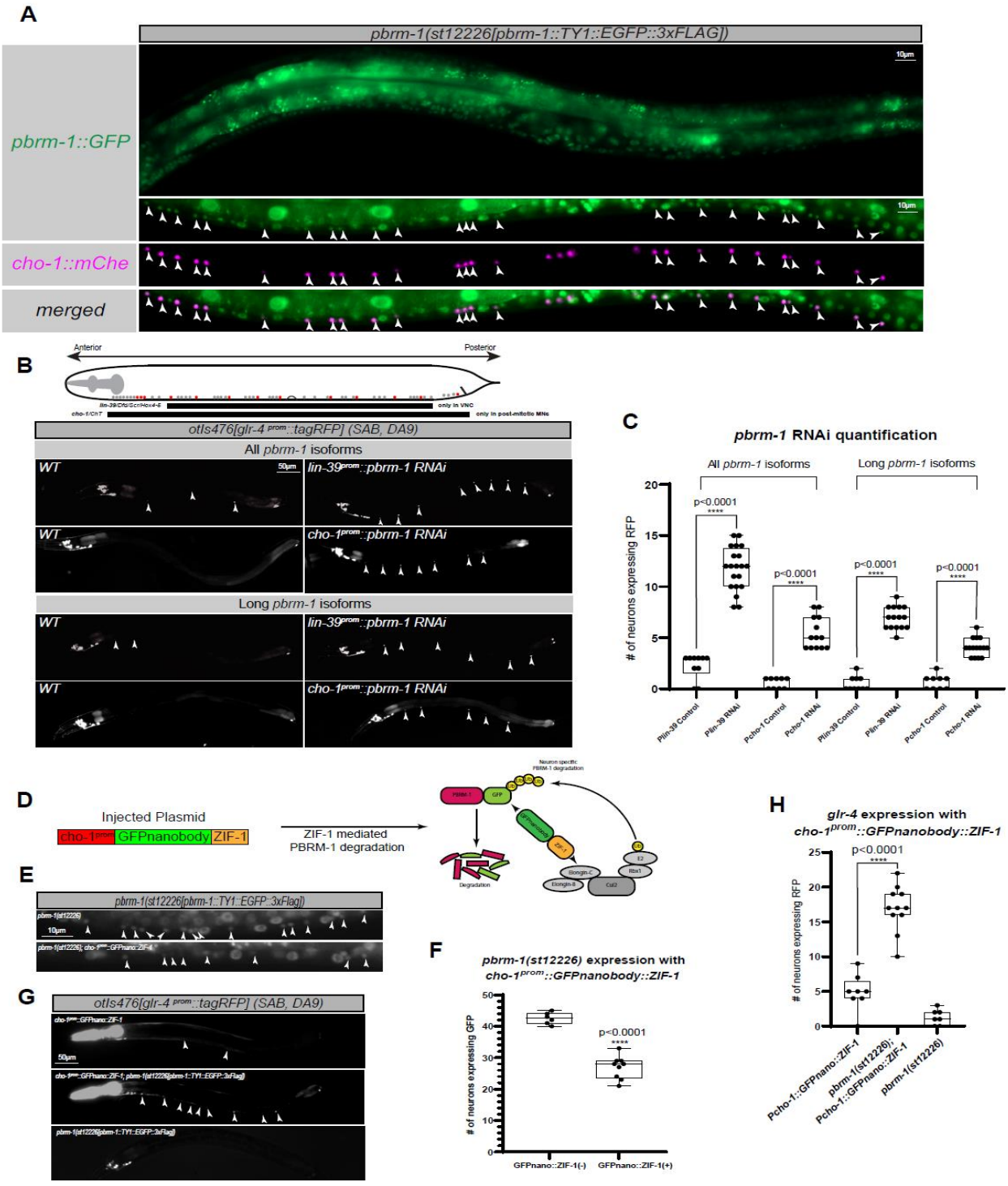

Figure 2.3. Cell-autonomous *pbrm-1/PBRM1* activity in post-mitotic MNs is required to repress *glr-4/GRIK4* in the VNC

(A) *pbrm-1::TY1::EGFP::3xFlag* endogenous reporter overlayed with cholinergic MN marker *cho-1*. Merged image reveals *pbrm-1* is expressed broadly and in cholinergic MNs (white arrowheads). Animals imaged at L4 stage.

Figure 2.3 cont.
(B) *pbrm-1* RNAi using *lin-39* and *cho-1* promoters, targeting long (top) and all (bottom) *pbrm-1* isoforms.

(C) Quantification of **B** showing number of MNs expressing *glr-4* in VNC. Knock-down animals recapitulate the mutant phenotype. Animals imaged at L4 stage. All isoform knock-down: *Plin-39* control n=10; *Plin-39* RNAi n=20; *Pcho-1* control n=9; *Pcho-1* RNAi n=13. Long isoform knock-down: *Plin-39* control n=10; *Plin-39* RNAi n=15; *Pcho-1* control n=9; *Pcho-1* RNAi n=15. Unpaired Welch's t-test, p<.05 = *; p<.01 = **; p<.001 = ***; p<.0001 = ****.

(D) Schematic of the microinjected plasmid (left), along with a cartoon depicting *GFPnanobody::ZIF-1* recruitment of E3 ubiquitin ligase complex, targeting GFP fused proteins for degradation (right).

(E) *PBRM-1::GFP* expression without (top) and with (bottom) *cho-1prom::GFPnano::ZIF-1*. Animals with the injected plasmid show *PBRM-1::GFP* depletion.

(F) Quantification of **E** showing number of MNs expressing *pbrm-1* in VNC. Animals imaged at L4 stage. *GFPnano::ZIF-1*(-) n=7; *GFPnano::ZIF-1*(+) n=8. Unpaired Welch's t-test, p<.05 = *; p<.01 = **; p<.001 = ***; p<.0001 = ****.

(**G**) Images show *glr-4* expression in 3 backgrounds: *cho-1^{prom}::GFPnano::ZIF-1* (top), *pbrm-1::TY1::EGFP::3xFlag* (bottom), and *cho-1^{prom}::GFPnano::ZIF-1*; *pbrm-1::TY1::EGFP::3xFlag* (middle).

(H) Quantification of **G** showing number of MNs expressing *glr-4* in VNC. Animals imaged at L4 stage. *Pcho-1::GFPnano::ZIF-1* n=8; *pbrm-1(st12226)*; *Pcho-1::GFPnano::ZIF-1* n=11; pbrm-1(12226) n=8. Unpaired Welch's t-test, p<.05 = *; p<.01 = **; p<.001 = ***; p<.0001 = ****.

Altogether, our genetic screen identified *pbrm-1* (PBRM1/BAF180) as a negative regulator of *glr-4* expression specifically in nerve cord MNs, pinpointing its involvement in regional MN identity.

2.3.3 *pbrm-1/PBRM1* activity in post-mitotic motor neurons is necessary to repress *glr-4/GRIK4*

To assess the expression pattern of *pbrm-1*, we obtained an available endogenous reporter (*pbrm-1::TY1::EGFP::3xFlag*). We observed that *pbrm-1::TY1::EGFP::3xFlag* is broadly

expressed in most (if not all) *C. elegans* neurons and other cell types (**Fig. 2.3a**). Its broad expression suggests that *pbrm-1* could act in post-mitotic MNs to control *glr-4* expression and/or in other cells to indirectly influence *glr-4* expression in MNs. To distinguish between these alternatives, we conducted MN-specific RNAi (Esposito et. al., 2007[28]). We used two *cis*-regulatory elements, *lin-39* (Feng et. al., 2022[29]) and *cho-1* (Kratsios et. al., 2011[30]), known to drive expression in post-mitotic MNs of the *C. elegans* nerve cord. RNAi against all *pbrm-1* isoforms and RNAi selectively targeting the long *pbrm-1* isoforms – using either the *lin-39* or *cho-1* elements – both resulted in ectopic *glr-4* expression in nerve cord MNs (**Fig. 2.2e, 2.3b-c**). We saw that RNAi targeting all *pbrm-1* isoforms using the *lin-39* regulatory element resulted in a phenotype similar to that of *ot792* mutants (11.75 ± 2.1 cells, $p < .0001$). RNAi selectively targeting the long isoforms of *pbrm-1* showed reduced *glr-4* expression in the nerve cord by comparison (~5-7 cells). We conclude that both long and short *pbrm-1* isoforms are necessary in post-mitotic MNs to repress *glr-4*. As the short *pbrm-1* isoforms contain only high mobility group (HMG) and zinc finger protein domains, and not the bromodomains and bromo-adjacent homology (BAH) domains present in the long isoforms (**Fig. 2.2e**), we suspect that each of these protein domains may be necessary for efficient *glr-4* repression.

To further address cell-autonomy, we used ZIF-1-mediated protein degradation to selectively deplete PBRM-1 in post-mitotic MNs (Wang et. al., 2017[31])(**Fig. 2.3d**). First, we generated transgenic animals expressing a GFP nanobody fused to ZIF-1 under the control of a MN-specific element (*cho-1^{element}::GFPnanobody::ZIF-1*). Next, we crossed these animals into an endogenously tagged *pbrm-1* reporter allele *(st12226)*.

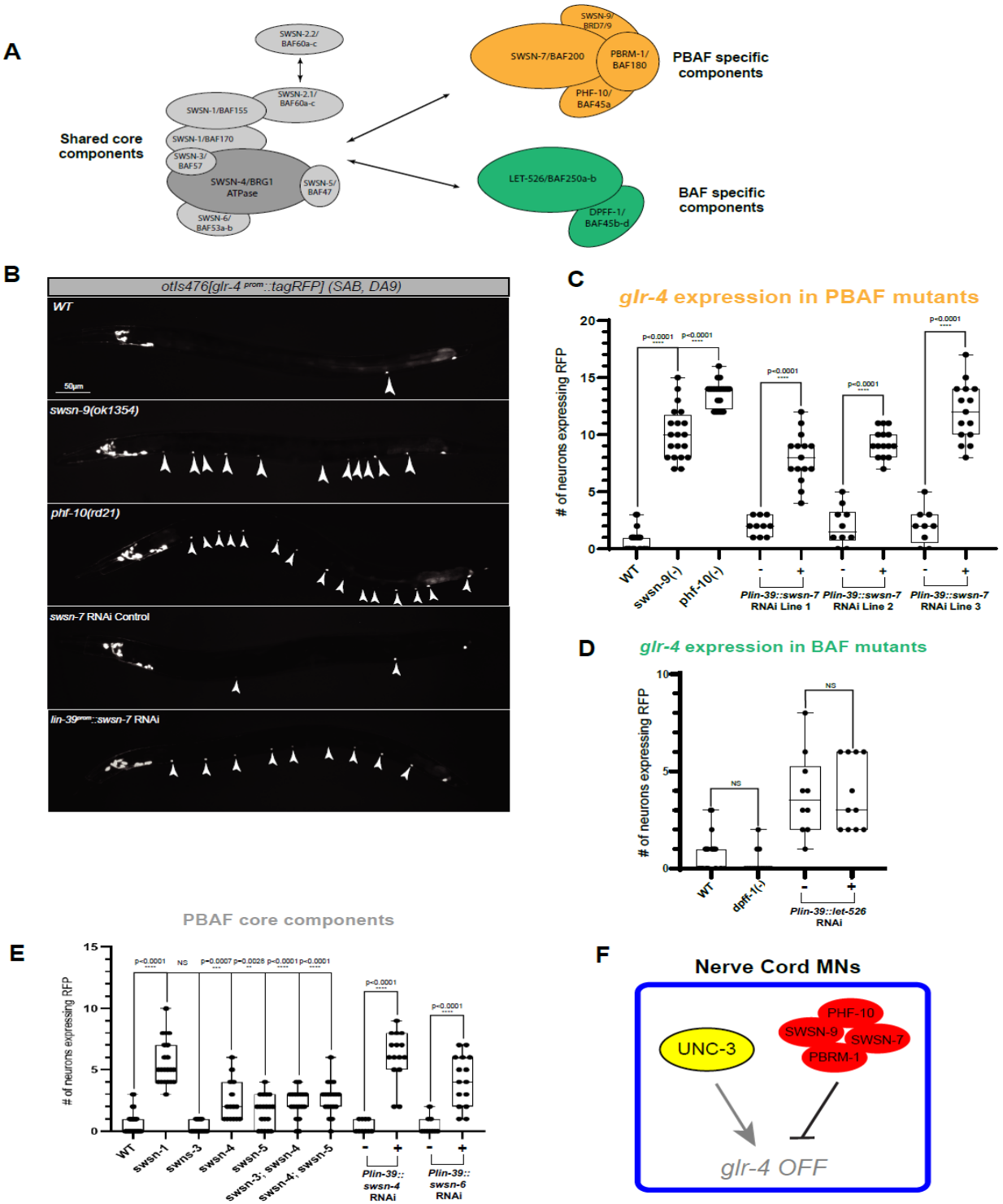

Figure 2.4. All PBAF-specific subunits repress *glr-4/GRIK4* in VNC MNs

(A) Cartoon of the BAF and PBAF chromatin remodeling complexes. Complexes share a core ATPase (dark gray) and its accessory components (light gray), with BAF specific subunits (green) and PBAF specific subunits (orange).

Figure 2.4 cont.
(B) *glr-4* expression in mutants for PBAF specific subunits *swsn-9*, *phf-10*, and *swsn-7* (RNAi).

(C) Quantification of PBAF mutants showing number of MNs expressing *glr-4* in VNC. Animals imaged at L4 stage. WT n=35; *swsn-9(-)* n=20; *phf-10(-)* n=20; *Plin-39::swsn-7* RNAi Line 1 (-) n=10, (+) n=15; *Plin-39::swsn-7* RNAi Line 2 (-) n=10, (+) n=15; *Plin-39::swsn-7* RNAi Line 3 (-) n=9, (+) n=15. Unpaired Welch's t-test, p<.05 = *; p<.01 = **; p<.001 = ***; p<.0001 = ****.

(D) Quantification of BAF mutants (*dpff-1, let-526* RNAi) showing number of MNs expressing *glr-4* in VNC. Animals imaged at L4 stage. WT n=35; *dpff-1* n=15; *Plin-39::let-526* RNAi (-) n=10, (+) n=11. Unpaired Welch's t-test, p<.05 = *; p<.01 = **; p<.001 = ***; p<.0001 = ****.

(E) Quantification of PBAF/BAF core component mutants (*swsn-1*, *swsn-3*, *swsn-4*, *swsn-5*, *swsn-3;swsn-4*, *swsn-4;swsn-5*, *swsn-4* RNAi, *swsn-6* RNAi) showing number of MNs expressing *glr-4* in VNC. Animals imaged at L4 stage. WT n=35; *swsn-1* n=21; *swsn-3* n=20; *swsn-4* n=15; *swsn-5* n=19; *swsn-3; swsn-4* n=19; *swsn-4; swsn-5* n=19; *Plin-39::swsn-4* RNAi (-) n=10, (+) n=15; *Plin-39::swsn-6* RNAi (-) n=10, (+) n=15. Unpaired Welch's t-test, p<.05 = *; p<.01 = **; p<.001 = ***; p<.0001 = ****.

(F) Schematic showing UNC-3 and PBAF effect on *glr-4* in the VNC.

We observed efficient PBRM-1::GFP degradation in nerve cord MNs, accompanied by ectopic *glr-4* expression (**Fig. 2.3e-h**). Altogether, our MN-specific RNAi and protein degradation experiments demonstrate a cell-autonomous role for PBRM-1 in post-mitotic MNs.

2.3.4 Essential roles for all PBAF-specific subunits in *glr-4/GRIK4* repression

PBRM-1/BAF180 is a key component of the highly conserved SWI/SNF (SWItch/Sucrose Non-Fermentable) ATP-dependent chromatin remodeling complex PBAF (Polybromo, BRG1-Associated Factor) (Hodges et. al., 2016[32]). This remodeler is comprised of four PBAF-specific subunits (PBRM-1/BAF180, SWSN-9/BRD7/9, SWSN-7/BAF200, and PHF-10/BAF45a), as well as a core set of proteins (SWSN-1/BAF155/170, SWSN-2/BAF60a-c, SWSN-3/BAF57, SWSN-4/BRG1, SWSN-5/BAF47, and SWSN-6/BAF53a-b) that are shared

with the highly related chromatin remodeler BAF (**Fig. 2.4a**). Through ATP hydrolysis, the PBAF and BAF complexes facilitate the ejection, sliding, and/or swapping of nucleosomes, thereby altering the state of chromatin to affect gene transcription in a positive or negative manner (Johnson et. al., 2005[33]).

To elucidate whether the effect on *glr-4* expression in nerve cord MNs is specific to *pbrm-1* or the PBAF complex as a whole, we first tested the three remaining PBAF-specific components (SWSN-9, SWSN-7, PHF-10). Similar to *pbrm-1* mutants, homozygous animals carrying loss-of-function alleles of *swsn-9(ok1354)* or *phf-10(rd21)* (Mathies et. al., 2022[34]) displayed ectopic *glr-4* expression in nerve cord MNs (**Fig. 2.4b, c**). Because null mutant animals for *swsn-7* are embryonic lethal (Large and Mathies, 2014[35]) and thereby do not allow evaluation of *glr-4* expression at L4, we conducted MN-specific RNAi against *swsn-7* and again observed the *glr-4* expression phenotype, similar to *pbrm-1*, *swsn-9,* and *phf-10* mutants (**Fig. 2.4b, c**). Hence, each PBAF-specific component is required for proper *glr-4* expression in nerve cord MNs.

Next, we conducted a similar analysis for five core subunits of PBAF (SWSN-1, SWSN-3, SWSN-4, SWSN-5, SWSN-6) using available mutant alleles or MN-specific RNAi. We observed ectopic *glr-4* expression in nerve cord MNs of *swsn-1* and *swsn-5* single mutants (but not *swsn-3* mutants), as well as in MN-specific RNAi against *swsn-6* (**Fig. 2.4e, Suppl. Fig. 2.4a**). In all these cases, *glr-4* is ectopically expressed in fewer MNs when compared to PBAF-specific mutants, indicating possible redundancy between these core subunits. We then focused on the ATPase *swsn-4/BRG1,* the "molecular engine" of the PBAF complex (Centore et. al., 2020[36]). Because homozygous animals for a null *swsn-4* allele are embryonic lethal (Large and Mathies, 2014[35]), we assayed ectopic *glr-4* expression in both hypomorphic *swsn-4(os13)*

mutants and in animals with MN-specific RNAi. In both cases, we observed ectopic expression of *glr-4* in nerve cord MNs. Of note, analysis of *swsn-3(tm3647); swsn-4(os13)* and *swsn-4(os13); swsn-5(ok622)* double mutants did not exacerbate the *glr-4* expression phenotype (**Fig. 2.4e**).

Lastly, we repeated the analysis for both BAF-specific components (DPFF-1/BAF45b-d and LET-526/BAF250a-b) (**Fig. 2.4a**). A mutant allele *dpff-1(tm4287)* (318 nucleotide deletion) was used while MN specific RNAi was again utilized targeting *let-526*. Disruption of either BAF-specific component showed no effect on *glr-4* expression (**Fig. 2.4d, Suppl. Fig. 2.4b**). Thus, we conclude that *glr-4* is negatively regulated in post-mitotic MNs by the PBAF complex, but not by BAF.

2.3.5 PBAF represses *glr-4/GRIK4* in specific classes of nerve cord motor neurons

Fifty-eight MNs from eight different classes (DA2-7 + DB3-7 + VA2-11 + VB3-11 + AS2-10 + VC1-6 + DD2-5 + VD3-11 = 58) populate the *C. elegans* nerve cord in hermaphrodites. Our genetic analysis with PBAF-specific mutants showed that up to 14 +\- 1 (mean +\- STDV) nerve cord MNs ectopically express *glr-4*^{prom}*::tagRFP*. Using a combination of criteria (stereotypic cell body position of MNs, birth order, and fluorescent reporters for specific MN classes), we determined with single-cell resolution that ectopic *glr-4* expression in all PBAF-specific mutants (*pbrm-1, phf-10, swsn-9*) selectively occurs in cholinergic MNs of the DA, VA, and AS classes (**Fig. 2.5a**). Specifically, ectopic *glr-4* expression occurs consistently in DA6, VA2, and in neurons of the AS class with cell bodies in the VNC (AS2-10).

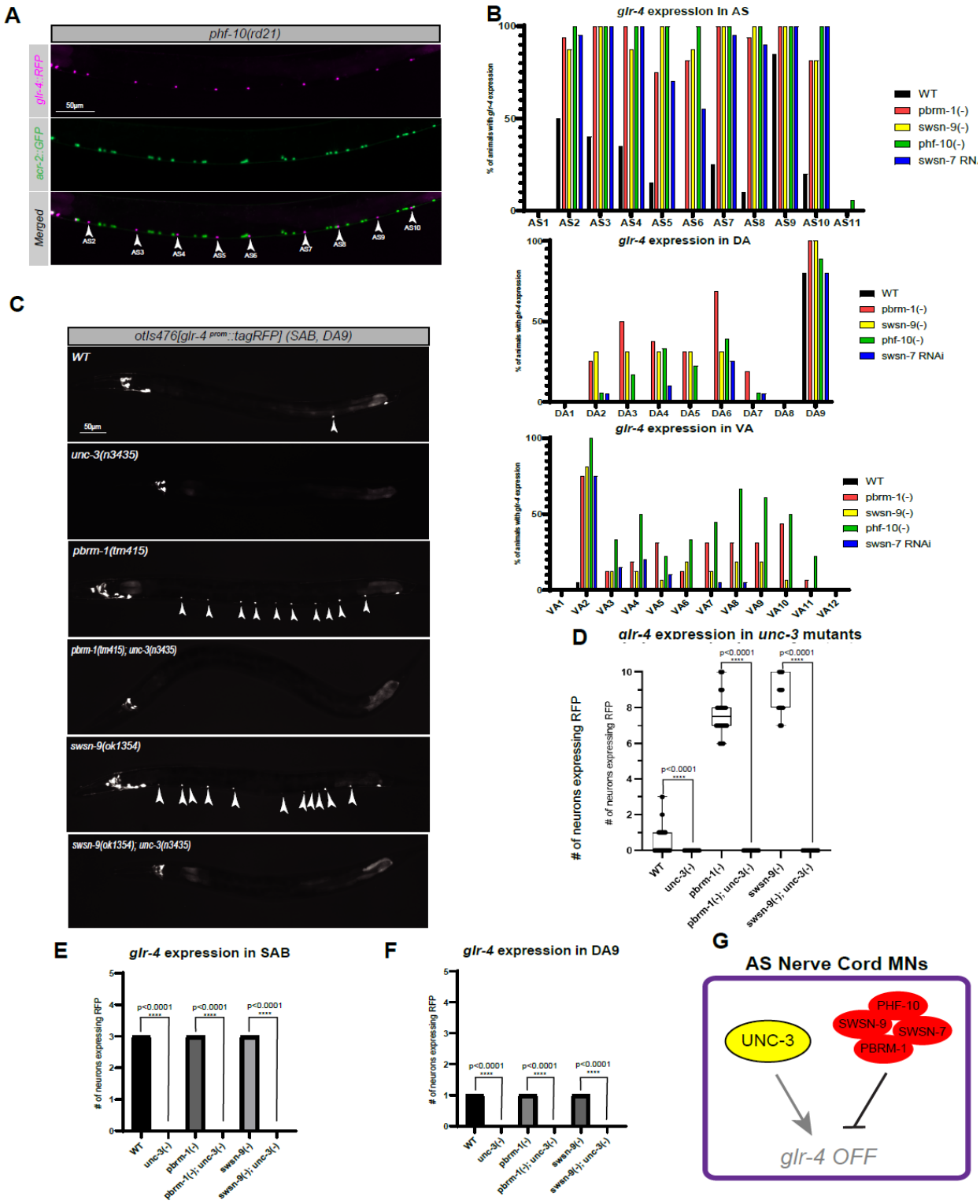

Figure 2.5. PBAF represses *glr-4/GRIK4* in AS, DA, and VA nerve cord MNs

(A) Single-cell analysis for *phf-10(rd21)* mutant animals. AS MNs shown with white arrowheads. Animals imaged at L4 stage.

Figure 2.5 cont.
(B) Results of single-cell analysis shown in **A** for all PBAF mutants. *glr-4* expression is affected in AS (top), DA (middle), and VA (bottom) neurons only in the VNC, not the RVG or PAG.

(C) *glr-4* expression in *unc-3* and *unc-3*/PBAF double mutants. *glr-4* expression is lost completely in RVG, VNC, and PAG MNs in all *unc-3* mutants.

(D-F) Quantification of **C** showing number of MNs expressing *glr-4* in RVG (**D**), VNC (**E**), and PAG (**F**). Animals imaged at L4 stage. WT n=35; *unc-3(-)* n=15; *pbrm-1(-)* n=20; *pbrm-1(-); unc-3(-)* n=15; *swsn-9(-)* n=20; *swsn-9(-); unc-3(-)* n=10. Unpaired Welch's t-test, p<.05 = *; p<.01 = **; p<.001 = ***; p<.0001 = ****.

(G) Schematic showing UNC-3 and PBAF effect on *glr-4* in AS MNs in the VNC.

Of note, we also observed differential effects in animals carrying PBAF mutant alleles. For example, multiple DA neurons (DA2-6) express *glr-4* only in *swsn-9* mutants. Multiple VA neurons (VA5-VA10) express *glr-4* only in *pbrm-1* and *phf-10* mutants (**Fig. 2.5b**). We conclude that the PBAF complex, despite being broadly expressed (**Fig. 2.3a, Suppl. Fig. 2.3**), selectively represses *glr-4* in specific subsets of nerve cord MNs.

2.3.6 The PBAF complex antagonizes the transcription factor UNC-3/Ebf in nerve cord motor neurons

Our lab has previously shown that the transcription factor UNC-3, sole ortholog of the Collier/Olf/Ebf (COE) family of transcription factors, acts as a terminal selector for cholinergic MN differentiation in *C. elegans* (Kratsios et. al., 2011[30]). Specifically, UNC-3 binds to and directly activates a plethora of effector target genes (including *glr-4*) in various classes of cholinergic MNs; *glr-4^{prom}::tagRFP* is robustly expressed in SAB neurons (anterior to VNC) and DA9 (posterior to VNC), and only weakly in 1-2 MNs along the nerve cord. This expression is completely lost in *unc-3* mutant animals (**Fig. 2.5c-f**), consistent with the previously documented

role of UNC-3 as transcriptional activator (Liberg et. al., 2002[37]). Thus, we hypothesized that *unc-3* is necessary for the ectopic *glr-4* expression in nerve cord MNs of PBAF mutants. Through double mutant analysis, we found that *glr-4* expression in nerve cord MNs is completely lost in p*brm-1(-); unc-3(-)* and *swsn-9(-); unc-3(-)* animals (**Fig. 2.5c-f**). These data suggest that the PBAF complex represses *glr-4* in nerve cord MNs by antagonizing the transcriptional activator UNC-3.

2.3.7 PBAF may act directly to repress *glr-4* transcription in nerve cord motor neurons

PBAF repression of *glr-4* is further evidenced by available ChIP-seq data via the ENCODE project (ENCODE Project Consortium[38]). ChIP-seq has been performed for both PBRM-1 and SWSN-7 in young adult and L1 stage animals respectively. In both cases, we observe binding of PBAF components to the *glr-4* locus (**Fig. 2.6g**), suggesting that PBAF directly represses *glr-4*. ChIP-seq data sets for PBAF core components in C. elegans was unavailable. We have also previously shown that UNC-3 directly binds upstream of the *glr-4* locus (Li et. al., 2020[39]), and that deletion of UNC-3 binding sites results in total loss of *glr-4* expression in SAB, VNC, and DA9 (Kratsios et. al., 2015[40]). However, as ChIP-seq for PBAF components was performed on whole animals, it remains unclear whether or not PBAF directly binds to the *glr-4* locus in nerve cord motor neurons.

2.3.8 MAB-9/Tbx20 represses *glr-4* in AS motor neurons in the nerve cord

The specificity of the observed effects PBAF has on *glr-4* in distinct classes (DA, VA,

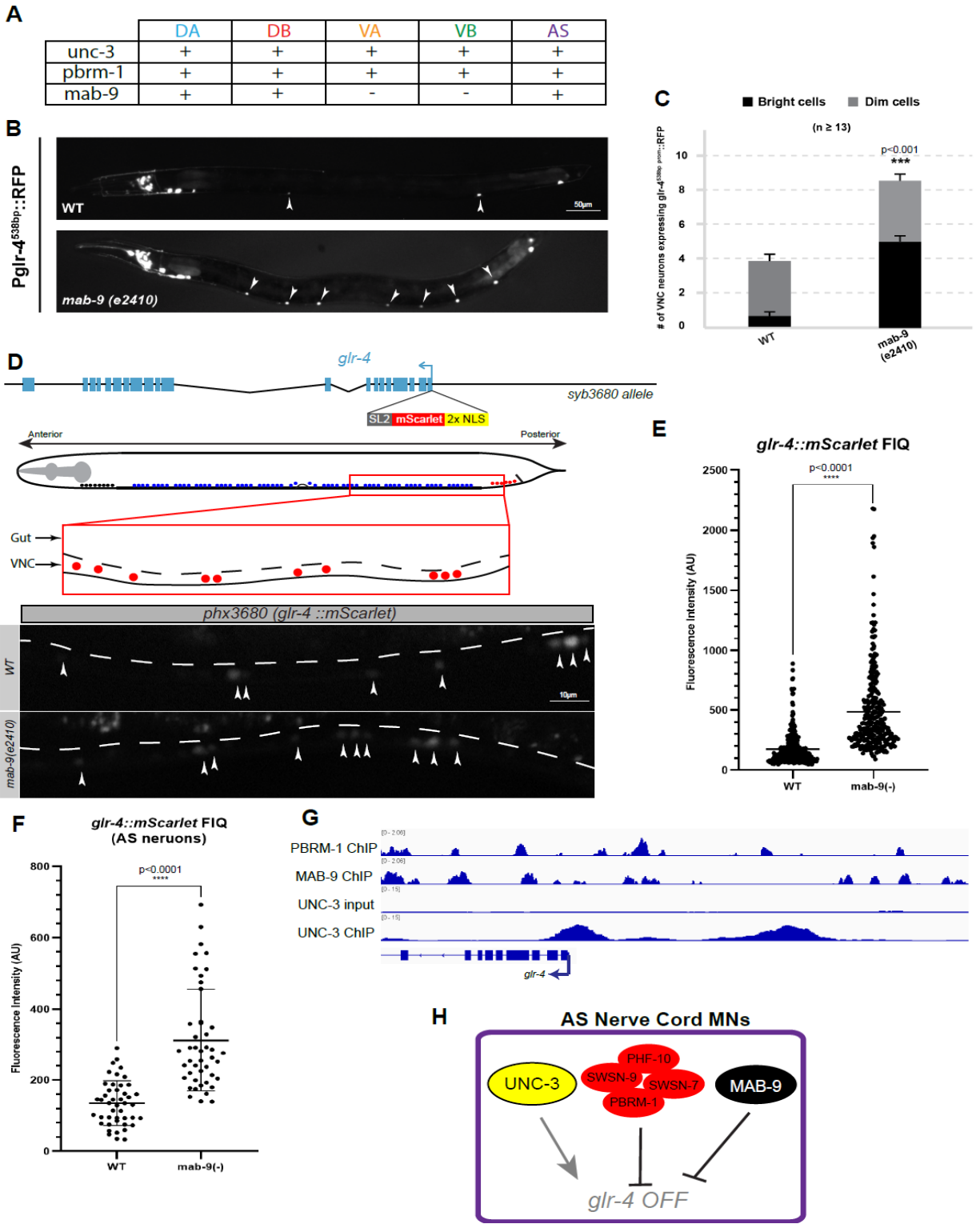

Figure 2.6. MAB-9/Tbx20 represses *glr-4/GRIK4* in AS motor neurons in the nerve cord

(A) Expression of *unc-3*, *pbrm-1*, and *mab-9* in cholinergic MN subtypes (DA, DB, VA, VB, AS).

Figure 2.6 cont.
(B) *glr-4* expression in WT and *mab-9(e2410)* mutant animals. *mab-9* mutants display ectopic expression of *glr-4* in the VNC.

(C) Quantification of **B** showing number of MNs expressing *glr-4* in VNC. Animals imaged at L4 stage. Unpaired Welch's t-test, p<.05 = *; p<.01 = **; p<.001 = ***.

(D) Diagram of endogenous *glr-4* reporter used in our analysis (top). Schematic of MNs in C. elegans VNC (middle). *glr-4* expressing neurons are indicated with white arrowheads (bottom).

(E) Graph showing the quantified fluorescence intenisty as a proxy for expression levels of *glr-4* in MNs of WT and *mab-9(e2410)* mutant animals. Animals imaged at L4 stage. WT n=271 (MNs); *mab-9(-)* n=293 (MNs). Unpaired Welch's t-test, p<.05 = *; p<.01 = **; p<.001 = ***; p<.0001 = ****.

(F) Graph showing the quantified fluorescence intenisty as a proxy for expression levels of *glr-4* in AS MNs of WT and *mab-9(e2410)* mutant animals. Animals imaged at L4 stage. WT n=45 (AS MNs); *mab-9(-)* n=45 (AS MNs). Unpaired Welch's t-test, p<.05 = *; p<.01 = **; p<.001 = ***; p<.0001 = ****.

(G) ChIP-seq tracks for PBRM-1, MAB-9, and UNC-3 showing binding at the *glr-4* locus. PBRM-1 and MAB-9 tracks are represented as fold change over control and using a log scale. ChIP-seq for PBRM-1 and MAB-9 were performed at the L1 stage. ChIP-seq for UNC-3 was performed at the L2 stage.

(H) Schematic showing UNC-3, PBAF, and MAB-9 effect on *glr-4* in AS MNs in the VNC.

AS) of nerve cord MNs is striking, given that PBAF subunit-encoding genes (*pbrm-1, swsn-7, swsn-9, phf-10*) are broadly expressed in neurons and other *C. elegans* cell types. What is the molecular basis for this specificity? We hypothesized that, in DA, VA, and AS neurons, transcription factors with repressor activity first recognize specific DNA sequences at the *glr-4* locus and subsequently recruit the PBAF complex to the locus. Supporting this hypothesis, it has been previously shown in oligodendrocyte precursor cells that SWI/SNF complexes can be recruited to their target genes by specific transcription factors (Yu et. al., 2013[41]).

To test this hypothesis, we focused on *mab-9* (ortholog of human Tbx20) because: (a) it is expressed in DA and AS neurons – two MN classes that show ectopic *glr-4* expression in

PBAF mutant animals, and (b) MAB-9 acts as a repressor in DA and AS neurons, as well as in MN classes DB, DD, and VD (Kerk et. al., 2017[42], Jafari et. al., 2011[43]). If our hypothesis is correct, we would expect ectopic *glr-4* expression in nerve cord MNs of *mab-9* mutant animals. Indeed, we observed ectopic *glr-4^{prom}::tagRFP* expression in AS neurons of *mab-9(-)* mutants, similar to what we observed in PBAF mutants (**Fig. 2.6a-c**). We obtained similar results using the endogenous *glr-4::mScarlet* reporter (**Fig. 2.6d-f**).

2.3.9 MAB-9 acts directly to repress *glr-4* transcription in nerve cord motor neurons

Available MAB-9 ChIP-seq data also showed binding at the *glr-4* locus, overlapping with that of PBRM-1 and SWSN-7. This supports our hypothesis that MAB-9 may recruit PBAF to the *glr-4* locus. To further test direct MAB-9 binding on *glr-4* locus, we mutated predicted MAB-9 binding sites located next to the UNC-3 binding site ~550 nucleotides upstream of the *glr-4* locus. Again, we observed ectopic *glr-4* expression in AS MNs of the nerve cord, indicating MAB-9 binds directly to the *glr-4* promoter to repress its transcription in AS MNs (data not shown). Altogether, this data supports the idea that the PBAF chromatin remodeling complex may be recruited to the *glr-4* locus in AS neurons by MAB-9, ultimately providing specificity to the broadly expressed PBAF complex.

2.3.10 PBAF prevents nerve cord MNs from adopting a "mixed" identity

Disruption of PBAF results in ectopic expression of *glr-4* in specific classes (DA, VA, AS) of nerve cord MNs, suggesting these neurons gain molecular features when PBAF gene activity is disrupted. (**Fig. 2.5b**). Next, we tested whether such gain is accompanied by a loss of

molecular identity features of these MNs. To this end, we evaluated the expression of nine genes known to be expressed in DA, VA, and/or AS neurons (*unc-17/VAChT, dbl-1/BMP7, del-1/SCNN1B/D/G, slo-2/KCNT1/2, acr-2/CHRNA3/6, unc-53/NAV1, unc-129/GDF10, nlp-7, flp-7/ Tachykinin family*) (**Suppl. Fig. 2.2 and 2.6**). We observed no change in expression among these fluorescent reporters in PBAF mutants. In summary, while *glr-4* exhibits ectopic expression in the nerve cord of PBAF mutants, several MN identity reporters remain unaffected, providing evidence that these cells do not undergo a complete cell-fate switch, but instead adopt a mixed MN identity. Thus, PBAF is required for MNs to acquire their complete regional identity.

2.3.11 PBAF controls the identity of caudal motor neurons

Because we observed de-repression of *glr-4* in VNC MNs in PABF mutants (while it's typically expressed in DA9 in the posterior near the tail), we hypothesized that other posteriorly expressed MN identity markers may also be de-repressed in the VNC (*itr-1/ITPR1, avr-15/GLRA1-3, glr-5/GRIK1/3, ser-2/HTR1A, flp-18/GPCRligand, sra-36/GPCRsubunit*). We did not observe any change in VNC expression for these markers in PBAF mutants. Instead, we found that PBAF is required for the expression of 4 genes (*itr-1/ITPR1, avr-15/GLRA1-3, glr-5/GRIK1/3, ser-2/HTR1A*). We first identified *itr-1/ITPR1* as a likely target of PBAF. Typically expressed only in DA9 in the posterior region, we found that ~75% of swsn-9 mutants lost *itr-1* expression in DA9 (**Fig. 2.7a, e**). This is a stark contrast to what we observed with *glr-4* and *unc-4* – instead of ectopic expression as we see in the nerve cord, *swsn-9* mutants showed loss of

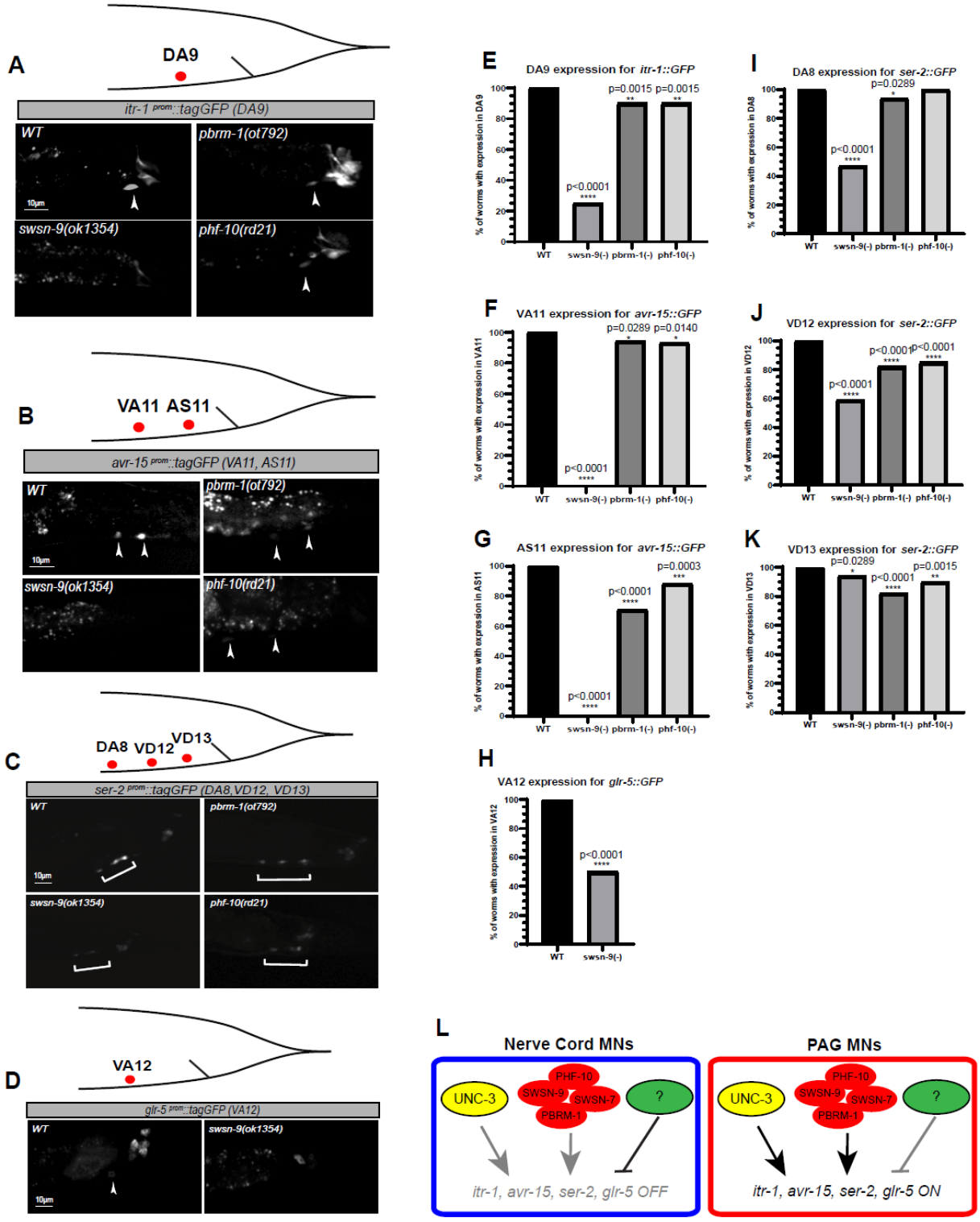

Figure 2.7. PBAF controls the identity of MNs in the pre-anal ganglion

(A) *itr-1* expression (DA9) in WT and PBAF mutants.

Figure 2.7 cont.
(B) *avr-15* expression (VA11, AS11) in WT and PBAF mutants.

(C) *ser-2* expression (DA8, VD12, VD13) in WT and PBAF mutants.

(D) *glr-5* expression (VA12) in WT and PBAF mutants.

(E) Graph showing percentage of animals with *itr-1* expression in WT and PBAF mutants. Animals imaged at L4 stage. WT n=21; pbrm-1(-) n=17; swsn-9(-) n=20; phf-10(-) n=19. Fisher's exact test, p<.05 = *; p<.01 = **; p<.001 = ***; p<.0001 = ****.

(F-G) Graph showing percentage of animals with *avr-15* expression in VA11 (**F**) and AS11 (**G**) in WT and PBAF mutants. Animals imaged at L4 stage. WT n=15; pbrm-1(-) n=17; swsn-9(-) n=26; phf-10(-) n=16. Fisher's exact test, p<.05 = *; p<.01 = **; p<.001 = ***; p<.0001 = ****.

(H) Graph showing percentage of animals with *glr-5* expression in WT and PBAF mutants. Animals imaged at L4 stage. WT n=13; swsn-9(-) n=9. Fisher's exact test, p<.05 = *; p<.01 = **; p<.001 = ***; p<.0001 = ****.

(I-K) Graph showing percentage of animals with *ser-2* expression in DA8 (**I**), VD12 (**J**), and VD13 (**K**) in WT and PBAF mutants. Animals imaged at L4 stage. WT n=24; pbrm-1(-) n=17; swsn-9(-) n=17; phf-10(-) n=20. Fisher's exact test, p<.05 = *; p<.01 = **; p<.001 = ***; p<.0001 = ****.

(L) Schematic showing UNC-3, PBAF, and other factor(s) effect on *itr-1*, *avr-15*, *ser-2*, and *glr-5* in VNC (left) and PAG (right) MNs.

expression of *itr-1* in PAG, suggesting that PBAF may activate gene expression in posteriorly located MNs. Indeed, we observed a similar effect with 3 other posterior MN reporters (*avr-15/GLRA1-3, glr-5/GRIK1/3, ser-2/HTR1A*). Expression of *avr-15* (expressed in VA11 and AS11) was completely lost in *swsn-9* mutants (**Fig. 2.7b, f-g**). Meanwhile *swsn-9* mutants displayed variable loss of *ser-2* (expressed in DA8, VD12, VD13), as well as loss of *glr-5* (expressed in VA12) in ~50% of animals (**Fig. 2.7c-d, h-k**). Taken together, our results indicate PBAF acts as both an activator and a repressor of gene expression in post-mitotic MNs in a region-specific manner, consistent with its previously described role as both an activator and repressor in pluripotent stem cells (Kaeser et. al., 2008[44]).

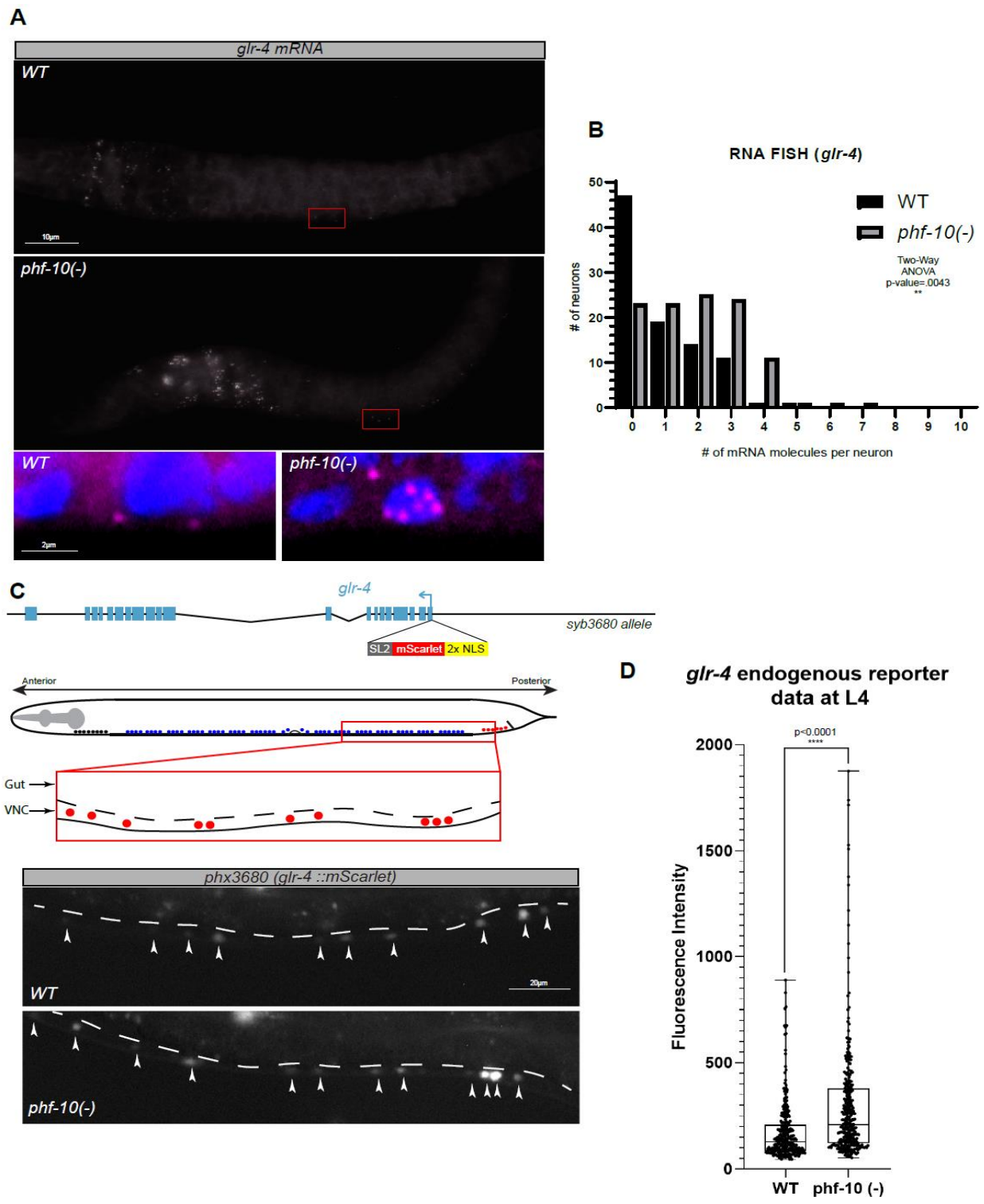

Supplementary Figure 2.1. smRNA FISH and an endogenous *glr-4/GRIK4* reporter validate that PBAF represses *glr-4/GRIK4* in VNC MNs

(A) RNA FISH for WT and *phf-10(rd21)* mutant animals at the L1 stage. Nuclei are stained with DAPI (blue). *glr-4* mRNA are labeled in magenta (bottom).

Supplementary Figure 2.1 cont.
(B) Histogram showing number of neurons against number of *glr-4* mRNA molecules per neuron for WT (black) and *phf-10(rd21)* mutants (gray). Animals imaged at L1 stage. WT n=19; *phf-10(-)* n=27. Two-Way ANOVA, p<.05 = *; p<.01 = **; p<.001 = ***; p<.0001 = ****.

(C) Diagram of endogenous *glr-4* reporter used in our analysis (top). Schematic of MNs in C. elegans VNC (middle). *glr-4* expressing neurons are indicated with white arrowheads in WT and *phf-10* mutant animals (bottom).

(D) Graph showing the quantified fluorescence intensity as a proxy for expression levels of *glr-4* in MNs of WT and *phf-10(rd21)* mutant animals. Animals imaged at L4 stage. WT n=271 (MNs); *phf-10(-)* n=334 (MNs). Unpaired Welch's t-test, p<.05 = *; p<.01 = **; p<.001 = ***; p<.0001 = ****.

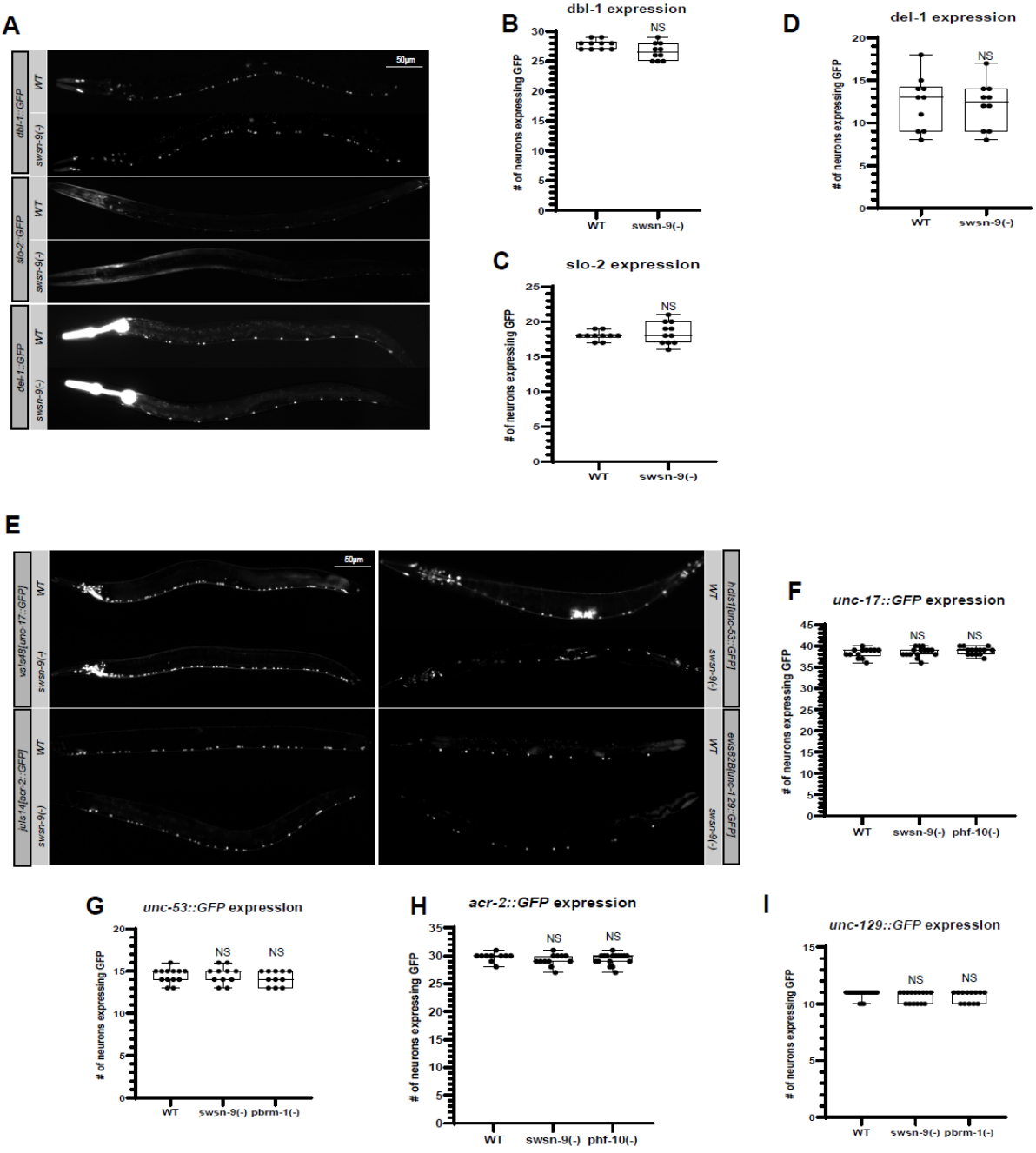

Supplementary Figure 2.2. Unaffected GFP markers show PBAF mutants adopt a "mixed" cell-identity

(A) MN sub-class specific GFP reporters for 3 terminal identity genes in WT and *swsn-9(ok1354)* mutants (*dbl-1*, *slo-2*, and *del-1*).

(B-D) Graphs showing quantification of unaffected GFP reporters from **A** in WT and *swsn-9* mutants. Animals imaged at L4 stage. *dbl-1* (**B**): WT n=10; *swsn-9(-)* n=10, *slo-2* (**C**): WT n=10;

Supplementary Figure 2.2 cont.
swsn-9(-) n=11, *del-1* (**D**): WT n=10; *swsn-9(-)* n=10. Unpaired Welch's t-test, p<.05 = *; p<.01 = **; p<.001 = ***; p<.0001 = ****.

(E) MN class specific GFP reporters for 4 terminal identity genes in WT and *swsn-9(ok1354)* mutants. *unc-17* (top left), *unc-53* (top right), *acr-2* (bottom left), and *unc-129* (bottom right).

(F-I) Graphs showing quantification of unaffected GFP reporters from G in WT and *swsn-9* mutants. Animals imaged at L4 stage. *unc-17* (**F**): WT n=13; *swsn-9(-)* n=15, *unc-53* (**G**): WT n=13; *swsn-9(-)* n=11, *acr-2* (**H**): WT n=10; *swsn-9(-)* n=12, and *unc-129* (**I**): WT n=20; *swsn-9(-)* n=15. Unpaired Welch's t-test, p<.05 = *; p<.01 = **; p<.001 = ***; p<.0001 = ****.

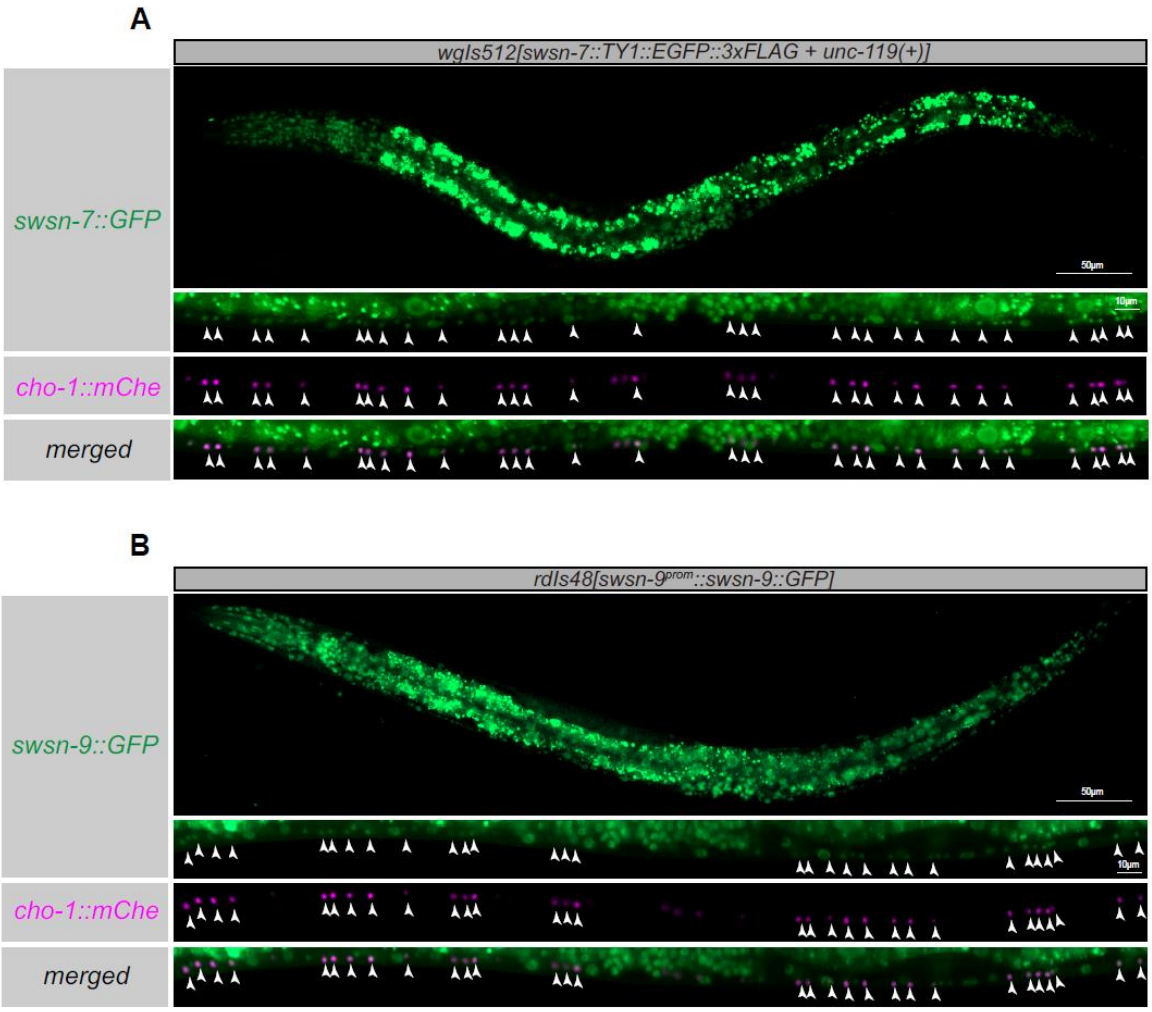

C

	DA	DB	VA	VB	AS
unc-3	+	+	+	+	+
pbrm-1	+	+	+	+	+
swsn-7	+	+	+	+	+
swsn-9	+	+	+	+	+

Supplementary Figure 2.3. PBAF reporters display broad expression in MNs and other cell types

(A) *swsn-7* endogenous reporter overlayed with cholinergic MN marker *cho-1*. Merged image (bottom) reveals *swsn-7* is expressed broadly and in cholinergic MNs (white arrowheads). Animals imaged at L4 stage.

(B) *swsn-9* transgenic reporter using the endogenous *swsn-9* promoter, overlayed with cholinergic MN marker *cho-1*. Merged image (bottom) reveals *swsn-9* is expressed broadly and in cholinergic MNs (white arrowheads). Animals imaged at L4 stage.

(C) Expression of *swsn-7* and *swsn-9* in cholinergic MN subtypes (DA, DB, VA, VB, AS).

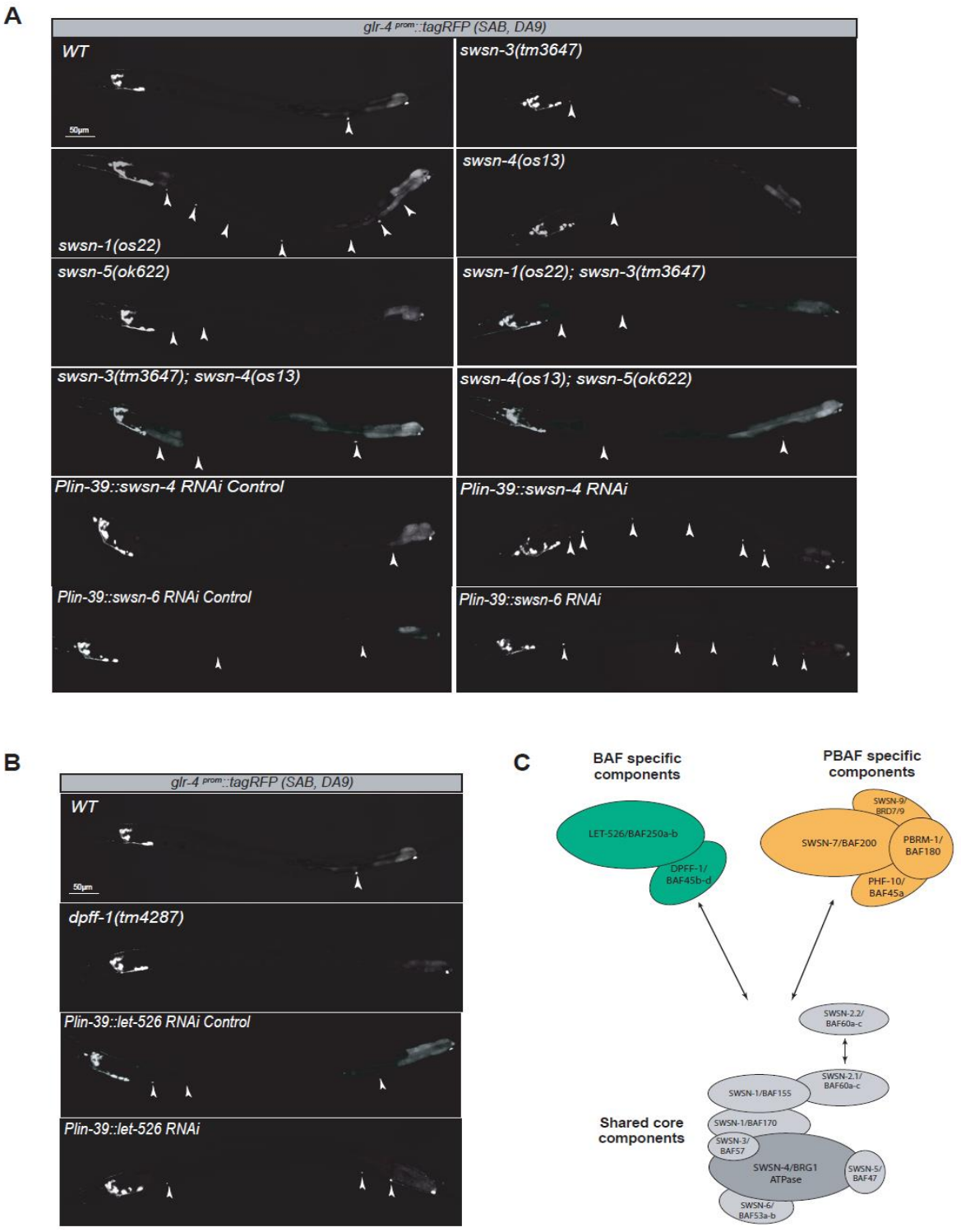

Supplementary Figure 2.4. BAF and core component mutants show variable effects on *glr-4/GRIK4* expression

(A) *glr-4* expression in PBAF/BAF core component mutants (*swsn-1*, *swsn-3*, *swsn-4*, *swsn-5*, *swsn-3;swsn-4*, *swsn-4;swsn-5*, *swsn-4* RNAi, *swsn-6* RNAi). Animals imaged at L4 stage.

Supplementary Figure 2.4 cont.
(B) *glr-4* expression in BAF mutants (*dpff-1*, *let-526* RNAi). Animals imaged at L4 stage.

(C) Cartoon of the BAF and PBAF chromatin remodeling complexes. Complexes share a core ATPase (dark gray) and its accessory components (light gray), with BAF specific subunits (green) and PBAF specific subunits (orange).

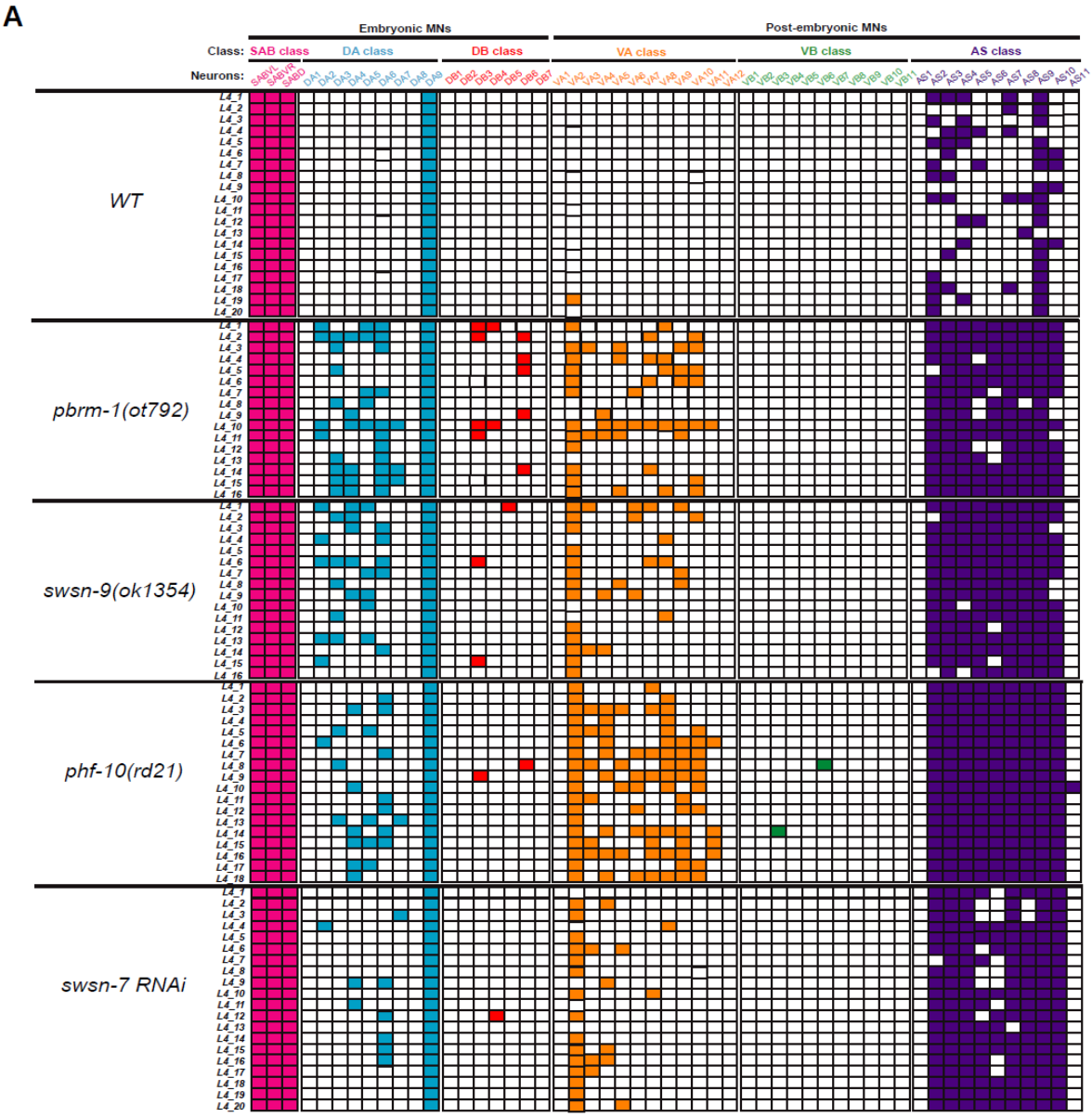

Supplementary Figure 2.5. Single-cell analysis of PBAF mutants shows *glr-4/GRIK4* is ectopically expressed in AS, DA, and VA, nerve cord MNs

(A) Single-cell analysis for WT and PBAF mutants. PBAF mutants show ectopic expression of *glr-4* in DA, VA, and AS MNs in the VNC (rows represent individual animals; columns represent individual MNs; six colors represent six cholinergic MN subtypes).

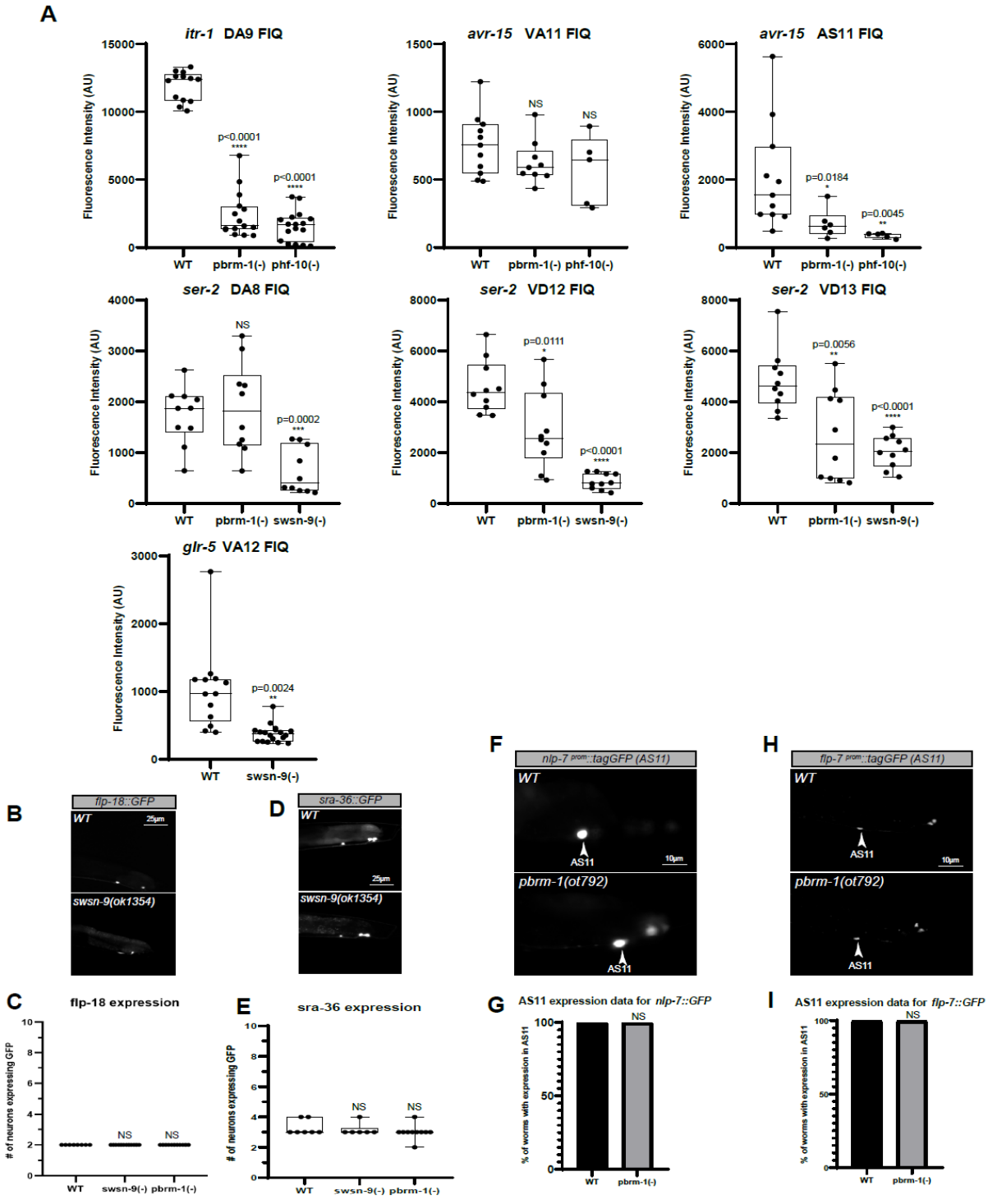

Supplementary Figure 2.6. Additional posterior markers validate that PBAF controls the identity of MNs in the pre-anal ganglion

(A) Graphs showing the quantified fluorescence intensity as a proxy for expression levels of 4 posterior MN markers tested in **Figure 2.7**. Unpaired Welch's t-test, p<.05 = *; p<.01 = **; p<.001 = ***; p<.0001 = ****.

Supplementary Figure 2.6 cont.
(B) Posterior MN marker *flp-18* expression in WT and *swsn-9(ok1354)* mutants.

(C) Graph showing quantification of *flp-18* expression in **B**. Animals imaged at L4 stage. WT n=8; *swsn-9(-)* n=12. Unpaired Welch's t-test, p<.05 = *; p<.01 = **; p<.001 = ***; p<.0001 = ****.

(D) Posterior MN marker *sra-36* expression in WT and *swsn-9(ok1354)* mutants.

(E) Graph showing quantification of *sra-36* expression in **D**. Animals imaged at L4 stage. WT n=7; *swsn-9(-)* n=6. Unpaired Welch's t-test, p<.05 = *; p<.01 = **; p<.001 = ***; p<.0001 = ****.

(F) Posterior MN marker *nlp-7* expression in WT and *pbrm-1(ot792)* mutants.

(G) Graph showing percentage of animals with *nlp-7* expression in WT and *pbrm-1(ot792)* mutants. Animals imaged at L4 stage. WT n=5; pbrm-1(-) n=5. Fisher's exact test, p<.05 = *; p<.01 = **; p<.001 = ***; p<.0001 = ****.

(H) Posterior MN marker *flp-7* expression in WT and *pbrm-1(ot792)* mutants.

(I) Graph showing percentage of animals with *flp-7* expression in WT and *pbrm-1(ot792)* mutants. Animals imaged at L4 stage. WT n=5; pbrm-1(-) n=5. Fisher's exact test, p<.05 = *; p<.01 = **; p<.001 = ***; p<.0001 = ****.

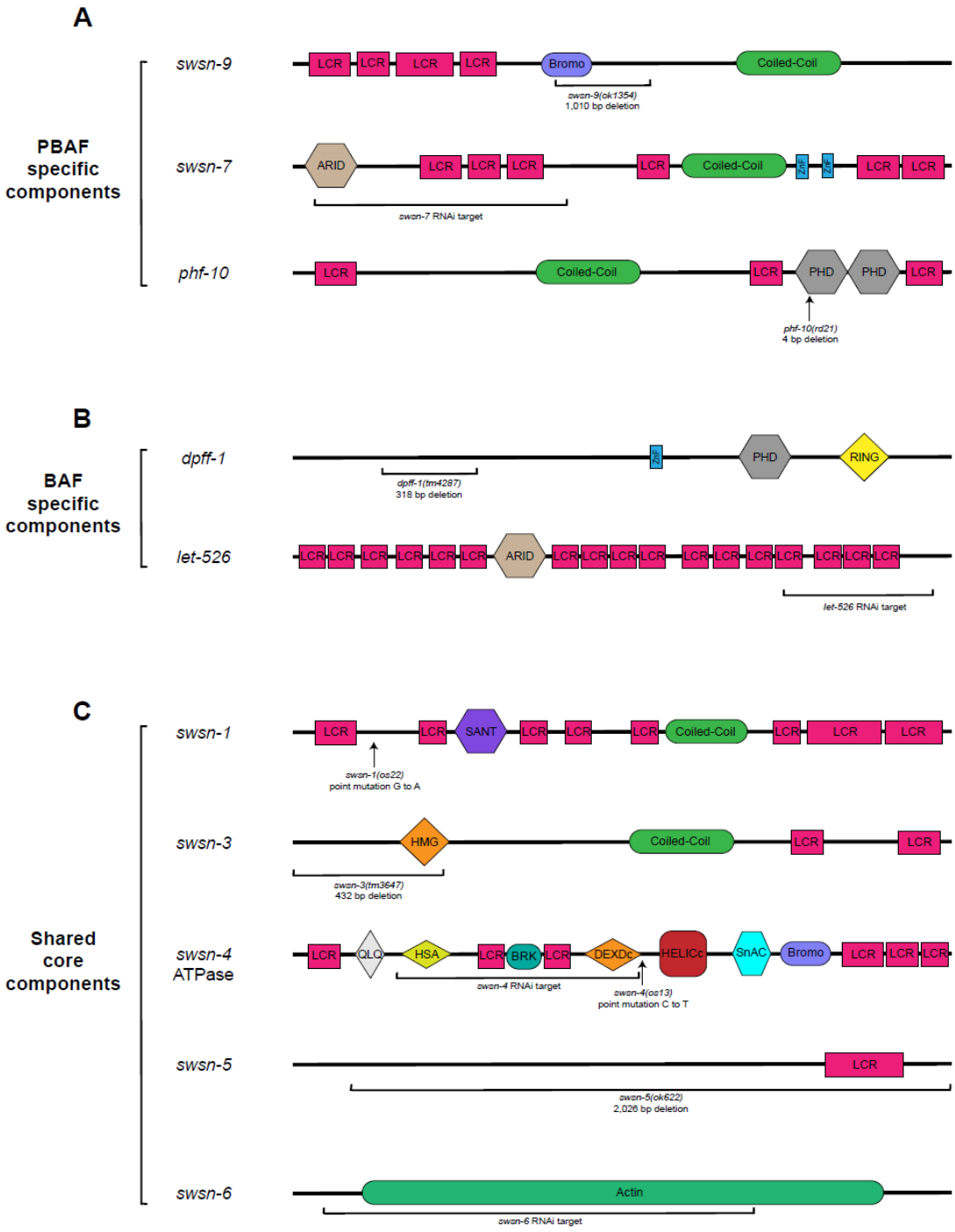

Supplementary Figure 2.7. PBAF, BAF, and core components' protein domains

(A) Protein domains of *C. elegans* PBAF specific components (*swsn-9*, *swsn-7*, and *phf-10*). Abbreviations: Bromo (bromodomains), LCR (low complexity region), Coiled-coil (coiled-coil region), ARID (AT-rich interaction domain), ZnF (zinc finger domain), PHD (plant homeodomain finger).

Supplementary Figure 2.7 cont.
(B) Protein domains of *C. elegans* BAF specific components (*dpff-1* and *let-526*). Abbreviations: RING (Really Interesting New Gene finger domain).

(C) Protein domains of *C. elegans* PBAF/BAF core components (*swsn-1*, *swsn-3*, *swsn-4*, *swsn-5*, and *swsn-6*). Abbreviations: SANT (Swi3, Ada2, N-CoR, TFIIIB), HMG (high mobility group), QLQ (Gln-Leu-Gln), HSA (helicase/SANT-associated), DEXDc (DEAD-box helicase), HELICc (helicase C-terminal domain), SnAC (Snf2-ATP coupling).

2.4 DISCUSSION

2.4.1 The Problem of Neuronal Identity – PBAF Likely Coordinates with Hox Genes to Control MN Regional Identity

In chapter 1.2, I outlined the central point of interest of this thesis – the problem of neuronal identity. How is it possible that, depending on the species, anywhere from hundreds to billions of neurons are able to differentiate into such a diverse array of cell types and obtain their unique function defining characteristics, all while synergizing with each other? To answer this question, we must better understand the molecular mechanisms which control neuron development. Thus far, we know that there exist vast gene regulatory networks in which DNA binding proteins (usually sequence-specific transcription factors) work with and against each other to control gene expression, and ultimately neuron identity. These networks are primarily led by the highly conserved Hox genes, differentially expressed across distinct regions along the A-P axis (Averof and Akam, 1995[10], Noden, 1991[11], Tumpel et. al., 2009[12]). However, gene transcription is only one piece of the equation. In order for DNA binding proteins to bind DNA, they first need access to their target promoter regions. Thus, it is usually necessary for ATP dependent chromatin remodelers to slide or eject nucleosomes and change chromatin conformation prior to any transcription events occurring. There is, however, a massive disparity

between the number of transcription and chromatin factors known to be involved in neuron development, highlighting the importance of furthering our understanding of roles for chromatin factors in establishing neuron identity.

In chapter 2, I presented data revealing PBAF as a key regulator of MN regional identity in the *C. elegans* motor system. While this research furthers our general understanding of chromatin factor involvement in neuron development, it is also important to consider the larger context in which PBAF achieves this. Previous work from our lab has shown that the conserved transcription factor *cfi-1/ARID3* also represses *glr-4/GRIK4* expression in VNC MNs (Li et. al., 2023[27]). Furthermore, it has also previously been shown that Hox genes *lin-39/Scr/Dfd/Hox4-5* and *mab-5/Antp/Hox6-8* control *cfi-1/ARID3* expression in cholinergic MNs, and by extension *glr-4/GRIK4* expression, while *egl-5/Abd-B/Hox9-13* controls expression of terminal identity genes in the posterior tail region such as *itr-1/ITPR1* and *avr-15/GLRA1-3* (Kratsios et. al., 2017[54]). This data combined with our new data concerning PBAF bring up interesting questions regarding PBAF and Hox gene coordination. Specifically, do *lin-39/Scr/Dfd/Hox4-5* and *mab-5/Antp/Hox6-8* control expression of *mab-9/Tbx20* in MNs? Preliminary data we have obtained suggests that this is indeed the case, and that expression of these Hox genes is required for proper activation of *mab-9/Tbx20*. Thus, PBAF and Hox genes likely coordinate to repress *glr-4/GRIK4* through activation of *mab-9/Tbx20*. In total, we are left with a working model implicating Hox factors, transcription factors, and chromatin remodeling factors in establishing MN identity (**Figure 2.8**). Elucidating the extent to which chromatin remodelers like PBAF coordinate with Hox factors, however, requires further investigation.

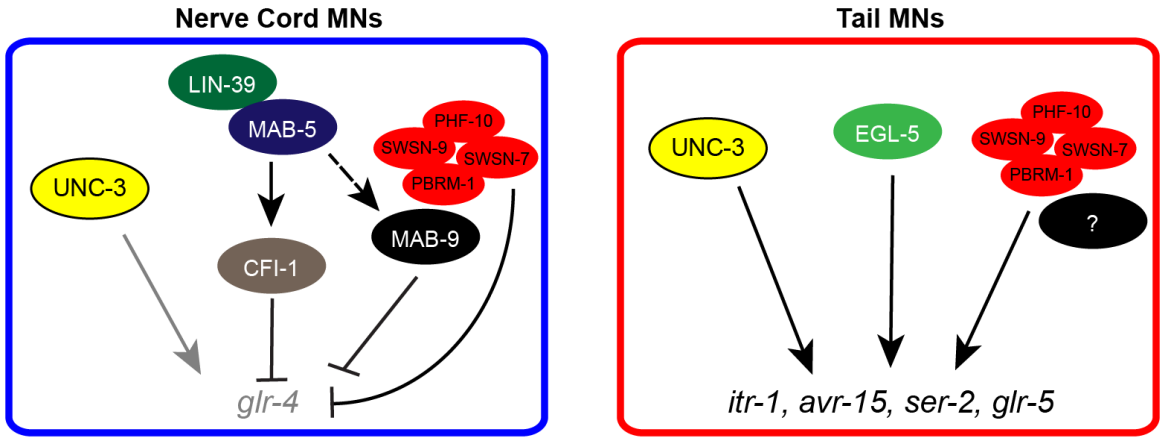

Figure 2.8 Coordinated activation and repression of *C. elegans* terminal identity genes

Schematic depicts an updated model of control over terminal identity gene expression, highlighting differences between the nerve cord (left) and tail (right) regions. PBAF represses *glr-4/GRIK4* in the nerve cord while activating several identity genes in the tail, likely recruited by a sequence-specific transcription factor. Such a model suggests that PBAF may indirectly coordinate with Hox factors to establish MN regional identity.

2.4.2 Known Roles for SWI/SNF Remodelers as an Activator and Repressor

In this thesis, I have presented data which demonstrates that the PBAF chromatin remodeler acts as a repressor of *glr-4/GRIK4* in *C. elegans* VNC, and also as an activator of several genes in the posterior region of the worm. While SWI/SNF remodelers are often associated with promoting gene activation (Centore et. al., 2020[55]), several recent studies have observed critical roles for PBAF as both a transcriptional activator and repressor. For example, PBAF has been observed to be required for transcriptional repression at sites of DNA breaks in actively transcribed chromatin regions in human U2OS cancer cells (Kakarougkas et. al., 2014[56]). Additionally, PBAF subunits are also required to facilitate chromatin binding by the repressor element 1-silencing transcription factor (REST) in human HEK293 cells (Ooi et. al., 2007[57]), and to facilitate REST repression of neuronal target genes in yeast (Battaglioli et. al., 2002[58]). Meanwhile, PBAF subunit PHF-10 has been shown to mediate transcriptional activation

by the bHLH transcription factor MYC in human melanoma cell lines (Soshnikova et. al., 2021[59]). Furthermore, another PBAF subunit, *swsn-9/BRD7*, has been demonstrated to be required for both target gene activation and repression in mouse embryonic stem cells (Kaeser et. al., 2008[60]). Altogether, these studies describe an established role for PBAF as both a transcriptional activator and repressor, thus supporting our results implicating the PBAF chromatin remodeler as a context dependent activator or repressor in *C. elegans* cholinergic MNs.

2.4.3 Recruitment of SWI/SNF to Target Promoters Confers Specificity

The similar phenotypes we observed in PBAF and *mab-9/Tbx20* mutants suggest that these two work together (or at least are involved in the same pathway) to repress *glr-4/GRIK4* in specific *C. elegans* VNC MN subtypes (DA, VA, AS) (**Fig. 2.9**). The hypothesis that PBAF may be recruited to the promoter regions of its target genes (in this case by *mab-9/Tbx20* to the *glr-4/GRIK4* promoter) is supported by similar studies in several species. Studies regarding this concept in yeast have been particularly robust. Early studies on SWI/SNF remodelers in *S. cerevisiae* introduced the catalytic model of SWI/SNF activity, in which the remodeler makes transient changes to the structure of chromatin in a catalytic and random manner (Owen-Hughes et. al., 1996[61]). Meanwhile, targeted, lasting changes to chromatin structure would only occur in the presence of sequence-specific transcription factors. This model, however, does not explain the observed specificity of SWI/SNF function and control over a limited number of genes. Instead, SWI/SNF recruitment to target loci by DNA binding proteins with sequence specificity has become a stronger model supported by several observations. For example, *in vivo* experiments in yeast have shown that the presence of SWI/SNF at the *HO* promoter is dependent

on the presence of transcriptional activator *Swi5* (Cosma et. al., 1999[62]). Other in vitro studies have shown that SWI/SNF displays preferential binding to DNA regions that are bound by transcriptional activators (Neely et. al., 1999[63]). Furthermore, this type of recruitment has been shown in mammalian oligodendrocyte precursor cells, in which the transcription factor Olig2 was observed to recruit SWI/SNF to target genes critical for oligodendrocyte differentiation (Yu et. al., 2013[26]). Finally, PBAF subunit *phf-10/PHF-10* has been shown to physically interact with the bHLH transcription factor MYC, facilitating the recruitment of PBAF to target gene promoters for activation in human melanoma cell lines (Soshnikova et. al., 2021[59]). Importantly, in addition to transcriptional activators, SWI/SNF has also been demonstrated to be recruited by transcriptional repressors, further highlighting its role as both an activator and repressor of transcription (Dimova et. al., 1999[64]). Together, these results from the literature further support our hypothesis that PBAF is recruited by sequence-specific transcription factors such as *mab-9/Tbx20* to repress *glr-4/GRIK4* expression in cholinergic MNs.

However, while our data and evidence from the literature support the hypothesis that PBAF is recruited by subtype-specific transcription factors, we have not shown experimentally that this is indeed the case. This leaves the door open for alternative hypotheses, such as PBAF instead recruiting subtype-specific transcription factors to their target loci. For example, perhaps PBAF, expressed in all neurons, first alters chromatin and is then able to recruit MAB-9 only in the neuron subtypes in which it is expressed (DA, DB, AS). Thus, the observed specificity would be inherent in MAB-9 expression. To test which of these hypotheses is correct, an experiment can be designed to answer two questions: 1.) What is the effect on *glr-4* expression when MAB-9 is overexpressed? 2.) What is the effect on *glr-4* expression when MAB-9 is overexpressed in a PBAF mutant background? Loss of *glr-4* expression would indicate that MAB-9 is sufficient to

repress *glr-4/GRIK4*, providing evidence for it first binding DNA with sequence-specificity and subsequently recruiting PBAF. If animals still show ectopic expression of *glr-4/GRIK4* in a PBAF mutant background while MAB-9 is overexpressed it would suggest that PBAF is necessary for MAB-9 to perform its function of repressing *glr-4/GRIK4*. This would indicate that PBAF likely first binds DNA in a non-sequence specific manner through its high mobility group (HMG) box protein domain, and subsequently recruits MAB-9 to directly bind and repress *glr-4/GRIK4*.

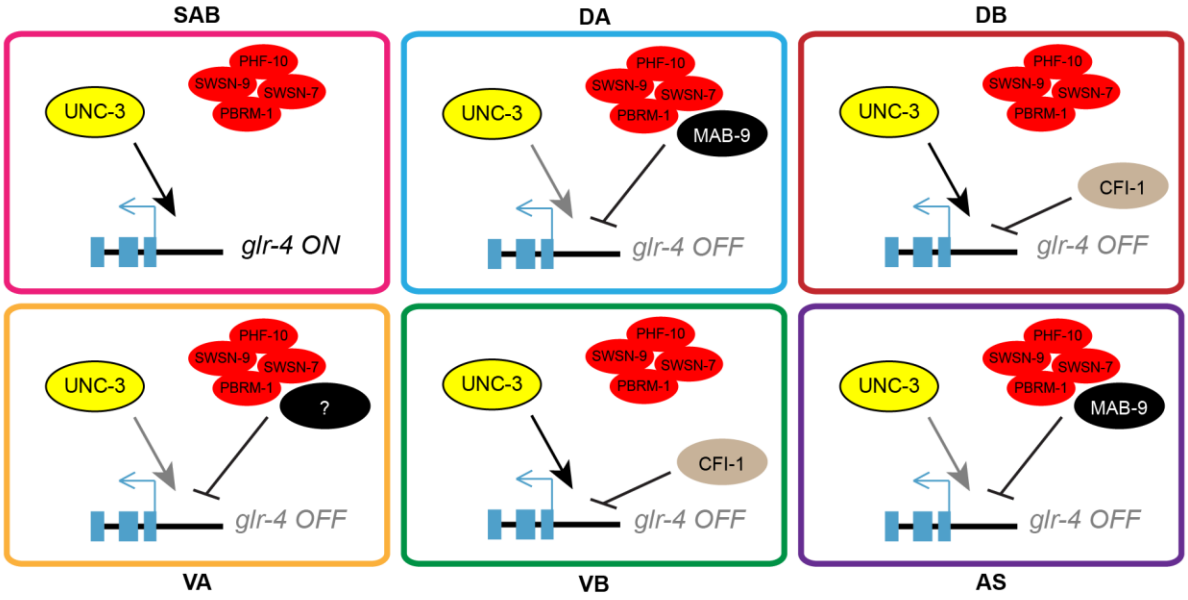

Figure 2.9 Specificity of PBAF is achieved via recruitment to target promoters by sequence-specific transcription factors

Schematic depicts PBAF activity on *glr-4/GRIK4* in *C. elegans* MN subtypes. Despite being broadly expressed, PBAF represses *glr-4/GRIK4* in only DA, VA, and AS subtypes. This specificity is likely due to recruitment of PBAF to the *glr-4/GRIK4* locus by the transcription factor MAB-9, which is expressed in both DA and AS MNs. Recruitment by an alternate transcription factor may be responsible for PBAF repression of *glr-4/GRIK4* in VA MNs, as they do not express MAB-9. In other subtypes which do not express MAB-9, PBAF does not repress *glr-4/GRIK4* despite being expressed. Instead, *glr-4/GRIK4* is repressed by other transcription factors such as CFI-1, as previously shown by our lab.

2.4.4 Roles for SWI/SNF in Hox Gene Function and Body Plan Specification

While PBAF's role as a regulator of MN regional identity has not been previously described, early studies on SWI/SNF indicate a role in Hox gene activation and body plan specification. SWI/SNF remodelers can have one of two distinct ATPases, brahma-related gene 1 (BRG1) and brahma (BRM), each of which is homologous to the SWI2/SNF2 ATPase found in yeast and provides both overlapping and mutually exclusive functions (Hoffman et. al., 2014[65], Jancewicz et. al., 2019[66]). Initial findings on BRM presented it as an activator of multiple homeotic genes (Hox genes, see chapter 1.4) in both the Antennapedia (*Scr*, *Antp*) and Bithorax complexes (*Ubx*) in *Drosophila*. Mutations in BRM were found to suppress homeotic transformation phenotypes in *Polycomb* and *Polycomb-like* mutant animals, revealing BRM as a homeotic gene activator and thus important for body segment identity (Kennison and Tamkun, 1988[67], Tamkun et. al., 1992[68]). While recent work has not focused on SWI/SNF remodeler functions in regional specification, these studies support our observations that PBAF plays a key role in establishing MN regional identity in *C. elegans*.

2.4.5 Examining the Role of PBAF During Repression of *glr-4/GRIK4*

As we interpret the results of our findings, it is imperative to consider the larger context in which PBAF functions to repress *glr-4/GRIK4*. As described previously PBAF does not act alone to repress *glr-4/GRIK4*; *mab-9/Tbx20* also represses *glr-4/GRIK4* in cholinergic MNs. Still, there are other genes whose loss results in a similar phenotype to that previously described (ectopic expression of *glr-4/GRIK4* in cholinergic MNs). For example, mutants for genes encoding the methyltransferase proteins *met-2/SETDB1* and *set-25/SETBP1* have been

previously shown to cause a strikingly similar phenotype (Li et. al., 2023[27]). Several of these genes' orthologs have also been seen to play roles in neuron development and fate specification in humans (SETDB1 and SETBP1, Park et. al., 2022[69], Cardo et. al., 2023[70]) and in flies (HP1α, Panteleeva et. al., 2007[71]). Thus, we envision a potential model of *glr-4/GRIK4* repression in cholinergic MNs that begins with *mab-9/Tbx20* recruitment of PBAF to the *glr-4/GRIK4* locus. PBAF recognizes a H3K9ac modification and binds to the locus, repressing *glr-4/GRIK4*. H3K9 is deacetylated and then subsequently methylated by *met-2/SETDB1* and *set-25/SETBP1*. Finally, *hpl-2/HP1/CBX5*, known to recognize H3K9me via its chromodomains (Nielson et. al., 2002[72]), along with *lin-61/L3MBTL2* and *lin-13* (these three interact to form a protein complex, DasGupta et. al., 2020[73]) then bind to the locus to silence *glr-4/GRIK4*. Altogether, this model presents a possible method through which PBAF synergizes with several other chromatin modifying proteins to ultimately repress *glr-4/GRIK4* in cholinergic MNs.

2.4.6 ATP-Dependent Chromatin Remodelers Control Gene Expression

As we consider the mechanisms through which PBAF represses *glr-4/GRIK4*, we highlight another interesting question. Why should the expression of neuron identity features depend on the presence and activity of a chromatin remodeler such as PBAF? Chromatin remodelers are ATP dependent, and thus expend a large amount of energy to regulate chromatin dynamics throughout the genome. How does it make sense to depend on a cost-ineffective method to regulate gene expression? One possible explanation for this may come from our results in chapter 2. I previously described that our transgenic reporter *glr-4::tagRFP* shows no *glr-4* expression in VNC MNs of WT animals and ectopic expression in PBAF mutants. On the other hand, our endogenous *glr-4::mScarlet* reporter shows low (baseline) levels of expression in

VNC MNs of WT animals, which is markedly increased in PBAF mutants. These data indicate that likely, the expression of *glr-4* is not an ON/OFF event. Instead, precise levels of *glr-4* may be required in each MN. Thus, it may be necessary to rely on dynamic transcriptional machinery like chromatin remodelers to achieve a consistent level of precise gene expression.

Supplementary Table 2.1 Strains and Primers Used

Reagent Type (*C. elegans* strain or primer)	Strain Name/Target Gene	Source	Genotype/Sequence(s)
Strain	HS1222	Caenorhabditis Genetics Center	pbrm-1(tm415)
Strain	RW12226	Caenorhabditis Genetics Center	pbrm-1(st12226[pbrm-1::TY1::EGFP::3xFlag])
Strain	VC887	Caenorhabditis Genetics Center	swsn-9(ok1354)
Strain	HS304	Caenorhabditis Genetics Center	swsn-1(os22)
Strain	RA437	Caenorhabditis Genetics Center	swsn-3(tm3647)
Strain	HS184	Caenorhabditis Genetics Center	swsn-4(os13)
Strain	RB810	Caenorhabditis Genetics Center	swsn-5(ok622)
Strain	CZ631	Caenorhabditis Genetics Center	juIs14[acr-2::GFP]
Strain	CB4605	Caenorhabditis Genetics Center	mab-9(e2410); him-5(e1490)
Strain	DA1299	Caenorhabditis Genetics Center	adEx1299 [avr-15::GFP + rol-6(su1006)]
Strain	OH2246	Caenorhabditis Genetics Center	otIs107[ser-2::GFP]
Strain	BW1935	Caenorhabditis Genetics Center	ctIs43[dbl-1p::GFP + dbl-1p::GFP::NLS + unc-119(+)]; him-5(e1490); unc-119(ed3)

Supplementary Table 2.1 cont.

Strain	NY225	Caenorhabditis Genetics Center	ynIs59[flp-18::GFP]
Strain	BC10749	Caenorhabditis Genetics Center	sEx10749[slo-2::GFP]
Strain	NC138	Caenorhabditis Genetics Center	wdIs3[del-1::GFP + dpy-20(+)]; dpy-20(e1282)
Strain	BC11976	Caenorhabditis Genetics Center	sEx11976[sra-36::GFP]
Strain	LX929	Caenorhabditis Genetics Center	vsIs48[unc-17::GFP]
Strain	VM133	Caenorhabditis Genetics Center	akEx31[glr-5::GFP+lin-15(+)]; lin-15B&lin-15A(n765)
Strain		Kratsios Lab	otIs453[itr-1::GFP]
Strain		Kratsios Lab	hdIs1 [unc-53p::GFP + rol-6(su1006)]
Strain		Kratsios Lab	evIs82B[unc-129::GFP]
Strain	MT10785	Bob Horvitz (MIT, Cambridge MA)	unc-3(n3435)
Strain		Laura Mathies (VCU, Richmond VA)	phf-10(rd21)
Strain		Laura Mathies (VCU, Richmond VA)	dpff-1(tm4287)
Strain		Genetic Screen	pbrm-1 (ot792)
Strain	KRA162	Genetic Cross	pbrm-1 (ot792) ; otIs476
Strain	KRA158	Genetic Cross	pbrm-1(tm415) ; otIs476
Strain	KRA120	Genetic Cross	pbrm-1(ot792); otIs476; kasEx42 [Ppbrm-1::pbrm-1::GFP] Line 1
Strain		Genetic Cross	pbrm-1(st12226[pbrm-1::TY1::EGFP::3xFlag]); otIs544[cho-1::mChe]
Strain		Genetic Cross	cho-1::GFPnanobody::Zif-1::NLS-Cre; otIs476
Strain		Genetic Cross	pbrm-1(st12226[pbrm-1::TY1::EGFP::3xFlag]); otIs476
Strain		Genetic Cross	cho-1::GFPnanobody::Zif-1::NLS-Cre; pbrm-1(st12226[pbrm-1::TY1::EGFP::3xFlag])

Supplementary Table 2.1 cont.

Strain		Genetic Cross	cho-1::GFPnanobody::Zif-1::NLS-Cre; otIs476; pbrm-1(st12226[pbrm-1::TY1::EGFP::3xFlag])
Strain	KRA160	Genetic Cross	swsn-9(ok1354); otIs476
Strain	KRA187	Genetic Cross	phf-10(rd21); otIs476
Strain	KRA188	Genetic Cross	dpff-1(tm4287); otIs476
Strain	KRA184	Genetic Cross	swsn-1(os22); otIs476
Strain	KRA186	Genetic Cross	swsn-3(tm3647); otIs476
Strain	KRA185	Genetic Cross	swsn-4(os13); otIs476
Strain	KRA183	Genetic Cross	swsn-5(ok622); otIs476
Strain	KRA199	Genetic Cross	swsn-3(tm3647); swsn-4(os13); otIs476
Strain	KRA200	Genetic Cross	swsn-4(os13); swsn-5(ok622); otIs476
Strain	KRA206	Genetic Cross	pbrm-1(ot792); otIs476; juIs14[acr-2::GFP]
Strain	KRA167	Genetic Cross	swsn-9(ok1354); otIs476; juIs14[acr-2::GFP]
Strain	KRA192	Genetic Cross	phf-10(rd21); otIs476; juIs14[acr-2::GFP]
Strain	KRA194	Genetic Cross	kasEx56[Plin-39::swsn-7] RNAi Line 1; otIs476[glr-4::RFP]; juIs14[acr-2::GFP]
Strain	KRA168	Genetic Cross	pbrm-1(tm415); otIs476; unc-3(n3435)
Strain	KRA169	Genetic Cross	swsn-9(ok1354); otIs476; unc-3 (n3435)
Strain		Genetic Cross	mab-9(e2410); otIs476
Strain		Genetic Cross	mab-9(e2410); syb3680[glr-4::mScarlet]; otIs532[cho-1::YFP]
Strain	KRA181	Genetic Cross	pbrm-1(ot792); otIs476; otIs453[itr-1::GFP]
Strain	KRA174	Genetic Cross	swsn-9(ok1354); otIs476; otIs453[itr-1::GFP]
Strain	KRA202	Genetic Cross	phf-10(rd21); otIs476; otIs453[itr-1::GFP]
Strain	KRA210	Genetic Cross	pbrm-1(ot792); otIs476; adEx1299 [avr-15::GFP + rol-6]
Strain	KRA214	Genetic Cross	swsn-9(ok1354); otIs476; adEx1299 [avr-15::GFP + rol-6]
Strain	KRA208	Genetic Cross	phf-10(rd21); otIs476; adEx1299 [avr-15::GFP + rol-6]
Strain	KRA182	Genetic Cross	pbrm-1(ot792); otIs476; otIs107[ser-2::GFP]
Strain	KRA175	Genetic Cross	swsn-9(ok1354); otIs476; otIs107[ser-2::GFP]
Strain	KRA203	Genetic Cross	phf-10(rd21); otIs476; otIs107[ser-2::GFP]
Strain	KRA190	Genetic Cross	swsn-9(ok1354); otIs476; akEx31[glr-5::GFP]
Strain		Genetic Cross	phf-10(rd21); phx3680[glr-4::mScarlet]; otIs532[cho-1::YFP]
Strain	KRA176	Genetic Cross	swsn-9(ok1354); otIs476; ctIs43[dbl-1::GFP]
Strain	KRA177	Genetic Cross	swsn-9(ok1354); otIs476; ynIs59[flp-18::GFP]
Strain	KRA213	Genetic Cross	swsn-9(ok1354); otIs476; sEx10749[slo-2::GFP]
Strain		Genetic Cross	swsn-9(ok1354); otIs476; wdIs3[del-1::GFP + dpy-20(+)]
Strain	KRA212	Genetic Cross	swsn-9(ok1354); otIs476; sEx11976[sra-36::GFP]

Supplementary Table 2.1 cont.

Strain	KRA166	Genetic Cross	swsn-9(ok1354); otIs476; vsIs48[unc-17::GFP]
Strain	KRA173	Genetic Cross	swsn-9(ok1354); otIs476;hdIs1[unc-53::GFP]
Strain	KRA161	Genetic Cross	swsn-9(ok1354) ; otIs476 ; evIs82B[unc-129::GFP]
Strain		Genetic Cross	syb3680[glr-4::mScarlet]; otIs532[cho-1::YFP]
Strain	KRA145	Injection	otIs476; kasEx168 [Plin-39::pbrm-1] RNAi all isoform
Strain	KRA146	Injection	otIs476; kasEx169 [Plin-39::pbrm-1] RNAi long isoform line 1
Strain		Injection	otIs476; Ex[Pcho-1::pbrm-1(all isoform)] RNAi Line 1
Strain		Injection	otIs476; Ex[Pcho-1::pbrm-1(long isoform)] RNAi Line 1
Strain		Injection	cho-1::GFPnanobody::Zif-1::NLS-Cre (integrated)
Strain	KRA135	Injection	otIs476; kasEx56 [Plin-39::swsn-7] RNAi line 1
Strain	KRA136	Injection	otIs476; kasEx57 [Plin-39::swsn-7] RNAi line 2
Strain	KRA137	Injection	otIs476; kasEx58 [Plin-39::swsn-7] RNAi line 3
Strain	KRA149	Injection	otIs476; kasEx172 [Plin-39::let-526] RNAi line 2
Strain		Injection	otIs476; Ex[Plin-39::swsn-4] RNAi line 3
Strain	KRA138	Injection	otIs476; kasEx59 [Plin-39::swsn-6] RNAi line 1
Strain	PHX3680	SunyBiotech	syb3680[glr-4::mScarlet]
Primer	*pbrm-1(ot792)* (genotyping)	Sigma-Aldrich	FRW: ATGACGTGTCTACGTAATCG RVS: tcacTTGAGATATGCTTCCG
Primer	*pbrm-1(tm415)* (genotyping)	Sigma-Aldrich	FRW 1: TCCACCTCCTACTCATAAAAGG FRW 2: TGCCATCTGCCAAACAATATCC RVS: TGATTCCTCATCATCAGATCC
Primer	*swsn-9(ok1354)* (genotyping)	Sigma-Aldrich	FRW: aagaagaagttccgaaagagc RVS 1: ttgtatcattccaggagttcc RVS 2: aagttggagatggaactgacg
Primer	*phf-10(rd21)* (genotyping)	Sigma-Aldrich	FRW: tctataaggtcgaaatcgtcc RVS: GACACAGCTCCATTCGTACG
Primer	*swsn-1(os22)* (genotyping)	Sigma-Aldrich	FRW: tcgcagacacgtattcaaatgg RVS: aattcaattttgggcgctgc
Primer	*swsn-3(tm3647)* (genotyping)	Sigma-Aldrich	FRW 1: taacgatgctcggcgagaac FRW 2: ttccaatatcccaaagctggg RVS: actcttgcaaaaaccacgtgc
Primer	*swsn-4(os13)* (genotyping)	Sigma-Aldrich	FRW: aaatgggctccatctgtaacc RVS: tactttctctcctgtagtcgc
Primer	*swsn-5(ok622)* (genotyping)	Sigma-Aldrich	FRW: tttgaacggtattcgcttctg RVS 1: aatagcaggctggaaaactgc RVS 2: aattgagaagagcgagcgag
Primer	*dpff-1(tm4287)* (genotyping)	Sigma-Aldrich	FRW: tcaagaacgtagtcatcacg RVS 1: tatgaacatcaaacggctacg RVS 2: tggacaatacgcaatttcgc

Supplementary Table 2.1 cont.

Primer	*mab-9(e2410)* (genotyping)	Sigma-Aldrich	FRW: aacccctaattttggcagtgg RVS: tatcgatttttttggcacaggc
Primer	*lin-39* intron 1+A7:A60 (pcr fusion)	Sigma-Aldrich	Primer A: TTGCCTCAAGTCAAGGACTG Primer A*: ATCCAATACTCGGAGATCAGg Primer B: GTCGTGATGGGTACTTGTTAC
Primer	*cho-1* 280 bp promoter (pcr fusion)	Sigma-Aldrich	Primer A: AGCTATGACCATGATTACGC Primer A*: ATAAGCTTGCATGCgagctc Primer B: TCCAAGGGTCCTCCTGAAAATG
Primer	all isoform *pbrm-1* RNAi sense (pcr fusion)	Sigma-Aldrich	Primer C: TTCAACACCTCCACAACATCC Primer D*: ATTTGCATCTGTGGATGAGG Primer D: tcacTTGAGATATGCTTCCG
Primer	all isoform pbrm-1 RNAi antisense (pcr fusion)	Sigma-Aldrich	Primer C: ATTTGCATCTGTGGATGAGG Primer D*: TTCAACACCTCCACAACATCC Primer D: AATCTCGATTATGGAAAGGC
Primer	long isoform *pbrm-1* RNAi sense (pcr fusion)	Sigma-Aldrich	Primer C: AGTTCAGGAAGAGGAAGAACC Primer D*: AAGTTTACAGCCAATGGACGG Primer D: TGCTTGATCCTCATCATATCC
Primer	long isoform *pbrm-1* RNAi antisense (pcr fusion)	Sigma-Aldrich	Primer C: AAGTTTACAGCCAATGGACGG Primer D*: AGTTCAGGAAGAGGAAGAACC Primer D: TTCAAGAACTTTTCGAGGCTGC
Primer	*swsn-7* RNAi sense (pcr fusion)	Sigma-Aldrich	Primer C: AAGCTTCCACATGTTCAAGG Primer D*: AAACTTCCACTCATCGAATGG Primer D: ATTCCATTTTGAGCCATTCGG
Primer	*swsn-7* RNAi antisense (pcr fusion)	Sigma-Aldrich	Primer C: AAACTTCCACTCATCGAATGG Primer D*: AAGCTTCCACATGTTCAAGG Primer D: GATCCACCTGAGAAGCAGAG
Primer	*swsn-4* RNAi sense (pcr fusion)	Sigma-Aldrich	Primer C: AGACACAACTCTCGAAACTGC Primer D*: TCAAACGATGTCCTTCGTCG Primer D: TGAGCATGGAAGAATCCGTTC
Primer	swsn-4 RNAi antisense (pcr fusion)	Sigma-Aldrich	Primer C: TCAAACGATGTCCTTCGTCG Primer D*: AGACACAACTCTCGAAACTGC Primer D: TGTCAATCTCCAAACTCAGg
Primer	*swsn-6* RNAi sense (pcr fusion)	Sigma-Aldrich	Primer C: ATACATTGCCGTTCAAGAAGC Primer D*: AAGAATCAACGAGTTTCCTCC Primer D: TAGAGCATAGTTGAGCCGTTC

Supplementary Table 2.1 cont.

Primer	swsn-6 RNAi antisense (pcr fusion)	Sigma-Aldrich	Primer C: TAGAGCATAGTTGAGCCGTTC Primer D*: TTGAGAAACAAGAGGCTATGG Primer D: ATACATTGCCGTTCAAGAAGC
Primer	*let-526* RNAi sense (pcr fusion)	Sigma-Aldrich	Primer C: ATTCCATCCGAGTCATCCTC Primer D*: actcacCATAGTGAAAGTTGC Primer D: TTGGAATGGATTCATCACGG
Primer	let-526 RNAi antisense (pcr fusion)	Sigma-Aldrich	Primer C: actcacCATAGTGAAAGTTGC Primer D*: ATTCCATCCGAGTCATCCTC Primer D: ACCTCAACAACATCCAGGTC

2.5 Materials and Methods

2.5.1 Genetics

Strains were grown at 15°C, 20°C, or 25°C on nematode growth media (NGM) plates with *E. coli* (OP50) (Brenner, 1974[45]). Mutant alleles used: *pbrm-1(ot792)* (point mutation, premature stop), *pbrm-1(tm415)* (427 nucleotide deletion, 5 nucleotide insertion), *swsn-9(ok1354)* (1,010 nucleotide deletion), *phf-10(rd21)* (4 nucleotide deletion), *unc-3(n3435)* (1,008 nucleotide deletion), *mab-9(e2410)* (single nucleotide substitution), *swsn-1(os22)* (missense mutation), *swsn-3(tm3647)* (432 nucleotide deletion), *swsn-4(os13)* (missense mutation), *swsn-5(ok622)* (2,026 nucleotide deletion), and *dpff-1(tm4287)* (318 nucleotide deletion).

All *C. elegans* strains and primers used in this study are listed in Supplementary Table 2.1.

2.5.2 Microscopy

To prepare slides for imaging, animals were anesthetized using 100mM sodium azide (NaN_3) while being mounted on a 4% agarose pad on glass slides. Images were taken with an automated fluorescence microscope (Zeiss, Axio Imager Z2). Several z-stacks were taken with each image (0.50 μm intervals between stacks) with Zeiss Axiocam 503 mono using the ZEN software (Version 2.3.69.1000, Blue edition). Images and z-stacks were then transferred and processed in ImageJ (Schindelin et. al., 2012[46]).

2.5.3 Generation of transgenic reporters

Reporter gene fusions were generated using PCR fusion (Hobert, 2002[47]). Target gene promoter fragments were fused to the *tagRFP* coding sequence. Gene fusion products were then injected into wild-type young adult animals at a total DNA concentration of 100 ng/ul. The fusion product was accompanied by a *myo-2::GFP* or *myo-2::mCherry* co-injection marker at a concentration of 3-5 ng/ul. Individual lines were isolated from F1 progeny.

2.5.4 Generation of RNAi constructs and lines

DNA fragments spanning 2-4 exons were selected from target genes and fused to enhancer elements sufficient to drive MN specific expression, *lin-39* (intron 1) and *cho-1* (280bp promoter fragment), by PCR fusion in both sense and antisense orientations (Esposito et. al., 2007[28]). Each fused construct was injected into young adult animals at a concentration of 100 ng/ul, along with *myo-2::GFP* or *myo-2::mCherry* co-injection marker plasmids at a concentration of 3-5 ng/ul. Individual lines were isolated from F1 progeny.

2.5.5 Motor neuron cell identification

A combination of criteria was used for MN cell ID: stereotypic cell body position of MNs (White et. al., 1986[48]), birth order (Sulston and Horvitz, 1977[49]), and previously characterized fluorescent reporters for specific MN classes (Jospin et. al., 2009[50], Stefanakis et. al., 2015[51], Pereira et. al., 2015[52]). Identity was determined based on co-localization with these previously characterized fluorescent reporters.

2.5.6 Fluorescence intensity quantification (FIQ)

Images of worms were taken with identical parameters, using z-stacks that span the entire cell bodies of nerve cord MNs. These stacks were processed in ImageJ, where background was subtracted to reduce background noise from the image (rolling ball radius = 50 pixels). The MN cell bodies were manually selected (by drawing an area over MN cell bodies to be measured), and the average fluorescence intensity was measured and recorded for each visible MN in the image.

2.5.7 ZIF-1 mediated protein degradation

A plasmid containing GFPnanobody fused to ZIF-1 (driven by MN specific 280bp *cho-1* promoter fragment) was injected into wild-type young adult animals along with co-injection marker *myo-2::mCherry*. GFPnanobody binds to GFP tagged proteins, while ZIF-1 recruits the E3 ubiquitin ligase complex to degrade tagged proteins (Wang et. al., 2017[31]). Individual lines were selected from F1 progeny. One line obtained underwent spontaneous integration into the genome and was subsequently used for our studies. This line was crossed with *pbrm-1::TY1::EGFP::3xFlag* to degrade PBRM-1::GFP tagged protein.

2.5.8 smRNA FISH

Animals were grown plates until full of gravid worms, and were subsequently collected in an egg prep to synchronize animals. Synchronized L1 animals were then incubated in 4% paraformaldehyde in 1xPBS for 45 minutes at room temperature, washed two times using

1xPBS, and then permeabilized with 70% ethanol at 4°C overnight. A *glr-4* probe was designed using the Stellaris Probe Designer website (Biosearch Technologies). The probe was mixed in hybridization buffer (0.1 g/mL dextran sulfate [Sigma D8906-50G], 1 mg/mL Escherichia coli tRNA [ROCHE 10109541001], 2 mM vanadyl ribonucleotide complex [New England Biolabs S1402s], 0.2 mg/mL RNase-free BSA [Ambion AM2618], 10% formamide) and added to the worms. The hybridization buffer was removed and worms were washed twice in wash buffer (DAPI was added during the second wash and incubated for 30 minutes in the dark for nuclear counterstaining). Worms were washed once in 2x SSC, incubated in GLOX buffer (0.4% glucose, 0.1 M Tris-HCl, 2x SSC) for 2 minutes for equilibration, and then resuspended in GLOX buffer with glucose oxidase and catalase added before imaging (Ji and van Oudenaarden, 2012[53]).

2.5.9 Statistical analysis

Individual data point dot plots and box and whisker plots were used to represent the quantification of our data. The horizontal line in the box represents the mean value, while the box itself represents the interquartile range. Unpaired t-test with Welch's correction was performed and p-values were annotated. Differences with $p < 0.05$ were considered significant. Asterisks in figures indicate statistical significance as follows: *$p < 0.05$, **$p < 0.01$, ***$p < 0.001$, ****$p<0.0001$. For plots comparing percentage of animals, chi-square analysis was performed to determine significance, while for comparison of histograms two-way ANOVA was used.

2.6 References

1. Sanes DH, Reh TA, Harris WA. Chapter 4 - Determination and differentiation. In: Sanes DH, Reh TA, Harris WA, eds. *Development of the Nervous System (Third Edition)*. Academic Press; 2012:77-104. doi:10.1016/B978-0-12-374539-2.00008-2

2. Khan YS, Lui F. Neuroanatomy, Spinal Cord. In: *StatPearls*. StatPearls Publishing; 2024. Accessed February 5, 2024. http://www.ncbi.nlm.nih.gov/books/NBK559056/

3. Jessell TM, Sürmeli G, Kelly JS. Motor Neurons and the Sense of Place. *Neuron*. 2011;72(3):419-424. doi:10.1016/j.neuron.2011.10.021

4. Guthrie S. Patterning and axon guidance of cranial motor neurons. *Nat Rev Neurosci*. 2007;8(11):859-871. doi:10.1038/nrn2254

5. Catela C, Kratsios P. Transcriptional mechanisms of motor neuron development in vertebrates and invertebrates. *Dev Biol*. 2021;475:193-204. doi:10.1016/j.ydbio.2019.08.022

6. Catela C, Chen Y, Weng Y, Wen K, Kratsios P. Control of spinal motor neuron terminal differentiation through sustained Hoxc8 gene activity | eLife. Accessed February 5, 2024. https://elifesciences.org/articles/70766

7. Stifani N. Motor neurons and the generation of spinal motor neurons diversity. *Front Cell Neurosci*. 2014;8. Accessed February 5, 2024. https://www.frontiersin.org/articles/10.3389/fncel.2014.00293

8. Hughes CL, Kaufman TC. Hox genes and the evolution of the arthropod body plan1. *Evol Dev*. 2002;4(6):459-499. doi:10.1046/j.1525-142X.2002.02034.x

9. Mallo M, Wellik DM, Deschamps J. Hox Genes and Regional Patterning of the Vertebrate Body Plan. *Dev Biol*. 2010;344(1):7-15. doi:10.1016/j.ydbio.2010.04.024

10. Averof M, Akam M. Hox genes and the diversification of insect and crustacean body plans. *Nature*. 1995;376(6539):420-423. doi:10.1038/376420a0

11. Noden DM. Cell movements and control of patterned tissue assembly during craniofacial development. *J Craniofac Genet Dev Biol*. 1991;11(4):192-213.

12. Tümpel S, Wiedemann LM, Krumlauf R. Chapter 8 - Hox Genes and Segmentation of the Vertebrate Hindbrain. In: *Current Topics in Developmental Biology*. Vol 88. Genes. Academic Press; 2009:103-137. doi:10.1016/S0070-2153(09)88004-6

13. Dasen JS, De Camilli A, Wang B, Tucker PW, Jessell TM. Hox Repertoires for Motor Neuron Diversity and Connectivity Gated by a Single Accessory Factor, FoxP1. *Cell*. 2008;134(2):304-316. doi:10.1016/j.cell.2008.06.019

14. Rousso DL, Gaber ZB, Wellik D, Morrisey EE, Novitch BG. Coordinated Actions of the Forkhead Protein Foxp1 and Hox Proteins in the Columnar Organization of Spinal Motor Neurons. *Neuron*. 2008;59(2):226-240. doi:10.1016/j.neuron.2008.06.025

15. Gieseler K, Qadota H, Benian GM. Development, structure, and maintenance of C. elegans body wall muscle. In: *WormBook: The Online Review of C. Elegans Biology [Internet]*. WormBook; 2018. Accessed March 10, 2024. https://www.ncbi.nlm.nih.gov/books/NBK426064/

16. Dubois L, Vincent A. The COE – Collier/Olf1/EBF – transcription factors: structural conservation and diversity of developmental functions. *Mech Dev*. 2001;108(1):3-12. doi:10.1016/S0925-4773(01)00486-5

17. Feng W, Destain H, Smith JJ, Kratsios P. Maintenance of neurotransmitter identity by Hox proteins through a homeostatic mechanism. *Nat Commun*. 2022;13(1):6097. doi:10.1038/s41467-022-33781-0

18. Clapier CR, Cairns BR. The Biology of Chromatin Remodeling Complexes. *Annu Rev Biochem*. 2009;78(1):273-304. doi:10.1146/annurev.biochem.77.062706.153223

19. Cairns BR, Kim YJ, Sayre MH, Laurent BC, Kornberg RD. A multisubunit complex containing the SWI1/ADR6, SWI2/SNF2, SWI3, SNF5, and SNF6 gene products isolated from yeast. *Proc Natl Acad Sci U S A*. 1994;91(5):1950-1954.

20. Stern M, Jensen R, Herskowitz I. Five SWI genes are required for expression of the HO gene in yeast. *J Mol Biol*. 1984;178(4):853-868. doi:10.1016/0022-2836(84)90315-2

21. Neigeborn L, Carlson M. Genes Affecting the Regulation of SUC2 Gene Expression by Glucose Repression in Saccharomyces Cerevisiae. *Genetics*. 1984;108(4):845-858. doi:10.1093/genetics/108.4.845

22. Zhou CY, Johnson SL, Gamarra NI, Narlikar GJ. Mechanisms of ATP-Dependent Chromatin Remodeling Motors. *Annu Rev Biophys*. 2016;45:153-181. doi:10.1146/annurev-biophys-051013-022819

23. Zeng L, Zhou MM. Bromodomain: an acetyl-lysine binding domain. *FEBS Lett*. 2002;513(1):124-128. doi:10.1016/S0014-5793(01)03309-9

24. Alfert A, Moreno N, Kerl K. The BAF complex in development and disease. *Epigenetics Chromatin*. 2019;12:19. doi:10.1186/s13072-019-0264-y

25. Sudarsanam P, Winston F. The Swi/Snf family: nucleosome-remodeling complexes and transcriptional control. *Trends Genet*. 2000;16(8):345-351. doi:10.1016/S0168-9525(00)02060-6

26. Yu Y, Chen Y, Kim B, et al. Olig2 Targets Chromatin Remodelers to Enhancers to Initiate Oligodendrocyte Differentiation. *Cell*. 2013;152(1):248-261. doi:10.1016/j.cell.2012.12.006

27. Li Y, Smith JJ, Marques F, Osuma A, Huang HC, Kratsios P. Cell context-dependent CFI-1/ARID3 functions control neuronal terminal differentiation. *Cell Rep*. 2023;42(3):112220. doi:10.1016/j.celrep.2023.112220

28. Esposito G, Di Schiavi E, Bergamasco C, Bazzicalupo P. Efficient and cell specific knock-down of gene function in targeted C. elegans neurons. *Gene*. 2007;395(1):170-176. doi:10.1016/j.gene.2007.03.002

29. Feng W, Destain H, Smith JJ, Kratsios P. Maintenance of neurotransmitter identity by Hox proteins through a homeostatic mechanism. *Nat Commun*. 2022;13(1):6097. doi:10.1038/s41467-022-33781-0

30. Kratsios P, Stolfi A, Levine M, Hobert O. Coordinated regulation of cholinergic motor neuron traits through a conserved terminal selector gene. *Nat Neurosci*. 2012;15(2):205-214. doi:10.1038/nn.2989

31. Wang S, Tang NH, Lara-Gonzalez P, et al. A toolkit for GFP-mediated tissue-specific protein degradation in C. elegans. *Dev Camb Engl*. 2017;144(14):2694-2701. doi:10.1242/dev.150094

32. Hodges C, Kirkland JG, Crabtree GR. The Many Roles of BAF (mSWI/SNF) and PBAF Complexes in Cancer. *Cold Spring Harb Perspect Med*. 2016;6(8):a026930. doi:10.1101/cshperspect.a026930

33. Johnson CN, Adkins NL, Georgel P. Chromatin remodeling complexes: ATP-dependent machines in action. *Biochem Cell Biol*. 2005;83(4):405-417. doi:10.1139/o05-115

34. Mathies LD, Blackwell G, Bettinger JC. New alleles of the SWI/SNF chromatin remodeling complex gene phf-10. *MicroPublication Biol*. 2022:10.17912/micropub.biology.000533. doi:10.17912/micropub.biology.000533

35. Large EE, Mathies LD. Caenorhabditis elegans SWI/SNF Subunits Control Sequential Developmental Stages in the Somatic Gonad. *G3 GenesGenomesGenetics*. 2014;4(3):471-483. doi:10.1534/g3.113.009852

36. Centore RC, Sandoval GJ, Soares LMM, Kadoch C, Chan HM. Mammalian SWI/SNF Chromatin Remodeling Complexes: Emerging Mechanisms and Therapeutic Strategies. *Trends Genet*. 2020;36(12):936-950. doi:10.1016/j.tig.2020.07.011

37. Liberg D, Sigvardsson M, Åkerblad P. The EBF/Olf/Collier Family of Transcription Factors: Regulators of Differentiation in Cells Originating from All Three Embryonal Germ Layers. *Mol Cell Biol*. 2002;22(24):8389-8397. doi:10.1128/MCB.22.24.8389-8397.2002

38. The ENCODE Project Consortium. An integrated encyclopedia of DNA elements in the human genome. *Nature*. 2012;489(7414):57-74. doi:10.1038/nature11247

39. Li Y, Osuma A, Correa E, et al. Establishment and maintenance of motor neuron identity via temporal modularity in terminal selector function. Desplan C, Bronner ME, Chuang CF, eds. *eLife*. 2020;9:e59464. doi:10.7554/eLife.59464

40. Kratsios P, Pinan-Lucarré B, Kerk SY, Weinreb A, Bessereau JL, Hobert O. Transcriptional Coordination of Synaptogenesis and Neurotransmitter Signaling. *Curr Biol*. 2015;25(10):1282-1295. doi:10.1016/j.cub.2015.03.028

41. Yu Y, Chen Y, Kim B, et al. Olig2 Targets Chromatin Remodelers to Enhancers to Initiate Oligodendrocyte Differentiation. *Cell*. 2013;152(1):248-261. doi:10.1016/j.cell.2012.12.006

42. Kerk SY, Kratsios P, Hart M, Mourao R, Hobert O. Diversification of C. elegans Motor Neuron Identity via Selective Effector Gene Repression. *Neuron*. 2017;93(1):80-98. doi:10.1016/j.neuron.2016.11.036

43. Jafari G, Appleford PJ, Seago J, Pocock R, Woollard A. The UNC-4 homeobox protein represses mab-9 expression in DA motor neurons in Caenorhabditis elegans. *Mech Dev*. 2011;128(1):49-58. doi:10.1016/j.mod.2010.09.005

44. Kaeser MD, Aslanian A, Dong MQ, Yates JR, Emerson BM. BRD7, a Novel PBAF-specific SWI/SNF Subunit, Is Required for Target Gene Activation and Repression in Embryonic Stem Cells. *J Biol Chem*. 2008;283(47):32254-32263. doi:10.1074/jbc.M806061200

45. Brenner S. The Genetics of Caenorhabditis Elegans. *Genetics*. 1974;77(1):71-94. doi:10.1093/genetics/77.1.71

46. Schindelin J, Arganda-Carreras I, Frise E, et al. Fiji: an open-source platform for biological-image analysis. *Nat Methods*. 2012;9(7):676-682. doi:10.1038/nmeth.2019

47. Hobert O. PCR Fusion-Based Approach to Create Reporter Gene Constructs for Expression Analysis in Transgenic C. elegans. *BioTechniques*. 2002;32(4):728-730. doi:10.2144/02324bm01

48. White JG, Southgate E, Thomson JN, Brenner S. The structure of the nervous system of the nematode Caenorhabditis elegans. *Philos Trans R Soc Lond B Biol Sci*. 1997;314(1165):1-340. doi:10.1098/rstb.1986.0056

49. Sulston JE, Horvitz HR. Post-embryonic cell lineages of the nematode, Caenorhabditis elegans. *Dev Biol*. 1977;56(1):110-156. doi:10.1016/0012-1606(77)90158-0

50. Jospin M, Qi YB, Stawicki TM, et al. A Neuronal Acetylcholine Receptor Regulates the Balance of Muscle Excitation and Inhibition in Caenorhabditis elegans. *PLoS Biol*. 2009;7(12):e1000265. doi:10.1371/journal.pbio.1000265

51. Stefanakis N, Carrera I, Hobert O. Regulatory Logic of Pan-Neuronal Gene Expression in C. elegans. *Neuron*. 2015;87(4):733-750. doi:10.1016/j.neuron.2015.07.031

52. Pereira L, Kratsios P, Serrano-Saiz E, et al. A cellular and regulatory map of the cholinergic nervous system of C. elegans. Shen K, ed. *eLife*. 2015;4:e12432. doi:10.7554/eLife.12432

53. Ji N, van Oudenaarden A. Single molecule fluorescent in situ hybridization (smFISH) of C. elegans worms and embryos. *Wormbook*. Published online December 13, 2012:1-16. doi:10.1895/wormbook.1.153.1

54. Kratsios P, Kerk SY, Catela C, et al. An intersectional gene regulatory strategy defines subclass diversity of C. elegans motor neurons. Dasen J, ed. *eLife*. 2017;6:e25751. doi:10.7554/eLife.25751

55. Centore RC, Sandoval GJ, Soares LMM, Kadoch C, Chan HM. Mammalian SWI/SNF Chromatin Remodeling Complexes: Emerging Mechanisms and Therapeutic Strategies. *Trends Genet*. 2020;36(12):936-950. doi:10.1016/j.tig.2020.07.011

56. Kakarougkas A, Ismail A, Chambers AL, et al. Requirement for PBAF in Transcriptional Repression and Repair at DNA Breaks in Actively Transcribed Regions of Chromatin. *Mol Cell*. 2014;55(5):723-732. doi:10.1016/j.molcel.2014.06.028

57. Ooi L, Belyaev ND, Miyake K, Wood IC, Buckley NJ. BRG1 Chromatin Remodeling Activity is Required for Efficient Chromatin Binding by the Transcriptional Repressor Rest and Facilitates Rest-Mediated Repression. *J Biol Chem*. 2006;281(51):38974-38980. doi:10.1074/jbc.M605370200

58. Battaglioli E, Andrés ME, Rose DW, et al. REST Repression of Neuronal Genes Requires Components of the hSWI·SNF Complex*. *J Biol Chem*. 2002;277(43):41038-41045. doi:10.1074/jbc.M205691200

59. Soshnikova NV, Tatarskiy EV, Tatarskiy VV, et al. PHF10 subunit of PBAF complex mediates transcriptional activation by MYC. *Oncogene*. 2021;40(42):6071-6080. doi:10.1038/s41388-021-01994-0

60. Kaeser MD, Aslanian A, Dong MQ, Yates JR, Emerson BM. BRD7, a Novel PBAF-specific SWI/SNF Subunit, Is Required for Target Gene Activation and Repression in Embryonic Stem Cells. *J Biol Chem*. 2008;283(47):32254-32263. doi:10.1074/jbc.M806061200

61. Owen-Hughes T, Utley RT, Côté J, Peterson CL, Workman JL. Persisent Site-Specific Remodeling of a Nucleosome Array by Transient Action of the SWI/SNF Complex. *Science*. 1996;273(5274):513-516.

62. Cosma MP, Tanaka T, Nasmyth K. Ordered Recruitment of Transcription and Chromatin Remodeling Factors to a Cell Cycle– and Developmentally Regulated Promoter. *Cell*. 1999;97(3):299-311. doi:10.1016/S0092-8674(00)80740-0

63. Neely KE, Hassan AH, Wallberg AE, et al. Activation Domain–Mediated Targeting of the SWI/SNF Complex to Promoters Stimulates Transcription from Nucleosome Arrays. *Mol Cell*. 1999;4(4):649-655. doi:10.1016/S1097-2765(00)80216-6

64. Dimova D, Nackerdien Z, Furgeson S, Eguchi S, Osley MA. A Role for Transcriptional Repressors in Targeting the Yeast Swi/Snf Complex. *Mol Cell*. 1999;4(1):75-83. doi:10.1016/S1097-2765(00)80189-6

65. Hoffman GR, Rahal R, Buxton F, et al. Functional epigenetics approach identifies BRM/SMARCA2 as a critical synthetic lethal target in BRG1-deficient cancers. *Proc Natl Acad Sci U S A*. 2014;111(8):3128-3133. doi:10.1073/pnas.1316793111

66. Jancewicz I, Siedlecki JA, Sarnowski TJ, Sarnowska E. BRM: the core ATPase subunit of SWI/SNF chromatin-remodelling complex—a tumour suppressor or tumour-promoting factor? *Epigenetics Chromatin*. 2019;12:68. doi:10.1186/s13072-019-0315-4

67. Kennison JA, Tamkun JW. Dosage-dependent modifiers of polycomb and antennapedia mutations in Drosophila. *Proc Natl Acad Sci U S A*. 1988;85(21):8136-8140.

68. Tamkun JW, Deuring R, Scott MP, et al. brahma: A regulator of Drosophila homeotic genes structurally related to the yeast transcriptional activator SNF2SWI2. *Cell*. 1992;68(3):561-572. doi:10.1016/0092-8674(92)90191-E

69. Park J, Lee K, Kim K, Yi SJ. The role of histone modifications: from neurodevelopment to neurodiseases. *Signal Transduct Target Ther*. 2022;7:217. doi:10.1038/s41392-022-01078-9

70. Cardo LF, de la Fuente DC, Li M. Impaired neurogenesis and neural progenitor fate choice in a human stem cell model of SETBP1 disorder. *Mol Autism*. 2023;14:8. doi:10.1186/s13229-023-00540-x

71. Panteleeva I, Boutillier S, See V, et al. HP1α guides neuronal fate by timing E2F-targeted genes silencing during terminal differentiation. *EMBO J*. 2007;26(15):3616-3628. doi:10.1038/sj.emboj.7601789

72. Nielsen PR, Nietlispach D, Mott HR, et al. Structure of the HP1 chromodomain bound to histone H3 methylated at lysine 9. *Nature*. 2002;416(6876):103-107. doi:10.1038/nature722

73. DasGupta A, Lee TL, Li C, Saltzman AL. Emerging Roles for Chromo Domain Proteins in Genome Organization and Cell Fate in C. elegans. *Front Cell Dev Biol*. 2020;8:590195. doi:10.3389/fcell.2020.590195

CHAPTER III: DISCUSSION

3.1 Summary and Significance of this Thesis

In summary, this thesis has provided evidence that the conserved chromatin remodeling complex PBAF acts as a key regulator of *C. elegans* MN regional identity in post-mitotic cholinergic MNs. These findings reveal multiple non-traditional roles for the PBAF chromatin remodeler and are significant for several reasons.

First, we found that animals lacking critical PBAF subunits display ectopic expression of *glr-4/GRIK4* in select MN subtypes (DA, VA, AS) in the VNC. Furthermore, we observed that PBAF repression of *glr-4/GRIK4* occurs cell-autonomously in post-mitotic MNs. Traditionally, chromatin remodelers are thought to act without sequence specificity to broadly control gene expression through changes in chromatin accessibility (Sudarsanam and Winston, 2000[1], Yu et. al., 2013[2], Quinn et. al., 1996[3], Côté et. al., 1998[4]). Acute control over gene expression and terminal differentiation in subsets of MN subtypes therefore is generally a role ascribed to other DNA binding proteins (i.e., transcription factors) as a part of complex gene regulatory networks. While the exact mechanism of PBAF's action to repress *glr-4/GRIK4* in select MN subtypes is still not entirely clear, this result challenges us to consider alternative, non-traditional roles for PBAF and other chromatin remodelers that may typically be thought of as roles for sequence specific transcription factors.

Second, we found that PBAF mutant animals also displayed loss of expression of several terminal identity features including *itr-1/ITPR1* and *avr-15/GLRA1-3*, indicating PBAF acts as an activator of these genes. This loss of expression occurred specifically in the posterior PAG region of the worm as opposed to the ectopic expression of *glr-4/GRIK4* previously seen in the

VNC. These MNs segregated by region adopt a "mixed" MN identity, and so we propose a novel role for the PBAF chromatin remodeler as a key regulator of MN regional identity in cholinergic MNs. While many previous studies have focused on the role of Hox genes in establishing MN regional identity during the early stages of development (Hughes and Kaufman, 2002[5], Mallo et. al., 2010[6], Averof and Akam, 1995[7], Noden, 1991[8], Tumpel et. al., 2009[9]), our findings help to illuminate the underlying molecular mechanisms which control MN regional identity during later (post-mitotic) stages of development.

Finally, we found that the conserved transcription factor *mab-9/Tbx20* acts directly to repress *glr-4/GRIK4* in AS MNs of the VNC. As this ectopic expression of *glr-4/GRIK4* occurs in a similar subset of MNs in *mab-9/Tbx20* mutants, we propose a mechanism through which transcription factors such as *mab-9/Tbx20* are able to effectively give PBAF its specificity. Specifically, we hypothesize that sequence-specific transcription factors may recruit the PBAF complex to its target loci, where it can locally recognize histone post-translational modifications and affect chromatin accessibility and gene expression. This hypothesis is consistent with other studies in the literature in yeast and mouse models, in which PBAF has been seen to be recruited to specific promoters by other sequence-specific transcription factors (Sudarsanam and Winston, 2000[1], Yu et. al., 2013[2], Yudkovsky et. al., 1999[10], Peterson and Workman, 2000[11]).

3.2 Limitations of this Thesis

3.2.1 Limitations of the *C. elegans* model

As with any research, there were several limitations that presented themselves throughout the course of this work. The first and largest of these limitations is the animal model I used in this

investigation, *C. elegans*. Although *C. elegans* is a fantastic model to study nervous system development (see chapter 1.5), its strengths as a model also serve as a limitation to the immediate impact and relevance of these findings as they relate to humans. Simply put, although we have uncovered a novel role for PBAF as a regulator of MN regional identity in this study, and while there is evidence that suggests this role may be conserved in other organisms (e.g., the conserved nature of PBAF, other conserved mechanisms of establishing MN regional identity such as Hox gene involvement, other studies showing the recruitment of PBAF to promoters of its target genes, etc.), we do not necessarily know if this is the case. Moving forward, similar studies must be done in more complex organisms (flies, mice, etc.) to further test the evolutionary conservation of our *C. elegans* findings. Finally, while a powerful genetic tool, *C. elegans* are less conducive to biochemistry experiments (such as co-IP, ChIP-seq, etc.). Thus, the model presents challenges to further dissecting the mechanism of MAB-9 recruiting PBAF. Going forward, biochemical experiments such as these can more easily be performed in mammalian cultured cell lines.

3.2.2 Limitations of quantification methods

Another form of limitation of this research lies in quantification of the data collected. An overwhelming majority of the data collected in this thesis came in the form of images taken. In quantifying these images, thresholds were often set to reduce noise in the image without removing or affecting visibility of neurons. However, the types of *C. elegans* reporter strains used in this thesis varied greatly in nature, producing inconsistent levels of fluorescence. For example, injected animals carry transgenes as an extrachromosomal array, and as a result show mosaicism (somewhat variable expression between animals) in the expression of these

transgenes. Meanwhile, endogenous reporter strains tend to be extremely dim and thus can cause thresholding errors during quantification. Both scenarios present challenges and therefore limitations to quantifications based on the type of reporter strain used. Furthermore, fluorescence intensity quantification of images was done in ImageJ by manually selecting individual MNs to be measured and quantified. This sort of quantification, while extremely useful, invites the potential for human error during the MN selection process, and thus provides a limitation to the accuracy of our quantification. Most importantly, however, I have done my utmost to maintain a high level of consistency in all images taken and quantifications performed. So long as these limitations apply to all animals quantified, we are able to minimize the effect they have (if any) on our results.

3.2.3 Limitations on scope of the project

Like every other thesis project before this one, a number of failed experiments presented limitations to the scope of this project. Notably, multiple initial attempts to test if PBRM-1 acts cell-autonomously, and at what timepoint PBRM-1 was required for the repression of *glr-4/GRIK4*, failed. We initially set out to utilize the auxin inducible degradation (AID) system, a well described system in *C. elegans* that has also previously been successful in our own lab, in order to deplete PBRM-1 upon the presence of auxin (Zhang et. al., 2015[12], Li et. al., 2020[13], Feng et. al., 2022[14], Feng et. al., 2020[15], Kerk et. al., 2017[16]). We were able to successfully generate an endogenously AID-tagged PBRM-1 reporter strain (*pbrm-1::mNG::3xFlag::AID*) via CRISPR/Cas9. However, this strain exhibited hypomorphic effects on *glr-4/GRIK4* expression (they displayed a partial ectopic expression phenotype as seen in *pbrm-1* mutants). Similarly, we attempted to use a heat-shock promoter to drive targeted RNAi of PBRM-1 in late

larval stage animals. However, again, these animals displayed hypomorphic effects on *glr-4/GRIK4* expression. We ultimately were able to successfully show evidence for cell-autonomy and a requirement for PBRM-1 in post-mitotic MNs by using a ZIF-1 mediated protein degradation approach (see chapter 2.3), but as a result we lacked precise control over the timing of PBRM-1 degradation, and thus limiting the extent of the results we were able to obtain from this experiment.

Another notable experiment which failed and ultimately was not able to be carried out was a MN-specific ChIP-seq experiment for PBAF component SWSN-9. The idea here was to perform ChIP-seq in *swsn-9* mutant animals which also carry an injected (and integrated) rescue construct for *swsn-9* driven by a MN-specific promoter. Thus, when pulldown of SWSN-9 occurred during the experiment it would only be pulled from MNs, allowing us to identify additional targets of PBAF in MNs. Although I used (followed as well as modified for optimization) previously established protocols from the literature as well as our own lab (Li et. al., 2020[13], Zhong et. al., 2010[17], Yu et. al., 2017[18]), roadblocks were met in pulling down enough (or any) DNA for the experiment, likely due to an inability to gather enough starting genetic material. Ultimately, I moved on from this experiment due to time constraints.

3.3 Future Directions for the Project

This thesis presents a starting foundation for future research on PBAF's (and possibly other chromatin remodelers) role in the developing nervous system. This work can and hopefully will be expounded upon in a number of different ways. One potential major step forward would be to generate a comprehensive list of target genes of PBAF in MNs. The easiest way to do this would

be to use an unbiased method such as RNA-seq or ChIP-seq in a MN-specific manner to identify downstream targets of PBAF. This data would not only broaden our understanding of PBAF role as a regulator of MN regional identity, but it also would help uncover potential new roles for PBAF in the developing motor system. Another potential direction for the project would be to pursue testing our proposed hypothesis that PBAF is recruited to its targets in MNs by sequence-specific transcription factors such as *mab-9/Tbx20*. This could be done by using methods to determine protein-protein interactions such as Co-IP. An alternative route could employ MN-specific ChIP-seq (see chapter 4.2.3) to determine PBAF binding in relation to the conserved binding sites of potential recruiting transcription factors like *mab-9/Tbx20*. I would also encourage the pursuit of improved behavioral data for *pbrm-1* and other PBAF mutant animals. The *pbrm-1(ot792)* strain used in this research showed clear locomotion defects, and we obtained preliminary behavioral data showing that this is the case for both *pbrm-1(ot792)* and *pbrm-1(tm415)* mutants (see Appendix A). However, further examination is required to better characterize their behavior and whether it constitutes a new behavioral phenotype or fits into an existing one. Finally, the PBAF complex should be closely studied in other species as well (mice, for example). PBAF has already been well studied in other disease contexts, and I believe it is important to investigate whether PBAF maintains a role in establishing MN regional identity in more complex, mammalian models.

3.4 References

1. Sudarsanam P, Winston F. The Swi/Snf family: nucleosome-remodeling complexes and transcriptional control. *Trends Genet*. 2000;16(8):345-351. doi:10.1016/S0168-9525(00)02060-6

2. Yu Y, Chen Y, Kim B, et al. Olig2 Targets Chromatin Remodelers to Enhancers to Initiate Oligodendrocyte Differentiation. *Cell*. 2013;152(1):248-261. doi:10.1016/j.cell.2012.12.006

3. Quinn J, Fyrberg AM, Ganster RW, Schmidt MC, Peterson CL. DNA-binding properties of the yeast SWI/SNF complex. *Nature*. 1996;379(6568):844-847. doi:10.1038/379844a0

4. Côté J, Peterson CL, Workman JL. Perturbation of nucleosome core structure by the SWI/SNF complex persists after its detachment, enhancing subsequent transcription factor binding. *Proc Natl Acad Sci U S A*. 1998;95(9):4947-4952.

5. Hughes CL, Kaufman TC. Hox genes and the evolution of the arthropod body plan1. *Evol Dev*. 2002;4(6):459-499. doi:10.1046/j.1525-142X.2002.02034.x

6. Mallo M, Wellik DM, Deschamps J. Hox Genes and Regional Patterning of the Vertebrate Body Plan. *Dev Biol*. 2010;344(1):7-15. doi:10.1016/j.ydbio.2010.04.024

7. Averof M, Akam M. Hox genes and the diversification of insect and crustacean body plans. *Nature*. 1995;376(6539):420-423. doi:10.1038/376420a0

8. Noden DM. Cell movements and control of patterned tissue assembly during craniofacial development. *J Craniofac Genet Dev Biol*. 1991;11(4):192-213.

9. Tümpel S, Wiedemann LM, Krumlauf R. Chapter 8 - Hox Genes and Segmentation of the Vertebrate Hindbrain. In: *Current Topics in Developmental Biology*. Vol 88. Genes. Academic Press; 2009:103-137. doi:10.1016/S0070-2153(09)88004-6

10. Yudkovsky N, Logie C, Hahn S, Peterson CL. Recruitment of the SWI/SNF chromatin remodeling complex by transcriptional activators. *Genes Dev*. 1999;13(18):2369-2374.

11. Peterson CL, Workman JL. Promoter targeting and chromatin remodeling by the SWI/SNF complex. *Curr Opin Genet Dev*. 2000;10(2):187-192. doi:10.1016/S0959-437X(00)00068-X

12. Zhang L, Ward JD, Cheng Z, Dernburg AF. The auxin-inducible degradation (AID) system enables versatile conditional protein depletion in C. elegans. *Dev Camb Engl*. 2015;142(24):4374-4384. doi:10.1242/dev.129635

13. Li Y, Osuma A, Correa E, et al. Establishment and maintenance of motor neuron identity via temporal modularity in terminal selector function. Desplan C, Bronner ME, Chuang CF, eds. *eLife*. 2020;9:e59464. doi:10.7554/eLife.59464

14. Feng W, Destain H, Smith JJ, Kratsios P. Maintenance of neurotransmitter identity by Hox proteins through a homeostatic mechanism. *Nat Commun*. 2022;13(1):6097. doi:10.1038/s41467-022-33781-0

15. Feng W, Li Y, Dao P, et al. A terminal selector prevents a Hox transcriptional switch to safeguard motor neuron identity throughout life. Desplan C, Bronner ME, eds. *eLife*. 2020;9:e50065. doi:10.7554/eLife.50065

16. Kerk SY, Kratsios P, Hart M, Mourao R, Hobert O. Diversification of C. elegans Motor Neuron Identity via Selective Effector Gene Repression. *Neuron*. 2017;93(1):80-98. doi:10.1016/j.neuron.2016.11.036

17. Zhong M, Niu W, Lu ZJ, et al. Genome-Wide Identification of Binding Sites Defines Distinct Functions for Caenorhabditis elegans PHA-4/FOXA in Development and Environmental Response. *PLoS Genet*. 2010;6(2):e1000848. doi:10.1371/journal.pgen.1000848

18. Yu B, Wang X, Wei S, et al. Convergent Transcriptional Programs Regulate cAMP Levels in C. elegans GABAergic Motor Neurons. *Dev Cell*. 2017;43(2):212-226.e7. doi:10.1016/j.devcel.2017.09.013

APPENDIX A

pbrm-1(ot792) mutant animals show partial lethality at early larval stages as well as clearly visible locomotion defects at late larval and adult stages of development. As a result, we aimed to further examine the locomotion defects of these mutants in comparison with wild type N2 animals. To accomplish this, animals were analyzed using automated worm tracking. Using this technology, the automated worm tracking program is able to follow individual animals while keeping a frequency count of various different locomotion behaviors seen in worms (forwards and backwards movement, body bends of specific directions, head turns, etc.). Wild type animals were analyzed alongside *pbrm-1(ot792)* and *pbrm-1(tm415)* mutant animals.

Our results show that *pbrm-1(ot792)* mutants show drastic changes to their observed locomotion in comparison with wild type animals, while *pbrm-1(tm415)* mutants show mild locomotion defects (**Figure A.1**). These results are consistent with our expected results based on the mutations present in each strain. *pbrm-1(tm415),* as shown previously in chapter 2, is a mutant strain characterized by a 427 bp deletion of the 4th exon, and targeting the long isoform of *pbrm-1* only. Conversely, *pbrm-1(ot792)* mutants are characterized by a single point mutation (C to T) in the 12th exon, and targeting all isoforms of *pbrm-1*. Furthermore, this point mutation results in a premature stop codon, likely resulting in the degradation of truncated *pbrm-1* mRNA via nonsense mediated decay. Going forward, additional behavioral analysis is required to fully categorize the *pbrm-1* mutant locomotion phenotype.

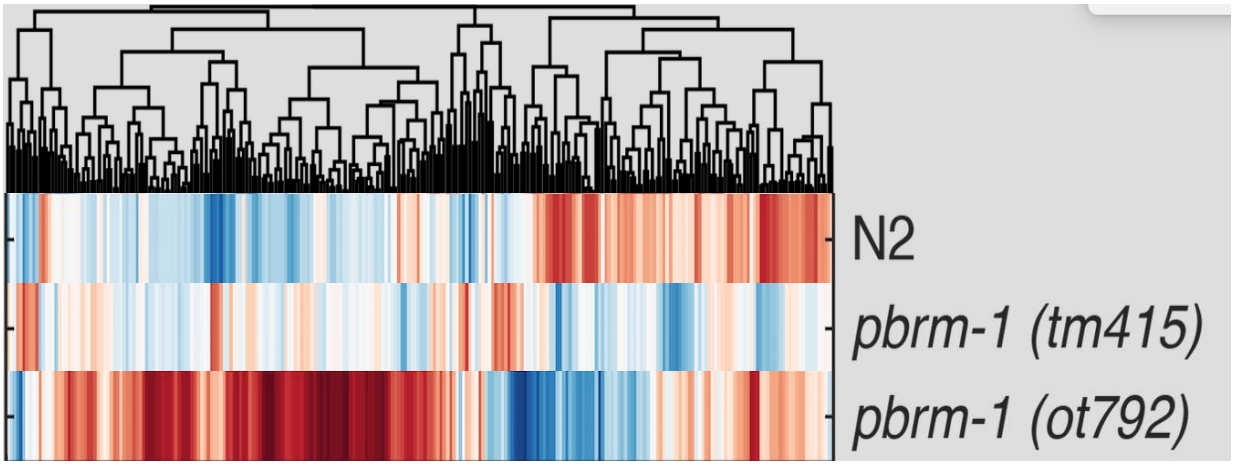

Figure A.1. *pbrm-1* mutants show behavior defects

Heatmap of C. elegans measurable locomotion in WT and *pbrm-1* mutant animals. Each vertical line represents another locomotion parameter, with red indicating high frequency and blue indicating low frequency. *pbrm-1(ot792)* mutants are especially affected, and these locomotion defects are clearly visible with the naked eye on agar plates. Additional data is needed to categorize a behavioral phenotype for *pbrm-1(ot792)*. Behavioral data collected in collaboration with Dr. Andre Brown, LMS, Imperial College London.

APPENDIX B

Previous studies have shown that two transcription factors, *unc-4/UNC-4* (a homeodomain transcription factor) and *unc-37/UNC-37* (a Groucho-like transcription factor) physically interact with each other to co-repress several VB specific terminal identity genes in VA MNs (Winnier et. al., 1999). As such, we were curious to see if these two transcription factors play a role in the repression of *glr-4/GRIK4* in the ventral nerve cord as we have seen for other subtype specific transcription factors such as MAB-9 and CFI-1. To investigate this question, *unc-4* and *unc-37* mutants were independently crossed to an extrachromosomal *glr-4/GRIK4* reporter, along with a cholinergic marker to identify individual MNs.

Our results show that both *unc-4* and *unc-37* mutants display ectopic expression of *glr-4/GRIK4* (**Figure B.1**). While wild type animals show ~8-9 MNs expressing *glr-4/GRIK4*, that expression is increased in *unc-4* mutants to ~14 MNs and in *unc-37* mutants to ~18 MNs. Interestingly, while this ectopic expression was seen across all cholinergic MN subtypes, it was observed primarily in the posterior half of the ventral nerve cord of the animals analyzed (between the vulva and tail). Although the *glr-4/GRIK4* expression was slightly variable from animal to animal, this likely was due to the use of an extrachromosomal reporter resulting in mosaic expression. Together, these results indicate that the transcription factors *unc-4* and *unc-37* may coordinate to assist in repressing *glr-4/GRIK4*. Of note, these results were not able to be recapitulated using an endogenous *glr-4/GRIK4* reporter. Quantification of fluorescence intensity was used as a proxy to observe expression levels of *glr-4/GRIK4*, an no significant difference was detected. As a result, more experiments must be conducted to elucidate the role of *unc-4* and *unc-37* as repressors of *glr-4/GRIK4*.

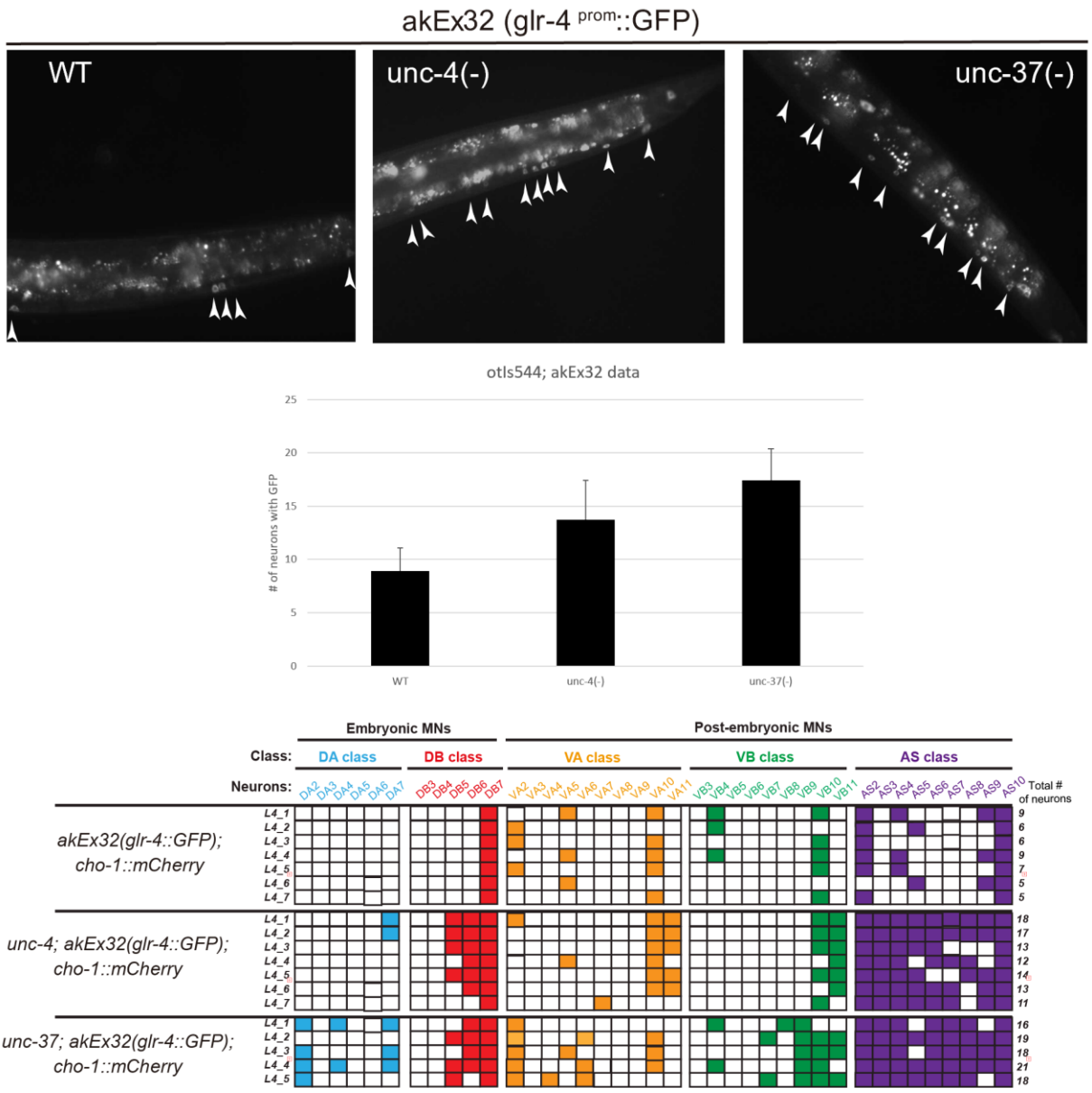

Figure B.1. Preliminary data shows transcription factors UNC-4 and UNC-37 also may repress *glr-4/GRIK4*

Top – Preliminary data for an extrachromosomal *glr-4/GRIK4* reporter (akEx32) shows de-repression in *unc-4(-)* and *unc-37(-)* animals. Expression was variable due to mosaicism of the extrachromosomal array. More data is required to further characterize this phenotype. Of note, *unc-37(-)* animals showed no observable phenotype when crossed with our endogenous *glr-4::mScarlet* reporter.

Bottom – Single-cell co-localization analysis of *unc-4(-)* and *unc-37(-)* animals crossed with akEx32 strain. De-repression is seen across all cholinergic MN subtypes.